Blue-Light Sensing in Arabidopsis: In Vivo Microscopy of Subcellular Localization, Endocytosis, and Vesicular Recycling of the Blue-Light Receptor Phototropin 1

Dissertation

zur

Erlangung des Doktorgrades (Dr. rer. nat.)

der

Mathematisch-Naturwissenschaftlichen Fakultät

der

Rheinischen Friedrich-Wilhelms-Universität Bonn

vorgelegt von

Yinglang Wan

aus

Sichuan, China

Bonn 2008

Angefertigt mit Genehmigung der Mathematisch-Naturwissenschaftlichen Fakultät der Rheinischen Friedrich-Wilhelms-Universität Bonn

1. Referent: Prof. Dr. František Baluška
2. Referent: Prof. Dr. Diedrik Menzel

Tag der Promotion: 13.02.2009

Erscheinungsjahr: 2009

Table of Contents

List of Figures

List of Tables

Abbreviations

AGC	Protein kinase A, cyclic GMP-dependent protein kinases and protein kinase C
APS	Ammonium persulfat solution
ARF	*A*DP-*R*ibosylation *F*actor
ARF-GEFs	(ARF-*G*uanine-nucleotide *E*xchange *F*actors)
BFA	Brefeldin A
BL	Blue Light
CEZ	Central Elongation Zone
CHX	Cycloheximide
Col 0	Columbia 0
CRY	Cryptochrom
DEZ	Distal Elongation Zone
DMSO	Dimethyl Sulfoxide
EDTA	Ethylenediaminetetraacetic acid
F-actin	Actin Filaments
Fig.	Figure.
FM1-43	N-(3-triethylammoniumpropyl)-4-(4-(diethylamino) styryl)pyridinium dibromide
FM4-64	N-(3-triethylammoniumpropyl)-4-(6-(4-(diethylamino) phenyl) hexatrienyl)pyridinium dibromide
GL	Green Light
GFP	Green fluorescence protein
GUS	ß-Glucoronidase
IAA	Indole-3-acetic acid
LB	Latrunculin B
LOV	Voltage, Oxygen and Light
MS	Murashige and Skoog
NPA	*N*-naphthylphthalmic acid
NPH	Nonphotptropic hypocotyls

PAGE	Polyacrylamide gel electrophoresis
PAT	Polar auxin transport
PHOT	Phototropin
PHY	Phytochrom
PID	PINOID
PINs	PIN-formed proteins
PM	Plasma membrane
PVC	Prevascular Vesicles
RC	Root Cap
RME	Receptor-Mediated Endocytosis
RL	Red Light
RTZ	Root Transition Zone
SDS	Sodium dodecyl sulfate
TEMED	N, N, N', N'-tetramethylethylenediamine
TGN	Trans Golgi Network
TIBA	2,3,5-triiodobenzoic acid
Tris	Tris (hydroxy methyl) aminomethane
WS	Wassilewskija
WT	Wild-Type

1. Introduction

1.1 Visible Light and Plant Photoreceptors

Light exists universally. As Albert Einstein, Luis de Broglie and many other scientists discovered in the 20th century, light has a wave-particle duality. The energy of light is carried by the elementary particle named photon, which is an undividable entity and therefore it is also called quantum. Einstein presented the following formula to describe the relationship between the photon-carried light energy (E) and the frequency (*f*) of electromagnetic light wave (Formula 1). Luis de Broglie formulated the hypothesis that not only light, but all matter, has the wave-particle duality. He described the relation between wavelength (λ) and momentum (ρ) as in Formula 2. These two formulas are equal to each other and can be linked by the light speed in vacuum (c) as Formula 3 and Formula 4 (reviewed by Bennett, 2005).

$$E = h f \quad \text{(Formula 1)}$$

$$\lambda = h / \rho \quad \text{(Formula 2)}$$

$$\rho = E / c \quad \text{(Formula 3)}$$

$$\lambda = c / f \quad \text{(Formula 4)}$$

(Planck's constant, $h = 6.626 \times 10^{-34}$ J s, light speed, $c = 299{,}792{,}458$ m/s)

Light and the majority other kinds of electromagnetic waves on the earth surface are radiated from the nearest star, the sun. It affects all aspects of life on our planet. During billions of years of evolution, life forms have developed several molecular systems to take advantage of sunshine directly and indirectly. Among them, the advent of oxygenic photosynthesis is one of the most important events in evolution of life on earth (Xiong et al., 2000). About 3.5 billions years ago, ancient cyanobacteria invented a mechanism to transform light energy into chemical energy using water as the electron donor (Xiong et al., 2000, Dyall et al., 2004). About 1.2 billions of years ago, such ancient cyanobacteria were engulfed by unicellular eukaryotes, giving rise to a stable endosymbiosis, and eventually the endosymbionts transformed in to chloroplasts (Des Marais, 2000, Xiong et al., 2000). Due to chloroplasts, light became the primary energy source for algae and the green plants and all the animals and heterotrophs, which live on green plants directly or indirectly, depend on this energy source as well.

Plants need to orient themselves in space and time in order to perceive light efficiently. Therefore, light does not only serve as energy source, but also as an environmental signal for plant lives. Light signals from the environment can influence the direction of growth in organs such as stems and roots, bending towards or away from the light source. These responses are called phototropism.

In *Arabidopsis*, the shoots react positive and the roots negative to incident blue light (BL) signals (reviewed by Iino, 2006), while red light (RL) causes reverse responses (Molas and Kiss, 2008, Kiss et al., 2003). Both qualities of light may also induce photomorphogenesis. Furthermore, excess light is destructive. Leaves may fold or rotate relative to the light vector, chloroplasts within the cells may reorient and tissues may accumulate photoprotective substances in order to prevent photo damages (Koller, 2000). All these implicate, that plants must have systems to sense and analyze light signals.

But unlike animals, plants do not have sensory organs such as eyes. In fact, the term “light” is derived from the physiological mechanism of the human eyes, which can detect electromagnetic waves with the wavelength range between 380-800 nm. Therefore this part of the electromagnetic wave spectrum is becoming visible light, or simply light. There are three kinds of cone cells in the human eye that are sensitive to three different ranges of wavelength (reviewed by Solomon and Lennie, 2007), and hence light is divided into three different color groups: blue light (BL, 380-500 nm), green light (GL, 500-600 nm) and red light (RL, 600-800nm). Plants detect a similar spectrum of lights as humans do, but mostly blue and red light signals, while they are blind for green light (Folta and Maruhnich, 2007).

Three families of photoreceptors have been discovered in plants and they are characterized in greater detail in the model plant *Arabidopsis*: phototropins (PHOT), cryptochromes (CRY) and phytochromes (PHY) (reviewed by Lariguet and Dunand, 2002). Phototropins and cryptochromes are activated by blue and ultraviolet-A (UV-A) light signals, while phytochromes are sensitive to red and far-red lights. The phototropin family has two members, named PHOT1 and PHOT2, which mediate most BL-initiated responses, such as phototropism, stomata opening, leaf expansion and chloroplast movement (reviewed by Christie, 2007). Cryptochrome has two known members, named CRY1 and CRY2. They regulate organ movements, physiological and morphogenetic responses in plants, such as inhibition of hypocotyl elongation, anthocyanin accumulation, promotion of stem and internode elongation,

circadian clock and day length perception, the latter of which helps plants to optimize their flowering time (reviewed by Li and Yang, 2007). The phytochome family has 5 members, named PHYA, PHYB, PHYC, PHYD and PHYE (Sharrock and Quail, 1989). They regulate several aspects of plant development and growth, such as seed germination, seedling de-etiolation, neighbour perception and avoidance, and flowing (reviewed by Schepens et al., 2004).

In this thesis work, my studies are focused on the BL receptor PHOT1, and PHOT1-mediated phototropic responses.

1.2 Phototropism and Polar Auxin Transport

Phototropism is the bending response of plant stem or root tissues under unilateral light illumination. The observation of this phenomenon is traced to the ancient civilizations, but scientific studies have only been started at the beginning of the 19th century (Poggioli, 1817, thanks to Prof. Winslow Briggs to unearth this history and introduced to me). Since then, numerous studies have been dedicated to the mechanisms of phototropic response. The most widely accepted theory was presented by Cholodny and Went independently (Went, 1928, Cholodny, 1926). They suggested that the asymmetric redistribution of the growth hormone auxin, namely indole-3-acetic acid (IAA), in response to gravity or unilateral light lead to organ curvature by causing unequal rates of cell elongation at opposite sides of the organ. After decades of physiological studies, this theory has recently been supported more directly by genetic and molecular biological studies addressing the polar auxin transport (PAT) as a central aspect of photo- and gravitropism. Molecular components have been discovered such as auxin efflux and influx transporters and transport facilitators in plant cells, and their roles in the tropic responses have been characterized (Friml et al., 2002, Blilou et al., 2005). Members of the PIN protein family have been identified as auxin efflux facilitators in *Arabidopsis* and their intracellular localization at the apical and/or basal plasma membrane (PM) domains in the cell files has been determined. PIN1 cycles between the PM domain and the endosomal compartment (Fig. 1) (Bonifacino and Jackson, 2008). Evidence for this cycling behavior comes from work with inhibitors of auxin transport. For example, *N*-naphthylphthalmic acid (NPA) and 2,3,5-triiodobenzoic acid (TIBA), as inhibitors of cellular auxin export, and brefeldin A (BFA) (inhibitor of protein secretion). All three

block auxin transport by inhibiting the endocytic recycling of PIN proteins (Geldner et al., 2001, 2003).

Brefeldin A is an antibiotic produced by the fungal organism *Eupenicillium brefeldianum* (Fujiwara et al., 1988). BFA binds to ARF-GEFs (ADP-Ribosylation Factor-Guanine-Nucleotide Exchange Factors) specifically, therefore blocks the activation of ARF by stopping the phosphate exchange between ARF-GDP (inactive) and ARF-GTP (active). ARF activation by GEF is important at least in two situations: the first one is when COPII vesicles form to be exported to the cis-Golgi cisterna. Inhibition of this GEF by BFA leads to inhibition of secretion; the second situation involving GEF-factors is when vesicles bud off the endosome to be exported to the plasmamembrane. This latter member of the ARF-GEF factor family in plants is named GNOM. GNOM is associated with endosome membranes and the

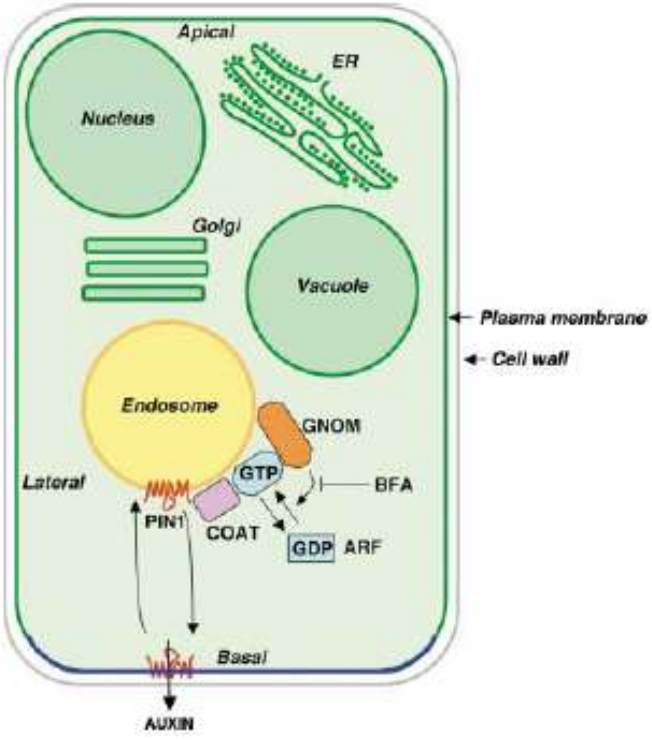

Figure 1. Schematic description of endosomal recycling of PIN proteins (Bonifacino and Jackson, 2003).

BFA inhibits the GNOM-mediated activation of ARF. ARF plays critical roles in the protein transportation via vesicle pathways. COP1, GGA1 and other coat proteins are involved. The recycling of PIN proteins is suggested to be related to this process.

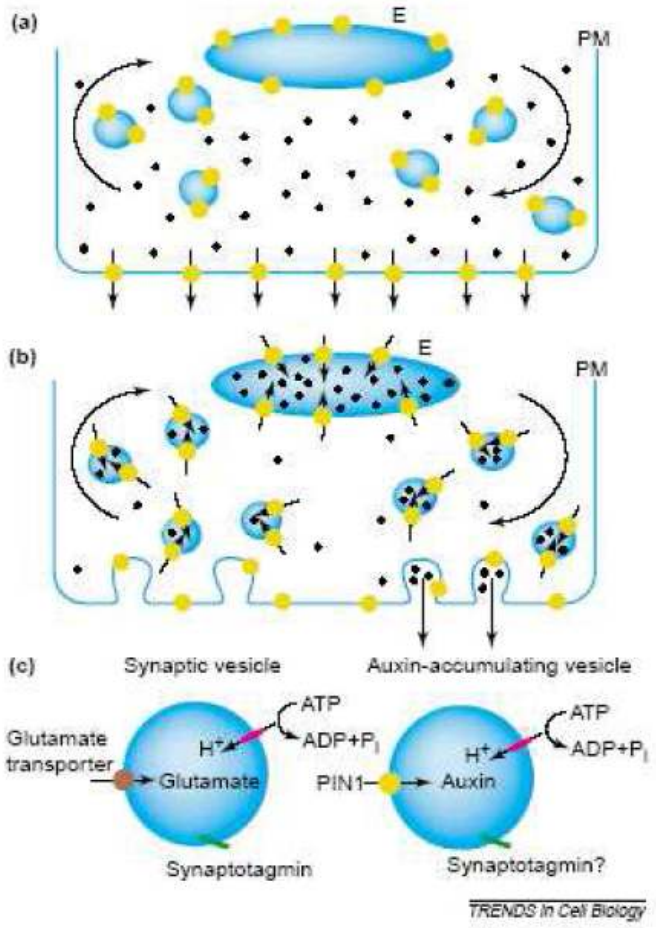

Figure 2. Vesicle transport of auxin mediated by PIN proteins (Baluška et al., 2003).
Detailed view of postulated PIN1 recycling at the apical pole of a hypothetical root cell. PIN1 (yellow circles) recycles between the apical plasma membrane (PM) and endosome (E). In (a), the conventional concept is shown, with PIN1 performing auxin (black dots) export (indicated with arrows) only when inserted into the plasma membrane. This model does not explain the transient nature of the PIN1 localization to the plasma membrane. In (b), the newly emerging model is summarized, based on the current breakthrough papers as well as on older data. According to this concept, PIN1 is the vesicular transporter that loads auxin (black dots) from the cytoplasm into vesicles and endosomes, while localization of PIN1 to the plasma membrane is only transient owing to its vesicular secretion and rapid retrieval back into internal membranes. In (c), the synaptic vesicle is shown in comparison with a putative auxin-accumulating vesicle. Both types of vesicles accumulate either glutamate or auxin, using a proton gradient as the driving force for crossing their limiting membranes.

blocking of GNOM by BFA results in disrupted membrane recycling between endosomes and plasma membranes whereas endocytosis from the plasma membrane is not blocked. Block of secretion and of endosomal recycling lead to a block of endosomal vesicular trafficking and consequently to the formation of BFA-induced compartments (Anders et al., 2008, Teh and Moore, 2002). Since PIN-proteins recycle between plasma membrane (PM) and endosomal compartment, their

correct distribution in the cell is also blocked and therefore processes depending on PIN-function are also blocked by BFA (Fig. 1, Bonifacino and Jackson 2008, Inoue and Randazzo, 2007, Dhonukshe et al., 2007). Therefore Baluška et al. (2003) hypothesized that auxin is transported in a vesicle manner inside plant cells (Fig. 2). This hypothesis about adjustable auxin transport in endosomal vesicles are supported by current studies of our group (Schlicht et al., 2006).

PIN-formed proteins (PINs) are relocalized under changes of both gravity and light conditions. For example, a member of the PIN family - PIN3 – has been reported to play an important role in the redistribution of auxin in the root cap following gravistimulation (Friml et al., 2002). After reorientation of the roots from vertical to horizontal position, the PIN3 proteins relocated from the horizontal to the vertical PMs

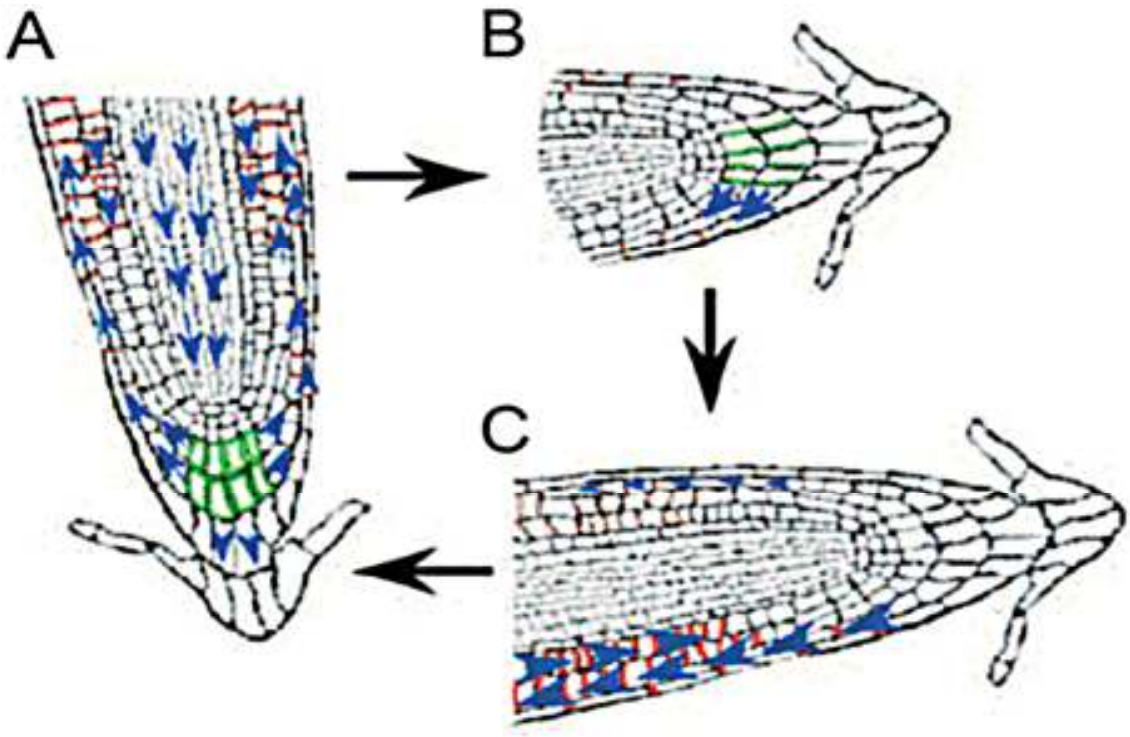

Figure 3. The polar auxin transport under gravitropic stimulation (Abas et al., 2006).

A: Auxin flow in the vertical position (blue arrows). PIN1 proteins are localized at the cross-walls of central cylinder cells, driving the apical transport of auxin. PIN2 proteins are at the polar domains of the plasma membrane in cortical and epidermal cells, and they transport auxin basally. PIN3 are localized in the root cap statocytes where they act as the re-distributor of auxin.

B: Auxin flow in the horizon position, changed by the relocalization of PIN3 proteins (green). Most of auxin is flowing to the lower part, with help from PIN3 proteins.

C: The auxin flow in the lower part of the elongation zone. The cellular concentration in the cells in this side is much higher than at the upper side. Cell elongation is inhibited and results in the root apex bending response to direction of gravity.

of the columella cells. This observation suggests that the PIN3 proteins determine the auxin distribution under reorientation of the organ. Another member of the PIN family, PIN1, becomes re-located in cells on the shaded side of the hypocotyl of wild-type *Arabidopsis* but is not similarly re-localized in a *phot1* mutant (Blakeslee et al., 2004). The localization of PIN2 is affected by light conditions as well. PIN2::GFP signals are stimulated inside vacuole in dark-grown seedlings while the seedlings grown under BL illumination did not have such pattern of localization (Laxmi et al., 2008). The mechanisms and the functional roles of this PIN2 relocalization are still unclear. And the roles of PINs in phototropic responses are still unknown either. Recently, the network built up by PIN1, PIN2 and PIN3 proteins and their roles in polar auxin transport are gravitropic stimulation is described in the Fig. 3 (Abas et al., 2006).

1.3 Phototropism and Interaction between Gravi- and Phototropism at Root Tip

Though the functions of PINs in *Arabidopsis* root under gravitropic stimulation are relative well studied, the phototropism of plant roots are only poorly studied. Because roots generally grow beneath the soil and light can only penetrate several millimeters into the soil, root phototropism is usually of little importance. However, when grown in light, root phototropism is generally masked by gravitropism. Although an early study on root phototropism surveyed 152 species and found 50% of these plants have negative phototropism in roots (Hubert and Funke, 1937), only a few of them have been characterized by modern technique in the absence of gravity.

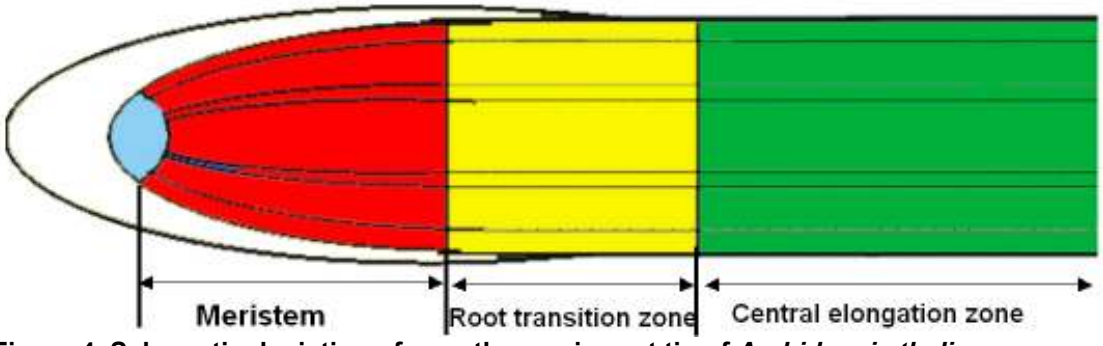

Figure 4. Schematic depiction of growth zone in root tip of *Arabidopsis thaliana*.
Regions are colored in different colors.
White: root cap; blue: quiescent center; red: meristem; yellow: root transition zone (distal elongation zone), green: central elongation zone.

Elongation rate of different tissues in phototropic response was detailed (Orbovik et al., 1993). A computer-feed back system was applied to observe the phototropism and gravitropism responses of *Arabidopsis* roots (Mullen et al., 2000). The response to light occurs at the central elongation zone (CEZ), while the roots respond to gravity at the root transition zone (RTZ), also known as distal elongation zone (DEZ) (distribution of growth zones is shown in the Fig. 4). The time that the roots need to respond is different too: the response to light is slower (40 minutes) than the response to gravity (10 minutes). These results suggest that the phototropic and gravitropic responses may share pathways of signal transduction, but each may evoke specific pathways as well, though it is considered, that the root cap is the organ for sensing both of gravity and light. Mullen and co-workers used optical fiber to illuminate the root cap and the RTZ of *Zea mays* (Mullen et al., 2002). They found that the illumination of the root cap (RC) led to significant, negative phototropic bending, but that the illumination to the RTZ did not. They concluded that the perception of light and the response to it are spatially separated.

The relationship between gravitropism and phototropism in a starchless mutant of *Arabidopsis* has been observed and analyzed (Vitha et al., 2000). It has been discussed, that the phototropism in the root region is a complex process determined by the intensity, direction and rhythm of illumination. Not surprisingly, the phototropism is unmasked by removing the gravitropic responses. Phototropic responses in starchless mutants are three times more intense than in the wild type root apices. Furthermore, roles of different light receptors in root tropic responses have been discovered by modern molecular biology. Roots of *Arabidopsis* are bending away from BL, but towards RL. This positive response to RL is mediated by phytochrome A and B (Kiss et al., 2003). Lariguet and Fankhauser have analyzed the interaction between gravitropic responses by using photoreceptor mutant plants. The Null mutant *phot1-5* shows non-gravitropic phenomena under weak BL illumination, while *phot2* and *phot1phyA* mutants have normal gravitropism under the same conditions. They suggest that activation of PHYA under BL inhibits gravitropic responses (Lariguet and Fankhauser, 2004), and that PhyA acts as a positive regulator of BL-caused phototropism, and thus it influences the phototropism induced by the PHOT1 BL receptor. It is therefore safe to conclude, that the signaling pathways under BL and RL interact with each other and that the gravitropic and phototropic signals influence each other, too (Correll et al., 2002, Folta et al., 2001,

Kiss et al., 2001). PKS1 (Phytochrome kinase substrate 1) links to PHOT1 and is supposed to be one of the interaction points in the complex signal transduction and response pathways (Schepend et al., 2008, Lariguet et al., 2006).

1.4 Phototropins

How can plants sense the direction of light? A gradient of light intensity between the illuminated and the shaded sides of a plant would be a logical answer to this question. Optical fibers have been used to measure the light gradient in the coleoptiles and hypocotyls of seedlings irradiated by unilateral BL (Vogelmann and Haupt, 1985). It has been determined, that light reaching the shaded side is 4-8 times weaker than the light hitting the illuminated side of maize hypocotyls. In order to sense the direction of light, plant cells must have mechanisms to sense and analyze this light gradient created by shading effects.

In the 1990s', Briggs and his colleagues have found that the level of membrane protein phosphorylation showed a gradient between illuminated and shaded side (Short et al., 1994, Palme et al., 1993), and therefore these results provided the evidences pointing at the involvement of a protein kinase . In 1995, mutant alleles named *nph* (nonphotptropic hypocotyls) were presented (Liscum and Briggs, 1995 and 1996). Among them, the *NPH1* gene encodes a flavoprotein with putative light and redox sensing domains, the LOV domains, which are activated by voltage, oxygen and light signals (Fig. 5). PHOT1 is phosphorylated even under weak BL illumination (mechanism is shown in the Fig. 6). Later, researchers found that the gene on the *NPH2* locus encoded a NPH1-like protein (NPL1), which was activated and phosphorylated under stronger light illumination (Sakai et al., 2001, Kagawa et al., 2001). Therefore, NPH1 and NPL1 were assigned to the same protein family and renamed phototropin 1 and 2 (Briggs et al., 2001).

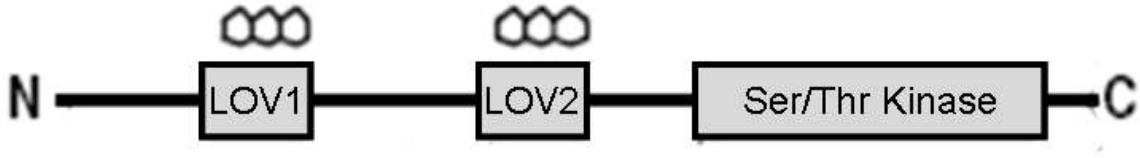

Figure 5. Schematic figure shows the domains of PHOT1 protein.
PHOT1 has two LOV domains at N-terminus, each LOV domain binds a FMN molecule non-covalently. There is a ser/thr kinase domain at C-terminus.

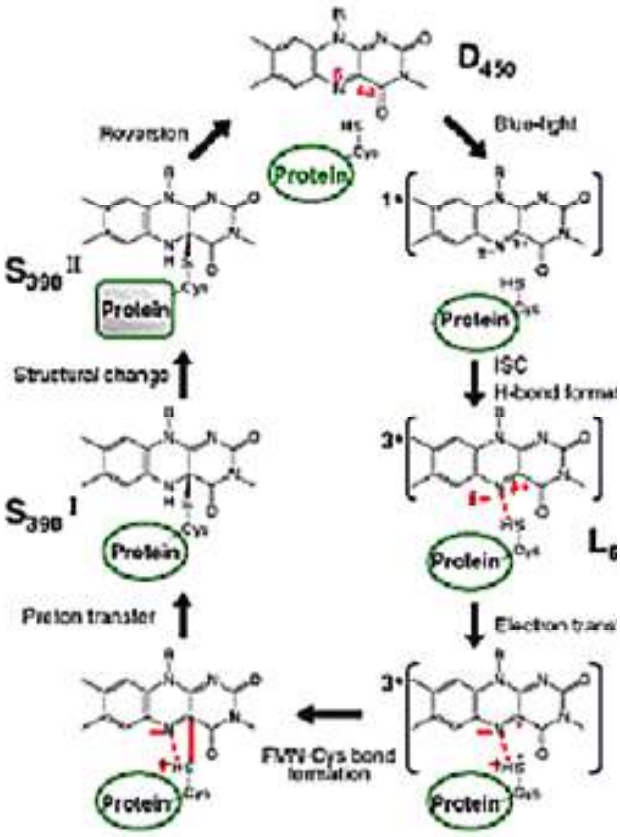

Figure 6. Proposed photocycle of LOV domains from PHOTs (Matsuoka et al., 2007).

Absorption of blue light results in the generation of the singlet excited-state FMN. Intersystem crossing results in the formation of the triplet-state, and this excited state is stabilized by protonation of the N5 atom of the isoalloxazine (high lighted in red) ring through the abstraction of a proton from the conserved Cys in the LOV domain polypeptide. This protonation of the triplet state FMN increases the electrophilicity of the C(4a) atom and promotes nucleophilic attack of the thiol anion at this position, resulting in the formation of the cysteinyl-FMN adduct (Arrows right side). This adduct is completely reversible in darkness. The catalytically reactive N5 and C(4a) atoms are highlighted on the ground state molecule, and their excited orbitals are highlighted in blue on the singlet and triplet state molecules. (arrows left side).

Phototropins are the most essential photoreceptors for the phototropic signaling. They trigger the BL-mediated signal transduction pathways. Both of them are sensitive to BL signals with peak wavelength at 450 nm. Already very weak BL (>0.01 $\mu mol \cdot m^{-2} \cdot s^{-1}$) can activate PHOT1, whereas the PHOT2 has less sensitivity to BL and requires much higher doses (> 1$\mu mol \cdot m^{-2} \cdot s^{-1}$) (Sakai et al., 2001). Besides the phototropic response, phototropins mediate also other BL mediated responses in plants. For instance, PHOT2 mediates dispersal of chloroplasts under strong BL, while both PHOTs together mediate intracellular chloroplast movements under weak BL (Kagawa et al., 2001, Suetsugu et al., 2005). Moreover, both PHOTs mediate stomata opening/closing (Kinoshita et al., 2001, 2003), expanding of leaves (Sakamoto and Briggs, 2002) and inhibition of hypocotyl elongation (Christie, 2007).

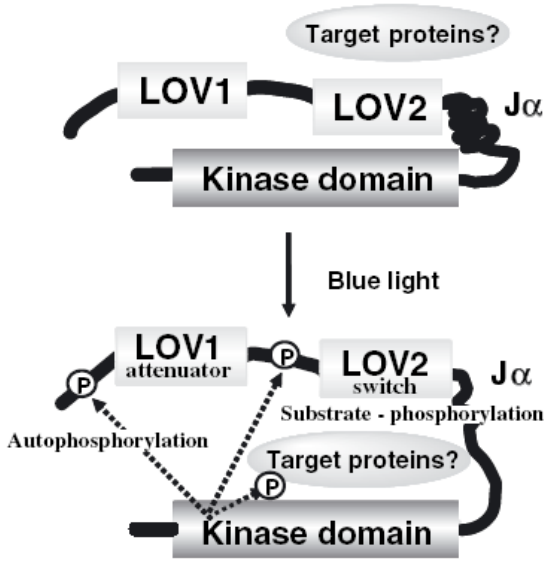

Figure 7. Schematic model describes the activation of C-terminus kinase domain of PHOT2 molecule (Matsuoka et al., 2007). Blue light releases of the FMN from LOV2 domain, which inhibits kinase activation at ground status in dark condition. After blue light illumination, C-terminus kinase is freed from the LOV2. Sites of phosphorylation of ser/thr amino acids are at N-terminus. Actually, 8 sites have been discovered (Salomon et al., 2003). Except phototropin itself, still no other substrate is known.

According to the photochemistry studies and structure analysis of PHOTs, the BL signals are received by the two N-terminus LOV domains, which then activate the ser/thr kinase domain at the C-terminus (Freddolino et al., 2006, Eitoku et al., 2007). LOV proteins exist widely in all kinds of eukaryotic organisms. Among all the LOV proteins, PHOTs are the only two members with two LOV domains for some unknown reasons. It is suggested that the LOV2 domain plays an essential role in the activation of the C-terminus kinase (Matsuoka et al., 2007), while the LOV1 domain helps in the dimeration of PHOT molecules (Salomon et al., 2004). Furthermore, the only known *in vivo* substrate of C-terminus ser/thr kinases is phototropin itself, though a common ser/thr kinase substrate, casein, is phosphorylated by the kinase domain of PHOT2 *in vitro* (Matsuoka and Tokutomi, 2005). Therefore, the signals are not transduced simply by the kinase cascade pathways. Though the exact mechanisms of phototropins-mediated pathways are still unknown, several cooperation partners of PHOTs were proved to mediate different BL responses. For example, NPH3, RPT2 (root phototropism 2) and CPT1 (coleoptile phototropism 1) belong to the same protein family and interact with PHOT1 directly (Motchoulski and Liscum, 1999, Inada et al., 2004, Haga et al., 2005). It has been suggested, that NHP3/RPT2/CPT1 act as scaffold proteins and mediate the signal transduction in phototropic responses, RPT2 can also control stomata movements (Inada et al., 2004). But neither of them plays roles in chloroplast movement responses. The mechanisms of the pathway via PHOT1/NPH3 have been described relative clearly (Motchoulski and Liscum, 1999, Pedmale and Liscum, 2007). Yeast two-hybrid and *in vitro* immunoprecipitation

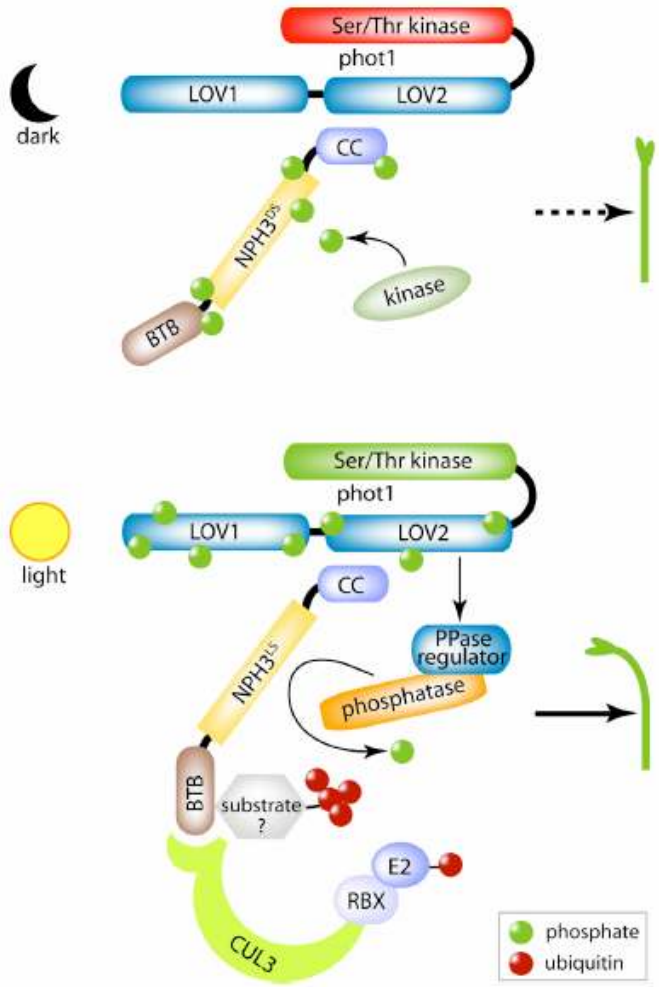

Figure 8. A model to describe the signal transduction via PHOT1/NPH3 pathway. (Pedmale and Liscum, 2007). NPH3 binds to PHOT1 directly via the coil-coiled domain (CC). LOV2 in the dark prevents the activation of the C-terminus kinase domain. Blue light illumination causes activation of the kinase domain of PHOT1 which is autophosphorylated. Blue light mediates dephosphorylation of NPH3 proteins via the regulatory subunit of PPase. The BTB domain at the N-terminus of NPH3 is activated by dephosphorylation. This then leads to downstream signal transduction.

suggests that the coiled-coil domain at C-terminus of NPH3 interacts with the N-terminus of PHOT1. BL irradiation causes the dephosphorylation of NPH3 *via* PHOT1-dependent pathways. They presented a common model to describe the PHOT1 mediated signal transduction via the PHOT1/NPH complex (Fig. 8).

Ion channels (Ca^{2+}, K^+, Na^+ , Cl^-, and H^+) are involved in the PHOT-mediated responses as well (Babourina et al., 2003; Baum et al., 1999; Fuchs et al., 2003; Harada et al., 2003; Stoelzle et al., 2003). PHOTs seem also to affect the distributions of myosin motor protein on the chloroplast surfaces (Krzeszowiec et al., 2007).

Recent clues in the discovery of the PHOTs mediated pathways are coming from the analysis of localization of PHOTs. Both PHOTs do not have transmembrane domains, but early studies with immuno-blotting methods indicated that the PHOTs are co-localized in the membrane fractions in etiolated *Arabidopsis* plants (Liscum and Briggs, 1995). Sakamoto (2002) observed and described the cellular localization

of PHOT1 proteins with PHOT1::GFP reporter constructs stably expressed in *Arabidopsis*. Interestingly, the illumination with the blue laser in the confocal microscope caused the release of PHOT1::GFP signals from plasma membrane (PM) into the cytoplasm. Knieb and colleagues reported that about 20% of the whole PHOT1::GFP was released from PM into the cytoplasm after illumination (2004), the level and speed of this process is dependent on the intensity and time of BL illumination (Wan et al., 2008). PHOT2 shows a similar behavior of BL induced internalization from the PM into cytoplasm and redistribution to the Golgi apparatus (Kong et al., 2005).

1.5 Modulation of PIN Localization

Polar localization and endosomal recycling of PIN proteins between PM and endosomal vesicles provide a plausible model to explain the mechanism for PAT in plant cells (Baluška et al., 2003, Blilou et al., 2005). The PINOID (PID) protein, a Ser/Thr kinase (Christensen et al., 2000, Friml et al., 2004) as well as the PP2A phosphatase (Michniewicz et al., 2007) act as modulators of PINs by controlling their phosphorylation and dephosphorylation. PID regulates the development of organs by enhancing polar auxin transport (Benjamins et al., 2001). For example, the development of inflorescences and lateral roots are affected by the PID kinase (Christensen et al., 2000, Benjamins et al., 2001). PID also affects the polarity of PIN localization (Friml et al., 2004). In shoot cells of wild-type plants (WT), PIN1 is localized on the apical membrane, whereas in the *pinoid* mutant plants PIN1 have basal membrane localization. In the root, where the *PID* gene is not expressed under normal conditions, PIN1, 2 and 4 proteins are basally localized. However, ectopic expression of *PID* in root cells results in apical membrane localization of PIN2 in root cells (Friml et al., 2004, reviewed by Kaplinsky and Barton, 2004, Fig. 9). There is still no report about the analysis of phototropism in *pinoid* mutants.

Interestingly, sequences of PID and PHOT1 kinases show some homology and they belong to the same AGC kinase family (named after protein kinase A, cyclic GMP-dependent protein kinases and protein kinase C) (Galván-Ampudia and Offringa, 2007). Furthermore, PID is interacting with NPY1, which again shows a homology to NPH3 (Cheng et al., 2007). Cheng et al. hypothesized that the PID/NPY1 and PHOT1/NPH3 act via similar pathways to modify polar auxin

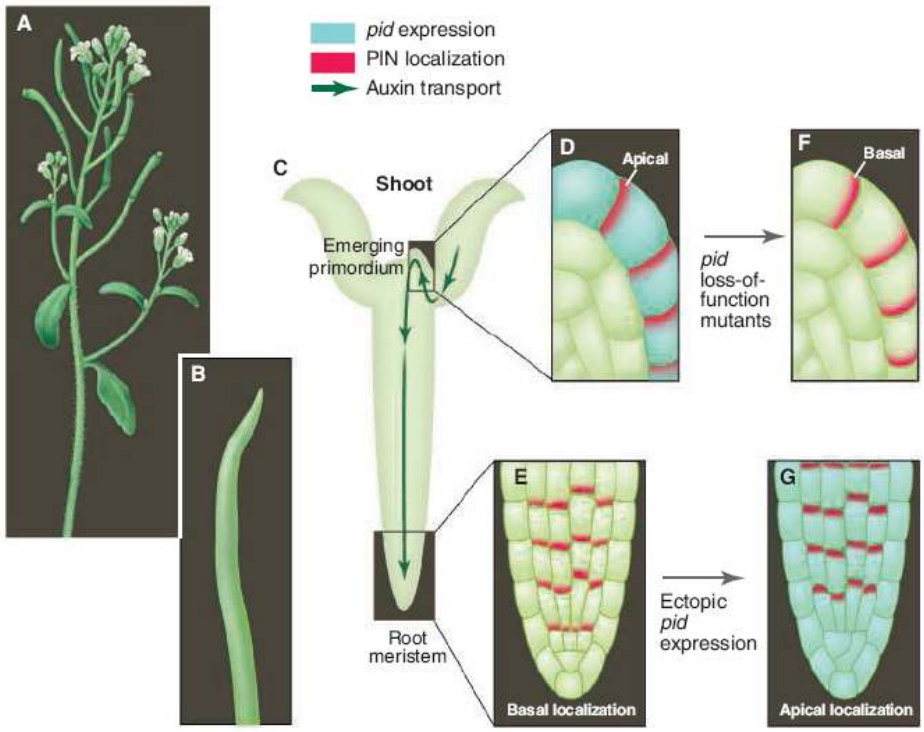

Figure 9. PINOID (PID) affects the development of inflorescence and polar localization of PIN proteins (Kaplinsky and Barton, 2004).

A: The inflorescence of wild-type *Arabidopsis*. B: Abscence of PIN1 or PID proteins causes the same phenotypes, which also appears, when the seedlings are treated by PAT inhibitors. C: Auxin is produced in young leaves and transported to the root tip, blue arrow depicts the route of PAT. D: In the shoot, where *PID* is expressed, PIN proteins have apical localization on the PM. E: In the root cells, where *PID* is not expressed normally, PINs are localized on the basal end of the PM, transport the auxin towards the meristem. F: In shoot of the *pid* mutant, PIN1 is localized at the basal pole of cells. This inhibits leaf primordium formation in the shoot. G: In the root ectopically expressing *PID*, PIN proteins are localized at the apical poles of cells. This results in decreased auxin level in meristem, inhibiting the root growth.

transport (Cheng et al., 2007). It is reasonable to postulate that the blue-light induced relocalization of phototropin1 will affect endosomal processes and auxin transport.

Actually, the PIN2::GFP reporter proteins also change their polar localization under BL illumination, while red and far red light did not affect it (Laxmi et al., 2008). In the Chapter 3.3, I will demonstrate the link between BL induced vesicular movement inside plant cells and polar auxin transport.

Endosomal vesicular movements have been suggested to be involved in the signal transduction process in animal cells (reviewed by Ibáñez, 2007). Membrane receptors exist in animal cells, such as the epidermal growth factor receptor (EGFR), present a receptor-mediated endocytosis (RME), which is a well-known signaling process in animal cells. It is not a surprising idea to search for the RME process in

plant cells. In model plants *Arabisopsis,* ligand-induced endocytosis of flagellin receptor was reported (Ali et al., 2007) and also the membrane-localized steroid receptor kinase BRI1 (brassinosteroid Intensive1) is involved in endosomal signaling pathways (Geldner et al., 2007). Importantly, BRI1 localizes on the plasma membrane as homodimers while BRI1 heterodimerizes together with BAK1 (BRI1-Associated Receptor Kinase 1) within endosomes (Russinova et al., 2004). Furthermore, the proteins that are essential for endosomal vesicle transport, such as SNAREs, Rabs and other proteins, are also found in plant cells. They are playing key roles in the transduction pathways (Chow et al., 2008, Anders et al., 2008, reviewed by Samaj et al., 2006). A dynamic motor protein, myosin VIII, has been found to be involved in the endosomal trafficking in *Arabidopsis* cells too (Sattarzadeh et al., 2008). However, the relationships between the cell surface receptor of plant cells and the intercellular signal transduction are still unclear.

1.6 Introduction to the Drugs Used in this Study

1.6.1 Brefeldin A

Brefeldin A (BFA) is a metabolite of the fungus *Eupenicillium brefeldianum*. After its rediscovery in 1988 (Fujiwara et al., 1988), it is now considered a very useful tool in cell biology, because BFA inhibits exocytosis effectively. This is due to the fact that BFA prevents vesicle formation in all anterograde exocytosis pathways by stabilizing the complexes between ADP Ribosylation Factor 1 (ARF1) and the Sec7 domain of its guanine nucleotide exchange factor (GEF) and such inhibiting the exchange of phosphate between GTP and the ARF1-GEF-GDP complex. Therefore, the assembly of coat protein complexes of budding vesicles named COPII is blocked, while the endocytosis is not affected or even stimulated (reviewed by Chardin et al., 1999). cis-Golgi elements merge with the ER in BFA treated cells (Nebenführ et al., 2002), whereas the trans-Golgi Network (TGN) and endosomes aggregate into so called BFA-induced compartments. This makes BFA a useful tool for studies of cell biology, in particular for the study of vesicle trafficking, endocytosis, exocytosis, sorting and secreting of proteins.

1.6.2 Cycloheximide

Cycloheximide (CHX) is an inhibitor of protein biosynthesis in eukaryotes, produced by the bacterium *Streptomyces griseus*. It blocks the protein synthesis by interfering with protein translation, i.e., the translocation of tRNAs and mRNA molecules on the ribosome (Obrig et al., 1971). By using ^{35}S-methionine as marker of new synthesis of proteins, I also determined if the conditions of experiments inhibited protein synthesis completely in root tissues (see the Chapter 2.3.5).

1.6.3 Latrunculin B

Latrunculin B (LB) is a marine toxin, first isolated from the red see sponge, *Latrunculia magnifica*. It has been utilized as a powerful drug that rapidly disassembles actin filaments (F-actin). LB causes F-actin depolymerization by binding with the actin monomer (G-actin), thereby inhibiting the addition of new G-actin units to the actin filaments (de Oliveira and Mantovani, 1988).

1.6.4 Wortmannin

Wortmannin is a furanosteroid metabolite of fungi *Penicillium funiculosum*. It is a specific inhibitor of phosphoinositide 3-kinases (PI3Ks) (Wymann et al., 1996), involved in the process of endocytosis. Treatment of wortmannin in plant cells inhibits the vesicular trafficking of membrane proteins from the PM to the endosomal compartment, the prevacuolar compartment (PVC) and the TGN. Enlarged PVC compartments are induced by wortmannin (Tse et al., 2004).

1.6.5 FM4-64 (Synaptored) and FM1-43

FM-dyes are nontoxic and water-soluble probes fluorescing only when bound to membranes. The abbreviation “FM” stands for the chemist’s name, Fei Mao, who developed the FM-dyes (Ribchester et al., 1994). Both FM1-43 and FM4-64 are membrane-selective fluorescent dyes. They insert into the outer leaflet of the plasma membrane lipid bilayer via their lipophilic tails, with the pyridinium dicationic head anchored at the membrane surface. The amphiphilic nature of these dyes is believed

to prevent them from freely crossing from the outer lipid leaflet of the membrane bilayer to the inner leaflet. The only possible way to internalize the FM dyes is by endocytosis via the formation of membrane vesicles. FM4-64 and FM1-43 differ slightly in their chemical structure, and these differences can result in different patterns of membrane staining and different excitation/emission peaks for the fluorescence nature (Bolte et al., 2004).

FM4-64 (N-(3-triethylammoniumpropyl)-4-(6-(4-(diethylamino) phenyl) hexatrienyl) pyridinium dibromide), has excitation/emission peaks at 560/635 nm. The emission wavelength in the red-domain is a significant advantage compared to FM1-43 (N-(3-triethylammoniumpropyl)-4-(4-(diethylamino) styryl) pyridinium dibromide), which shows a green fluorescence. The red fluorescence of FM4-64 is also advantageous in studies with GFP-transformed plants (Bolte et al., 2004). Synaptored^{TM} is the product name of FM4-64 from company Sigma^{TM}, it is equal to FM4-64.

2. MATERIALS AND METHODS

2.1 Plant Materials

2.1.1 Growth Condition

Seeds of *Arabidopsis thaliana* were sterilized in 6% NaClO solution with 0.01% Triton X-100 for 5 minutes. The sterilized seeds were washed with sterilized water for 5 x 1 minute and then planted on agar plates containing 1/2 MS culture medium (Murashige and Skoog, 1962) and 1% saccharose. Agar plates with seeds were kept in the refrigerator over night and then placed in the cultivation chamber at 22^{o} C temperature and 16 hours illumination per day. Etiolated seedlings were kept in petri-dishes covered with aluminium foil, after the initiation of germination by 2 hours illumination with white light at 22^{o} C.

2.1.2 Genetically Transformed *Arabidopsis* Lines

1. *ProPHOT1::PHOT1::GFP* fusion constructs were expressed on the *phot1-5* mutant back ground under control of its native promoter (Sakamoto and Briggs, 2002).

2. *ProPIN1::PIN1::GFP* and *proPIN2::PIN2::GFP* fusion constructs were also expressed on the *pin1* (*pin1-1*) and *pin2 (eir1-4)* mutant background (Delivered from Rujin Chen, Nobel foundation, USA).

3. *ProS35::NPH3::GFP* plasmids were made by my colleague Dr. Jan Jasik, the transformation of this construct into *Arabidopsis thaliana* is described in Chapter 2.3.1.

4. The *proCYCB1::GUS* transformed *Arabidopsis* line (Ferreira et al., 1994), was used to observe the effects of BL on the root meristem. Cyclin B is a member of the cyclin family of cell cycle control genes. It binds to the Cdk1 (cyclin-dependent kinase 1). The CYCB/Cdk1 complex promotes expression of genes required during mitosis (Azzam et al., 2004). Therefore, the activation of cyclin B promoter activity is only detectable in dividing cells. In plant roots, the presence of dividing cells circumscribes the region of the root meristem (Hauser and Bauer, 2000). The GUS staining method will be described in part 2.3.4.

5. DR5 is a highly active auxin response promoter element (Ulmasov et al., 1997). A reporter gene, such as *GFP,* driven by DR5 is showing the distribution of auxin signaling, indicating the presence of IAA indirectly. *Arabidopsis* seedlings were stably transformed with the *proDR5::GFP* construct, and by observing the GFP-fluorescence, a map of auxin distribution in root tips was established under different enviromemtal signals.

6. The mutant lines of *eir 1-4* (*pin2* null mutant, Luschnig et al., 1998) and *pin 3-3 (pin3* null mutant, Friml et al., 2002*)* were used for the phototropic analysis. Both lines show agravitropic root growth.

7. All *Arabidopsis* lines were based on the Columbia 0 (Col 0) ecotype except *pin3-3* mutant line, which was based on the Wassilewskija (WS) ecotype.

2.2 Chemicals

In this study, the *Arabidopsis* seedlings were treated with the inhibitors which are described in the Chapter 1.6. The concentrations and details of chemical treatments are shown in the Table 1. The light condition during treatment was carefully controlled in order to minimize the unwanted light effects from environments. The controlling of blue light conditions is described in the Chapter 2.3.4.

For labeling of the plasma membrane and endosome compartments, both FM dyes were used at concentration of 10 μM in 1/2 MS medium. In the experimental part of Chapter 3.1 and 3.2, FM4-64 and FM1-43 (Molecular Probe ®) are used. In the Chapter 3.3, synaptored (Sigma ®) was used. Synaptored is the product name of FM4-64 by Sigma ®. It is chemically equal to the compound originally known as FM4-64. To avoid quick dye uptake by endocytosis, the seedlings were kept at 4 ˚C for 15 minutes and then treated with the pre-cooled FM working solution at 4˚C for 10

Table 1. List of chemicals.

Name	Storage	Working solution	Company
Brefeldin A	10 mg/ml in DMSO, -20 ºC	50 μM in 1/2 MS	Sigma
Cycloheximide	100 mg/ml in DMSO, 4 ºC	50 μM in 1/2 MS	Sigma
Latrunculin B	2 mM in DMSO, -20 ºC	50 μM in 1/2 MS	Sigma
Wortmannin	10 mg/ml in DMSO, 4 ºC	30 μM in 1/2 MS	Sigma
FM1-43	100 mM in H_2O, 4 ºC, dark	10 μM in 1/2 MS	Molecular Probe
FM4-64 (Synaptored)	100 mM in H_2O, 4 ºC, dark	10 μM in 1/2 MS	Molecular Probe (Sigma)

minutes. The labeling of shoot epidermal cells needed 60 minutes incubation. Stepwise labeling of both FM dyes is described in the Chapter 2.3.3.

2.3 Methods

2.3.1 Crossing of transgenic lines of Arabidopsis

1. Transgenetic lines have been planted into soil in the cultivation chamber at 22^{o}C temperature and 16 hours illumination per day. After around 4 weeks of growth, when plants started to develop inflorescences, the largest buds of mother plants were chosen for crossing. In my studies, the mutant line of *phot1-5* was chosen as mother plant to cross with the PIN2::GFP transformed line, and *nph3-1* mutation was chosen as mother plant to cross with the PHOT1::GFP lines (See the Chapter 2.1.2).

2. The inflorescence was fixed under a binocular by hands gently, only the buds in right sizes were remained by removing the meristem of the chosen inflorescence. All the petals and sepals were removed by forceps. Emasculated inflorescences were marked and the plants were let to grow for 2 overnights. Then the pollens on an anther of a matured flower of father plants were crossed on matured stigmata. The seeds matured after about 4 weeks.

3. Seeds were germinated and grown in the above described conditions. The seedlings were sprayed with herbicide Basta (Bayer CropScience, 1:1000 diluted) to destroy the uncrossed seedlings. These F1 plants were self-pollinated and grown to the F2 generation. F2 seeds were cultured on the agar surface as described in the Chapter 2.1.1, the seedlings with phenotype of *phot1-5* and *nph3-1* were chosen and grown on soil to get the F3 generation. The phenotype of lines of F3 have been analyzed statistically to ensure the homozygous mutant background as described in the Chapter 2.3.5.

2.3.2 Methods to Produce Transgenic Line of *Arabidopsis*

1. Preparation of Competent Cells of *Escherichia coli* and *Agrobacterium tumefaciens.*

E. coli bacteria were cultured on the 2% agar plate of LB medium (10g/l Tryptone, 5g/l Yeast extraction, 5g/l NaCl, pH7.0) with selective antibiotics overnight at 37 ^{o}C.

A single colony was chosen and cultured in liquid LB medium (around 3 ml) overnight at 37 °C on a shaker with speed of 280rpm. 1 ml of this culture medium was added into 100 ml LB medium, incubated at 28 °C on the shaker until OD_{600} reached 0.4. After chilled on ice for 20 minutes, the medium was centrifuged at 4500 rpm for 10 minutes, in order to spin down the cells. The pellets were resuspended into ice cold TB buffer (10 mM PIPES, 55mM $MnCl_2$, 15 mM $CaCl_2$, 250mM KCl) and incubate for 30 minutes on ice. After spinning down the cells, these were resuspended into TE buffer (1/10 volumn) again, divided into tubes as 1.6 ml aliquots with 0.4 ml glycerol, freezed in N2 and stored in -70 °C.

The method for preparation of competent cells of *A. tumefaciens* bacterium is similar to the *E. coli*, but the YEP medium (1g/l Peptone, 1g/l yeast extraction, 5g/l beef extract, 5g/l sucrose, 2mM $MgCl_2$, pH 7.0) was used in this case.

2. Transformation of the Competent Cells by Heat Shock

Stored competent cells were taken from freezer and defrosted on ice. 10 µl plasmid DNA was added into each tube (40 µl), incubated on ice for 1 hour before a heat shock in waterbath for 45 seconds. Then, the tubes were put on ice again and incubated for 2 minutes. 0.5 ml prewarmed LB medium (37ºC) was added to the tubes and incubated at 37 ºC for 45 minutes on a shaker. As the last step, culture was spread on antibiotic-containing LB medium plate and cultured over night in 37 ºC overnight. In case of *A.tumefaciens,* YEP medium was used to instead of LB medium.

3. Isolation of the plasmid DNA from *E. coli* by miniprep

Single *E. coli* clonies were chosen from the agar plates, and cultured in 2 ml liquid medium at 28ºC on shaker with speed of 180 rpm overnight. The cell suspension was transferred into 1.5 ml tubes. The cells were spinned-down briefly, the suppernant medium was discarded, and 100µl solution I (25mM Tris, pH 8.0; 50 mM glucose, 10 mM EDTA, added RNAse freshly) was added into each tubes. The cells were suspended completely, then 200 µl solution II (0.2M NaOH + 1% SDS, mixed freshly) was added and mixed gently, and incubated for 3 minutes. 150 µl Solution 3 (3M potassium acetat, pH5.5) was added to each tube and mixed gently, then centrifuged for 10 minutes on 13000rpm. The suppernant was transferred into new tubes

carefully, without any of the pellets. Double volume of pure ethanol was added into the suppernant, incubated 10 minutes at 4ºC, the mixture was centrifuged for 20 minutes at 13000rpm. The suppernant was discarded, 70% ethanol was used to wash the pellet twice, and left to dry out on ice.

4. Transformation of the Competent Cells of *A. tumefaciens* by Heat Shock

In this step, the plasmid DNA isolated by miniprep was transformed into *Agrobacterium tumefaciens.* The methods were same as described in the step 2, except that the YEP medium was used to instead of the LB medium.

5. Transformation of *Arabidopsis* plants by *Agrobacterium*

The plants to transform were planted at the condition described in the Chapter 2.1.3. The first inflorescence was cut in order to remove apical dominance. 4-5 inflorescences were developed in 4-5 days, then the plants were ready for transformation.

The culture medium (YEP) with transformed Agrobacterium was collected into 50 ml falcon tubes and centrifuged at 3000 rpm for 5 minutes. The cells were resuspended in infiltration medium (1/2 MS liquid medium, 5% Sucrose, 1mM Benzylamino Purine (BAP), 0.01% vitamin B5 and 0.01% Silwel) of the same volume. The inflorescences of the target plants were put into the infiltration media upside down, incubate in vacuum for 20 minutes for each transformation.

After vacuum infiltration, the inflorescences were inserted into plastic bags and grown in the culture chamber for two days. Then the bags were removed and the plants were grown for 4 more days before the vacuum infiltration was repeated once again to get better transformation rate.

2.3.3 Stepwise Staining of Membrane Fractions in FM Dyes

Seedlings were pre-cooled at 4 ˚C before staining with FM1-43 solutions (5 μM in the ½ MS medium) at 4˚C for 5 minutes. The stained seedlings were kept in the 1/2 MS medium at room temperature for 5 minutes then incubated with FM4-64 solution (5 μM in the ½ MS medium) at 4˚C for 5 minutes. After a wash with the ½ MS medium

for 5 minutes, the seedlings were treated by BFA solution (50 µM) in the dark or under BL illumination.

2.3.4 Confocal Laser Scanning Microscopy and Blue-Light Illumination

The first two parts of my studies were conducted at the Carnegie Institution (Department of Plant Biology, San Francisco), with a Biorad MRC1024 confocal laser scanning microscope, using a Nikon 60x water immersion objective, NA = 1.3. Excitation of GFP was achieved with the 488 nm laser line of the Ar/Kr-mixed gas laser. With the Biorad 30% transmittance neutral density filter in place, the fluence rate at the sample with the 63x water-immersion objective lens was 25 $\mu mol \cdot m^{-2} \cdot s^{-1}$. Fluorescence emission was detected between 505 and 530 nm for PHOT1::GFP fluorescence and at 650 nm for FM4-64 fluorescence. The external light source used in some experiments was a halogen lamp (Phillips 20 MR 16, New Jersey, USA) passed through Corning glass filters: Corning number 5032 for blue light, number 4015 for green light, and number 2404 for red light.

During the third part of my studies microscopy was conducted at the *Institut für physikalische und theoretische Chemie* of the University of Bonn, which is equipped with a LSM 510 meta confocal microscope (Zeiss, Germany), a 60x oil - immersion objective was used for detailed images and 20x air objective for overviews. An Argon laser was used to produce the 488 nm blue laser line. Another adjustable BL source for continous BL illumination came from a halogen bulb. A filter glass (Knight Optical® with Cat. Number 476FCS5050) was used to provide peak wavelength at 475nm. The blue laser intensities were measured with a powermeter model 841-PE (Newport®) equipped with a detector model 818-3T.

2.3.5 Analysis of Whole Seedling Fluorescence

Fluorescence images of whole seedlings were obtained with a Leitz MZFLIII binocular combined with a digital camera (Leica JVC KY-F708, Leitz,Wetzlau, Germany). Relative fluorescence intensities were measured with ImageJ software (Wayne Rasband, National Institutes of Health, Bethesda, Maryland, USA). Images were background subtracted and intensities of the different regions of the seedlings were measured for 10 seedlings and averaged for each region. The ‘re-slice’ function

of Image J allowed me to construct the cross-section images shown in result Figs. 3 and 5. The dimensions were calculated from the original z-series slices.

2.3.6 Histochemical ß-Glucoronidase (GUS) Staining

Seedlings of stably transformed promoter-GUS plants were stained for ß-Glucoronidase activity. Samples were vacuum infiltrated for 10 min with substrate solution (100 mM sodium phosphate buffer, pH 7.0, 10 mM EDTA, 0.1% Triton X-100, 0.5 mM potassium ferricyanide, 0.5 mM potassium ferrocyanide, and 1 mM 5-bromo-4-chloro-3-indolyl glucuronide) and incubated at 37°C for 2h up to 8h. The stained seedlings were cleared in absolute ethanol and rehydrated by passing through a graded ethanol series diluted with H_2O. The seedlings were kept in H_2O, transferred to microscope slides, and mounted using an anti-fade mounting medium containing *p*-phenylenediamine. Roots were examined using a Leica MZ FL III binocular equipped with a CCD camera (see 2.3.3).

2.3.7 Determine the New Protein Synthesis by ^{35}S-Methionine

1. Treatment by ^{35}S-Methionine and CHX

About 0.1 g plant seedlings were collected into 1.5 ml tubes, 0.5 ml TBS buffer (150 mM NaCl, 10 mM Tris, pH8.0) was added into it. The seedlings were touched with the buffer but not soaked in it. 0.05 ml CHX (from 5 mM stock solution) was added into the TBS and treated for 30 minutes, before add 50 micro curies of ^{35}S-Methionine to the buffer. Samples were incubated at room temperature for 30 minutes before protein extraction.

2. Protein extraction

The buffer was discarded carefully as radioactive waste. Plant tissues were grinned in extractions buffer (50 mM Tris, 10 mM EDTA, 0.2% Triton X100, 10 mM mercaptoethanol, pH 7.2, protease inhibitor cocktail (Sigma) 1:2000 and PMSF 100µM were added freshly). After centrifugation briefly (5000rpm, 5 min, 4˚C), the suppernatant was collected in new tubes as protein solution.

3. SDS-PAGE

The extracted proteins were separated on the polyacrylamide gel by electrophoresis in this step. Both the stacking gel and the resolving gel were diluted from the 40% Acrylamid mixture solution (Acrylamid:Bisacrylamid=37.5:1, Gel 40® from Rotiphorese®). After solidification of the electrophoresis system with resolving gel (for 20 ml 8% gel: H_2O 10.6 ml, Gel 40® 4ml, 1,5M Tris 5 ml pH8.8, 10%SDS 200µl, 10% ammonium persulfat solution 200µl, 20 µl TEMED) and stacking gel (for 5 ml 4% gel: H_2O 3.645 ml, Gel 40® 0.625ml, 1.0M Tris 0.63 ml pH6.8, 10%SDS 50µl, 10% ammonium persulfat solution 50µl, 5µl TEMED), the whole system was put into 1Xelectrophoresis buffer (Tris base 3g, Glycine 14.4g, SDS 1g, add H_2O to 1l). The protein samples were mixed up with 1 volume 2Xloading buffer (1M Tris-HCl pH6.8 1.6 ml, 20% SDS 2ml, glycerol 2 ml, beta-mercaptoethanol 1.0ml, bromophenol blue 0.004 g, add H_2O to 10ml), then cooked in the boiling water for 2 minutes before loading gel. Gels were electrophoresed at 120 V in the electrophoresis buffer for 1 hour. The samples were dried in a gel dyer.

4. Recording of radioactive signals

Dried polyacrylamide gel was stacked with an X-ray film (BioMax MR-1 film, Kodak®) and was exposed for 1 hour in darkness. This experiment suggested that the 1 hour treatment by 50 µM CHX inhibited the protein synthesis completely.

2.3.8 Phototropic Analysis

Seeds of *Arabidopsis* plant lines were sterilized and planted as described above (see the Chapter 2.1.1). Because the seedlings of mutant *eir1-4* and *pin3-3* lost both gravitropism and phototropism, the seeds were put on the plates in two paralleled lines. White fluorescent light was filtered by blue foils to create parallel side illumination with an intensity of 2 $\mu mol \cdot m^{-2} \cdot s^{-1}$ (methods to create and measure the adjustable blue light source are described in section 2.3.2). This blue light intensity was sufficient to activate the PHOT1 kinase but not the PHOT2.

In the case of *proPHOT1::PHOT1::GFP* transformed seedlings, they were cultured under dark condition for 3 days before side illumination with 2 $\mu mol \cdot m^{-2} \cdot s^{-1}$ blue light. After 6 and 12 hours illumination, pictures were taken with a digital camera

Kodak Z710, only contrast and brightness of pictures were modified as required to see the images clearly. The separation angles between the position of the root or shoot tip and the vertical position were measured by the software ImageJ (NIH, USA).

3 Results

3.1 Subcellular Localization of Phototropin 1::GFP in Etiolated Seedlings of *Arabidopsis thaliana*

PHOT1 is expressed in different tissues of 4-days old dark-grown *Arabidopsis* seedlings. Because PHOT1 is a photoreceptor which mediates various responses to BL such as chloroplast movements, opening of stomata, spread of hypocotyls and phototropism, the description of its distribution could give clues as to understand the physiological processes behind these responses.

3.1.1 Phototropic Analysis of *proPHOT1::PHOT1::GFP* Tansformed Seedlings

Before attempting to relate blue-light-induced changes in PHOT1::GFP to any physiological responses in wild-type plants, it was necessary to determine the relative physiological sensitivity of the transgenic seedlings to BL compared to wild-type seedlings. Therefore, both the wild-type (Col 0) seedlings and the *phot1-5* seedlings expressing the PHOT1::GFP gene driven by the PHOT1 promoter were exposed to 2 $\mu mol \cdot m^{-2} \cdot s^{-1}$ unilateral BL for different periods of time to obtain a time course for the development of curvature in each case. The results are shown in Table 2.

Table 2. Complementation of phototropism in etiolated *Arabidopsis* hypocotyls by PHOT1::GFP.

Exposure time (hours)	*proPHOT1::PHOT1::GFP*	*Wild-Type*
6	19.0 ± 1.5	40.8 ± 3.7
24	49.7 ± 4.5	74.1 ± 4.1

3.1.2 Cellular and Subcellular Localizations of PHOT1::GFP in Etiolated Seedlings

PHOT1::GFP distribution was examined in whole 4-days old dark-grown seedlings by fluorescence microscopy. At low magnifications, the strongest signals were found in the hook and the elongation regions of the hypocotyl, and across the abaxial faces of the cotyledons (Fig. 10A, cotyledon abaxial face view; Fig. 11, cotyledon edge view). The fluorescence signal declined concomitantly with elongation of the hypocotyl and expansion of the cotyledons. Whether this decline is simply the consequence of dilution through cell enlargement or a reduction in gene expression is not resolved in this study. Surprisingly, a strong signal arose from the shoot–root transition region (Figs. 10A and B). This strong signal could arise because the cells are not elongating and diluting the signal, or because PHOT1::GFP expression is higher in these cells, or both. Fluorescence declined sharply below this region, but became considerably stronger in the more apical tissues of the root. The average brightness of GFP signal detected in different tissues of 10 of 4 days old seedlings

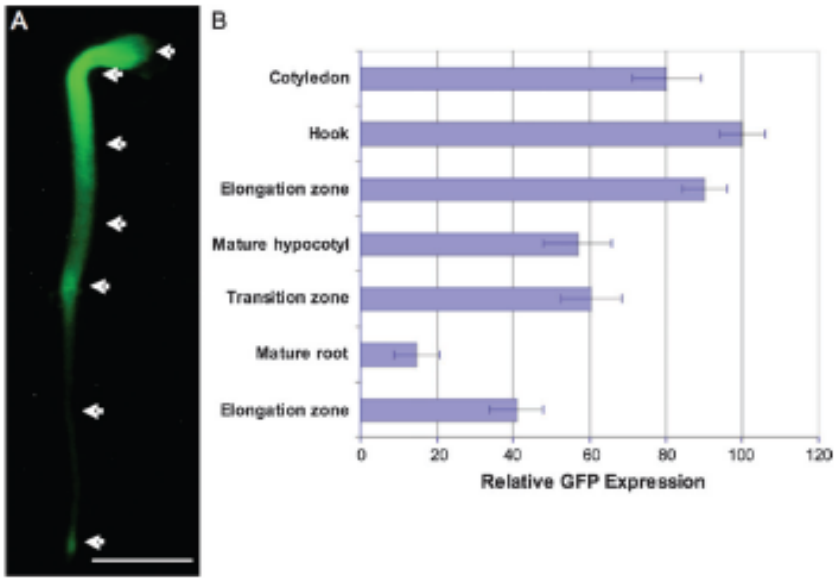

Figure 10. PHOT1::GFP expression in dark-grown *Arabidopsis* seedlings.

(A) PHOT 1::GFP expression in a 4 days old *Arabidopsis* seedling. Image taken with a binocular low-power fluorescence microscope (Bar = 1 mm).

(B) Quantification of the intensities of the PHOT1::GFP fluorescence was obtained with ImageJ software. Arbitrary units, value for highest reading (hook) set to 100. White arrows in Figure 1A indicate where measurements were taken. Values in Figure 10 B were averaged from 10 seedlings. For details, see Materials and Methods. Error bars indicate standard error of the mean.

was measured and the results are shown in Fig. 10B. Table 3 shows the expression level of PHOT1::GFP in different cell layers of different tissues. Detailed descriptions of the subcellular expressions and localizations are shown in the Figs. 11 – 18.

Table 3. Expression level of PHOT1::GFP in various tissues of etiolated *Arabidopsis* seedlings.

	Epidermis	**Cortex**	**Stele**
Cotyledon	moderate	moderate	N/A
Apical hook	moderate	strong	moderate
Mature hypocotyl	weak	moderate	moderate
Transition area	weak	strong	weak
Mature root	none	moderate	weak
Root elongation zone	weak	moderate	Moderate
Root cap	none	N/A	N/A

3.1.3 Distribution in the Cotyledons.

At higher magnification, confocal images resolved major differences in the tissue and cellular distribution of PHOT1::GFP in various tissues and organs. The strong signals seen from the cotyledons in the Fig.11 arise both from the epidermis on the abaxial face and the adjacent underlying mesophyll cells. It is almost undetectable from the adaxial tissues. As shown in the Fig. 12A, the signal from the epidermis at the margin of the cotyledon is extremely weak (arrows). However, the fluorescence from the underlying cell layers is far stronger, particularly on certain walls at right angles to the cotyledon surface (Fig. 12A). These walls are likely the ones most recently laid down during cell division that precedes cotyledon expansion. They are much more common near the cotyledon margin where the marginal meristem was located than toward the center.

The epidermal cells on the abaxial face of the cotyledon are heavily fluorescent (Figs. 12A and 12B). However, the signal appears enriched at the anticlinal walls and weaker or undetectable from the inner and outer periclinal walls (Figs. 12 A, B and D). Using the re-slice option of ImageJ from z-series scanning data, it is possible to reconstruct transverse images from composite longitudinal images for the Figs. 12C, 12D (see below). Guard cells from 4 days old seedlings as visualized in median

transverse section (Fig. 12C) shows signal predominantly on their anticlinal walls. These anticlinal walls lies at different angles with respect to the vertical walls, this fact suggests that the intensity of these fluorescence in not an artefact from the optical axis of scanning. Individual epidermal cells thus resemble imaginative cookie cutters (Figs. 12A and 12B). There was weak fluorescence at the walls of the mesophyll cells facing the epidermis (Figs. 12A and 12B). In 4 days old seedlings, the anticlinal walls of both guard cells show PHOT1::GFP (Fig. 12B). However, in seedlings 3 days old, incipient guard cells appears as dark circles with weak fluorescence apparent only around the periphery (Fig. 12E, arrow, cf. Fig. 12B, arrows). Thus, PHOT1::GFP expression is delayed in guard cells compared with its expression in adjacent epidermal cells.

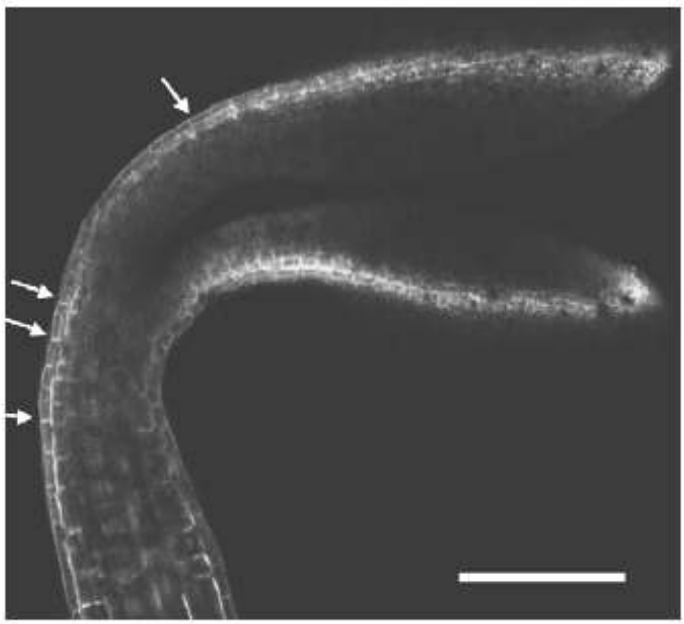

Figure 11. Single confocal optical section showing PHOT1::GFP localization in the cotyledon and apical hook region.

PHOT 1::GFP is preferentially localized at the epidermal anticlinal walls through the hook to the base of the cotyledon (arrows). The underlying adjacent cortical cells along the hook also show strong fluorescence at their outer periclinal walls adjacent to the epidermis and at their anticlinal walls, with little signal at their inner periclinal walls. Thus, each cell forms a 'C' shape. Only the abaxial cell layers of the cotyledon show strong PHOT1::GFP expression (Bar=100 μm).

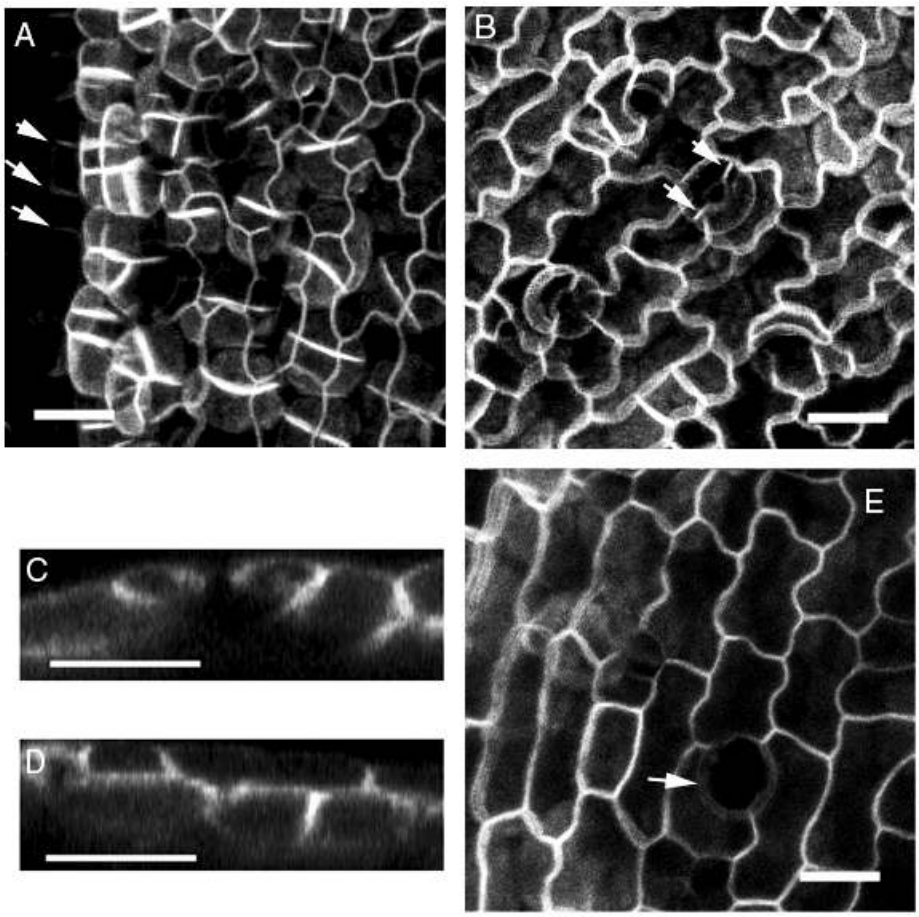

Figure 12. Distribution of PHOT1::GFP in the cotyledons of 4days old seedlings.

(A) and (B): Projection of the abaxial face of a cotyledon near the cotyledon margin of etiolated seedlings. The image was constructed from a z-series of optical sections of the surface of the cotyledon to a depth of 30 µm. (A): Epidermal cells at the left margin show only very weak PHOT1::GFP fluorescence, localized largely to the anticlinal walls in a polar fashion (long arrows). The epidermal anticlinal walls are uniformly labeled and there is almost no detectable signal from the outer or inner periclinal walls. Note the especially strong signal from cell plate-like structures in the center of the mesophyll cells. (B): The oblique angle of observation shows the strong signal on the anticlinal walls of the epidermal cells and the lack of signal at inner or outer walls. The signal is fairly weak in underlying mesophyll cells except for an occasional strongly fluorescent cell plate-like structure. Note PHOT1::GFP fluorescence from the two pairs of guard cells where they meet (arrows). (C) and (D): Computer-reconstructed cross-sectional image of guard cells of etiolated seedlings. Images were produced with ImageJ software by vertically slicing the original z-series dataset. C: Cross-section of epidermis of 4 days old seedling showing guard cells (top center of image). PHOT1::GFP fluorescence is strongest at the anticlinal walls of the guard cells. Note that the adjacent epidermal cell to the right lacks fluorescence along its inner periclinal wall. D: Cross-section of epidermis and first layer of cortical cells. PHOT1::GFP fluorescence is detectable only on the anticlinal walls of the epidermal cells, the anticlinal walls of the underlying cortical cells, and the common walls between them. E: Projection of abaxial face of cotyledon of 3 d old light-grown seedling. Image was constructed from a z-series of images of the surface of the cotyledon to a depth of 30 µm. Note lack of PHOT1::GFP expression at the inner walls in the guard cells (arrow). (Bars = 20 µm).

Another interesting discovery was the localization of PHOT1 on the membrane surface of chloroplasts. When the seedlings were grown under white light illumination in order to allow maturation of chloroplasts, the green fluorescence came only from the surface of chloroplasts facing outwards (Fig.13), therefore only partly overlapping with the red autofluorescence from chloroplast, whose emission wave length of autofluorescence is at red region of spectrum (Bolte et al., 2004). From the top view of projections, images are rebuilt from z-series scanning pictures (Fig. 13A), the two fluorescence signals are mostly colocalized together, but the green fluorescence signals is slightly shifted from the red signals (arrows). Observing this region at higher magnification by step scanning pictures, surfaces of chloroplasts show colocalization with the PHOT1::GFP signals, but lost the colocalization in images derived from optical section taken 2 µm deeper into the cell (Fig. 13B, arrow heads).

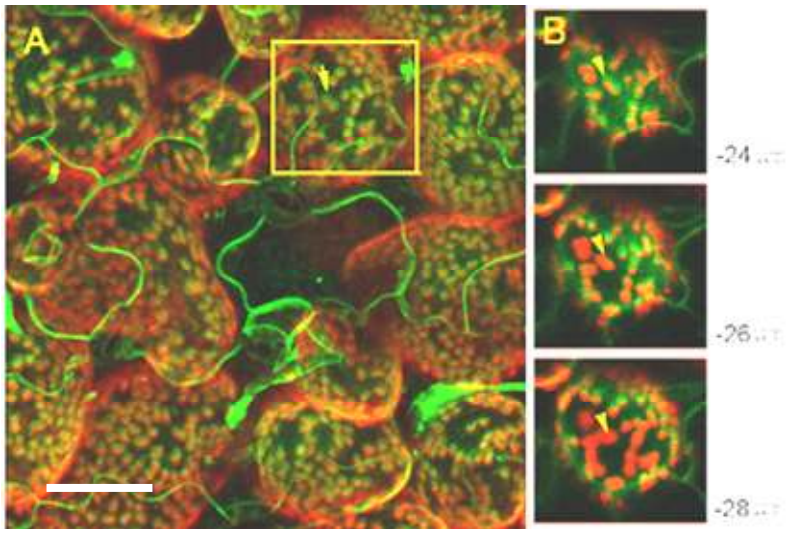

Figure 13. Localization of PHOT1 on surface of chloroplasts in mesophyll cells.

A: Projections reconstructed from series of images from surface of leaves to 60 µm deep inside. B: Single images chosen from this z-series image sequence. Upper: 24 µm, middle: 26µm, down: 28 µm from leave surface. (Bar = 20 µm)

3.1.4 Distribution in the Hook

Epidermal cells in the apical hook region show lower expression than the underlying cortical cells (Figs. 14A and 14B). The epidermal cells on the margins of the image show that as with the epidermal cells of the cotyledons, there is weaker signal at the outer periclinal walls (Fig. 14A, arrows). In longitudinal section, it appears that it is the end walls of cortical cells and the wall adjacent to the epidermal

cells that are most heavily labelled (Fig. 14B, thick arrows). This distribution forms a ‘C’ in longitudinal section with the open side facing inward. The heavy signal marks the contact between the outer periclinal wall of the cortical cell and the inner periclinal wall of the adjacent epidermal cell arose exclusively from the cortical cells (Fig. 14B, dashed arrows). Some PHOT1::GFP fluorescence also marks the deeper cells, likely pith and developing vascular tissue (Figs. 14A and 14B). Because of light scattering, the resolution is insufficient to provide more structural detail. Note that the end walls of these inner cells were generally more heavily labelled than the side walls (Fig. 14B)—a polarity of PHOT1 distribution that occurs to varying degrees throughout the seedling.

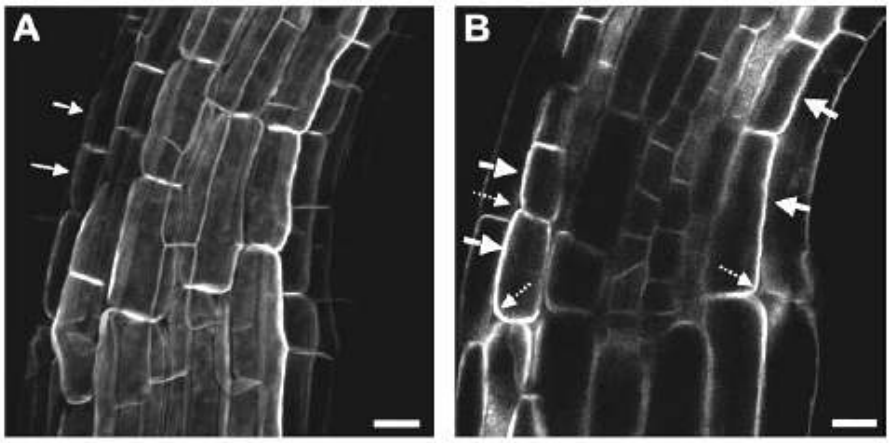

Figure 14. Localization of PHOT1::GFP in the apical hook region.

(A) Projection of optical sections from the surface of the hook to a depth of 50 μm. Note smooth labeling of surfaces of underlying cortical cells, polar distribution of signal in both epidermal and cortical cells, with strong fluorescence arising from the region of contact between cortical and epidermal cells. Outermost epidermal walls weakly labeled (thin arrows).

(B) Single image chosen from z-series images. Note ‘C’-like pattern of cortical cells (thick arrows). Prevascular tissue is marked weakly, and also shows somewhat polar distribution of PHOT1::GFP fluorescence. Where there is clear physical separation of cortical cells from epidermal cells, it is obvious that the strong signal at the common faces arises from the cortical cells and not the epidermal cells (B, dashed arrows) (Bar = 20 μm).

3.1.5 Changes from Hook to Root-Shoot Transition Region as Visualized in Cross-Section

Transverse images were reconstructed from stacks of longitudinal images in Figs. 15 (1–4), illustrating the distribution of PHOT1::GFP in sections through the hook (1), elongation zone (2), mature zone (3), and the shoot–root transition region (4). The pattern of strong fluorescence at the anticlinal walls of the epidermal cells, noted above for the cotyledon epidermis, persists down the hypocotyl axis. In the hook, the first layer of cortical cells beneath the epidermis also showed the 'C'-shaped pattern with the opening facing inwards, just as was the case in longitudinal section (Fig. 15-1). Further down in the elongation zone, all of the longitudinal walls of the first row of cortical cells below the epidermis are labelled and the next layer inwards show the inward-facing 'C'-shaped distribution of signal (Fig. 15-2). The pattern of labelling in the shoot at the transition zone is similar to the pattern seen in the elongation zone (Fig. 15-4). Unlike to the "C" shape of Fig. 14B and Fig. 15-1, this kind of C-shaped pattern could be artefact, because the superimposition of the laser scanning may create the strong signals from parallel cell borders. But the differences of cellular localization of PHOT1::GFP are presented here clearly.

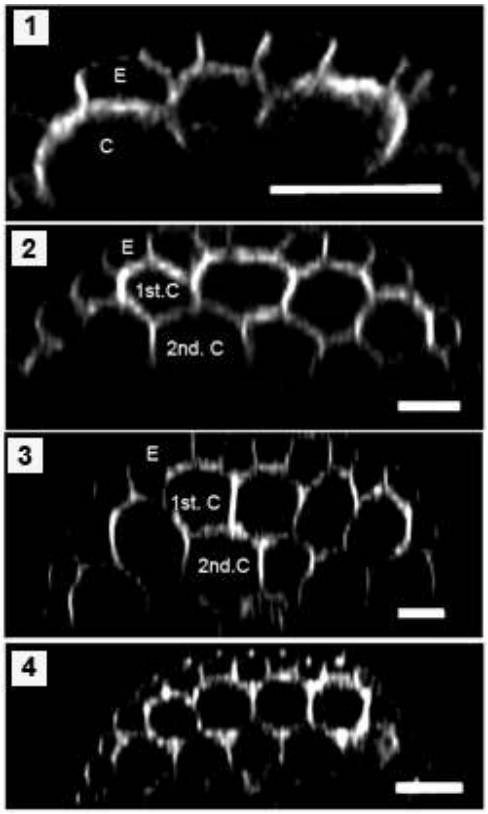

Figure 15. Computer-reconstructed cross-sectional images of hypocotyl cortex and epidermis.
These images were produced with ImageJ software by vertically re-slicing the original z-series data set.
1: Hook region. Note absence of PHOT1::GFP at inner periclinal walls of cortical cells (C), outer periclinal walls of epidermal cells (E), strong signal on outer periclinal and anticlinal walls of cortical cells (C).
2: Elongation region. Note continued absence of signal at outer periclinal walls of epidermal cells (E); first underlying layer of cortical cells (1st C) with stronger signal on anticlinal than periclinal walls; and labeling of anticlinal walls of next cortical layer in (2nd C).
3: Mature hypocotyl. The outer periclinal walls of epidermal cells show a trace of signal and both outer and inner cortical cells show strongest signal on anticlinal walls.
4: Shoot side of the shoot/root transition region. Outer periclinal walls of epidermal cells lacks signals either. The signals from the first layer of cortex are relative fairly and uniformly distributed (Bar = 50 µm).

3.1.6 Distribution of PHOT1 in Elongating and Mature Hypocotyl Tissues

In both the hypocotyl elongation and maturation zones, as in the hook, the epidermal signal is considerably weaker than that in the cortical cells (Figs. 16A and B). The pattern of heavy signal seen at the outer periclinal wall and the anticlinal walls of the cortical cells adjacent to the epidermis of the hook, forming a 'C' in longitudinal section, is not as distinct in the elongation zone, although the 'C' shape is still evident (Fig. 16A, arrows). In the elongating and mature regions, the cortical cells had moderate signal on all faces (Fig. 16B). A tendency toward bipolar distribution of the signal remains there. A strong polarity appears in cortical cells, epidermal cells, and in the stele cells. As in the hook, some GFP fluorescence is present in the inner tissues (Fig. 16B). These inner cells, possibly vascular parenchyma, show a tendency toward polar distribution of signal (Fig. 16B, arrows).

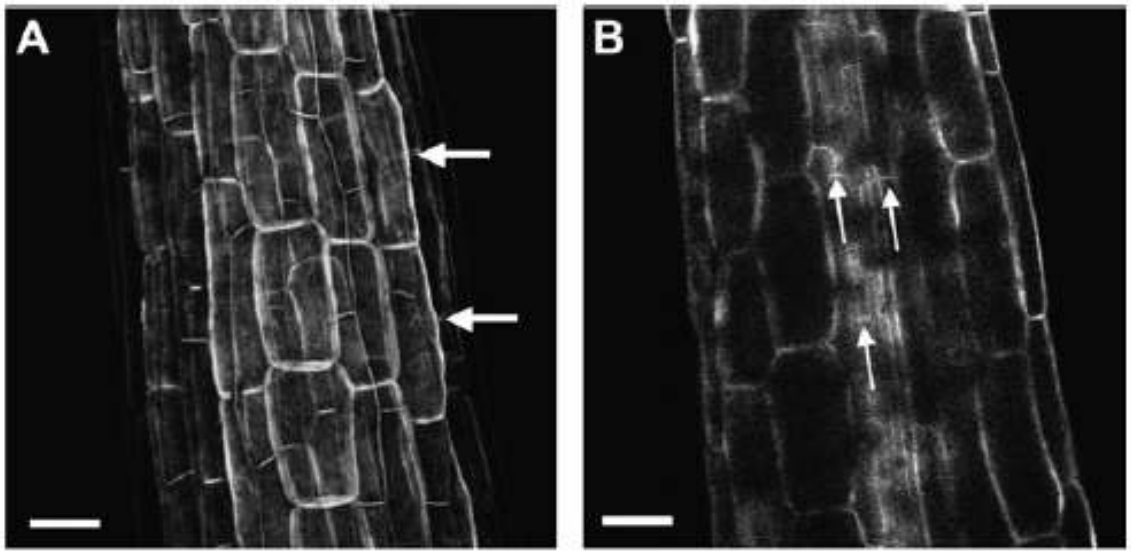

Figure 16. Localization of PHOT1::GFP in the elongation zone.

A: Projection of optical sections from the surface of the hook to a depth of 80 µm. Epidermal cells (weaker signal) show uniform distribution on their anticlinal and outer periclinal walls; cortical cells (stronger signal) show more uniform labeling, i.e., less polar distribution on all of their walls than in the hook region. Hence, the 'C' pattern of signal distribution is weaker than in the hook (arrows).

B: Single image chosen from the z-series of Fig. 16A. Epidermal cells are uniformly labeled and the inner periclinal walls of the outer cortical cells are now also labeled so that the 'C' pattern is weaker (arrows). The developing vascular strand (center) shows fairly heavy signal with a suggestion of stronger fluorescence at the end walls. (Bar=20µm)

3.1.7 Distribution at the Shoot–Root Transition Zone

As noted above, there is strong expression of green fluorescence detectable in the shoot–root transition zone (Fig. 10A). Whether the strong signals reflect a real increase in *PHOT1::GFP* expression in this region or simply appear, because these cells have not elongated as much as their counterparts above them, or both, is an open question. Both cortical and epidermal cells on the shoot side show the same pattern of fluorescence as the hypocotyl cells above them—- weaker in the epidermis than in the cortex, with only slight polarity in both cases (Figs. 17A and B). The transition from shoot to root is marked by a dramatic and abrupt overall decrease in signal. Note that GFP fluorescence is completely absent from the root epidermal cells. The elongated root cortical cells show only very weak signal, largely concentrated at their end walls in a highly polar fashion (Fig. 17, arrows).

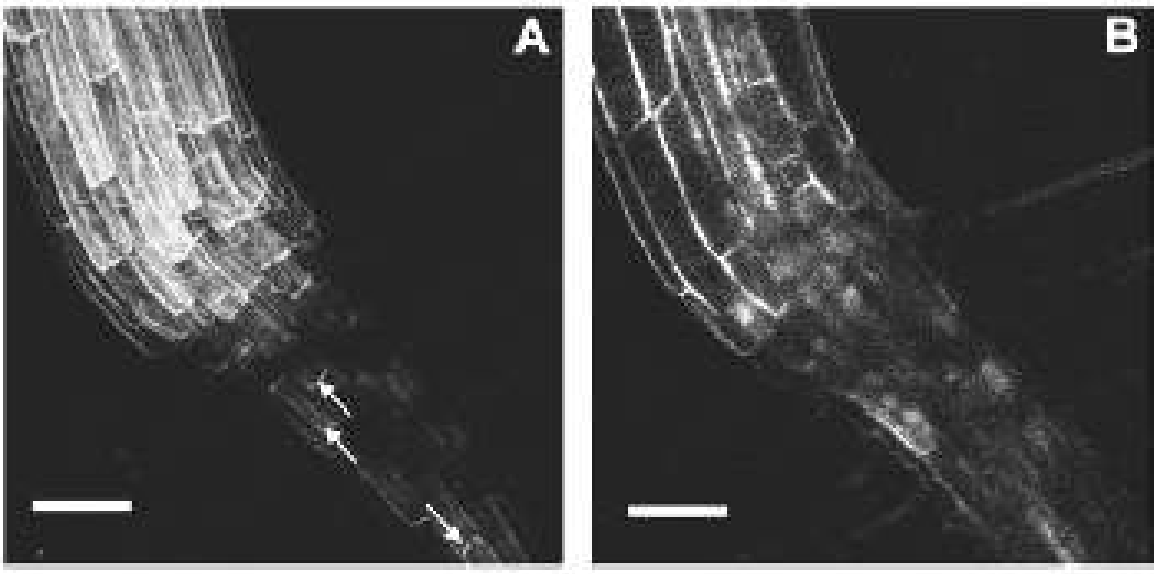

Figure 17. Localization of PHOT1::GFP at the shoot–root transition zone.

A: Projection of optical sections from the surface of the hook to a depth of 100 µm. Cortical (strong fluorescence) and epidermal (weak fluorescence) cells on the shoot side are relatively uniformly labeled on all walls. Cortical cells on the root side, by contrast, show sharp polar distribution (arrows).

B: Single median image from z-series showing somewhat polar PHOT1::GFP distribution in vascular strand in addition to that in cortical cells. Note complete absence of PHOT1::GFP expression in the root epidermis (Bar = 100 µm).

3.1.8 Distribution of PHOT1::GFP in Mature and Elongating Root Tissues

The expression pattern of PHOT1::GFP in root tissues is different from the pattern in the shoot region. The epidermal cells of roots of 4 days old etiolated seedlings lack any detectable expression of PHOT1::GFP. The absence of PHOT1::GFP in the root epidermis is even more dramatically illustrated in images of roots stained with the red-fluorescing membrane marker FM4-64 (Fig. 18A–D). Not surprisingly, root hairs, of epidermal origin, also fail to express PHOT1::GFP (Fig.18B, arrows). The root cortical cells show polar distribution of PHOT1::GFP through the mature zone and into the elongation zone (Fig. 18B). The central stele is also labelled as indicated by the diffuse fluorescence seen in all four images in Fig. 18. Again, technical limitations (e.g. light scattering and self-shading) prevented resolving individual cell types. The elongating cortical cells closer to the root tip also show a strong bipolar distribution of signal (Figs. 18B–D). Along the whole plant bodies, all the cortical and central stele tissues have expression of PHOT1::GFP, which show strong polar localization in cells.

3.1.9 Subcellular Distribution of PHOT1::GFP in the Root Apex

As shown in the Fig. 18C, there is relatively strong signal in the elongating region basal to the root cap. In the more mature region of the root tip, the most intense fluorescence arises from the stele (Fig. 18B). The red fluorescence from the membrane stain FM4-64 clearly defines the epidermis in the Figs. 18B–D, verifying a lack of detectable GFP signal from these cells. As shown in the Fig. 18D, signal is also undetectable within either the root cap or root apical meristem in these 4 days old seedlings. Signal first appears in cells destined to become cortex and endodermis, and only appears more basally in the inner prospective stelar tissues (Figs. 18C and D). In parallel with the absence of signal at any face of the epidermal cells, there is only a trace of signal at the outer periclinal walls of the cortical cells. However, their inner periclinal walls adjacent to incipient endodermal cells share strong signal with the adjacent endodermal cells and their anticlinal walls are also strongly labelled, giving them once again the appearance of a ‘C-form’, but this time with the open side facing outwards (Figs. 18C and D). The smaller endodermal cells also show a ‘C’-shaped pattern, sharing heavy signal with the cortical cells and additional signal

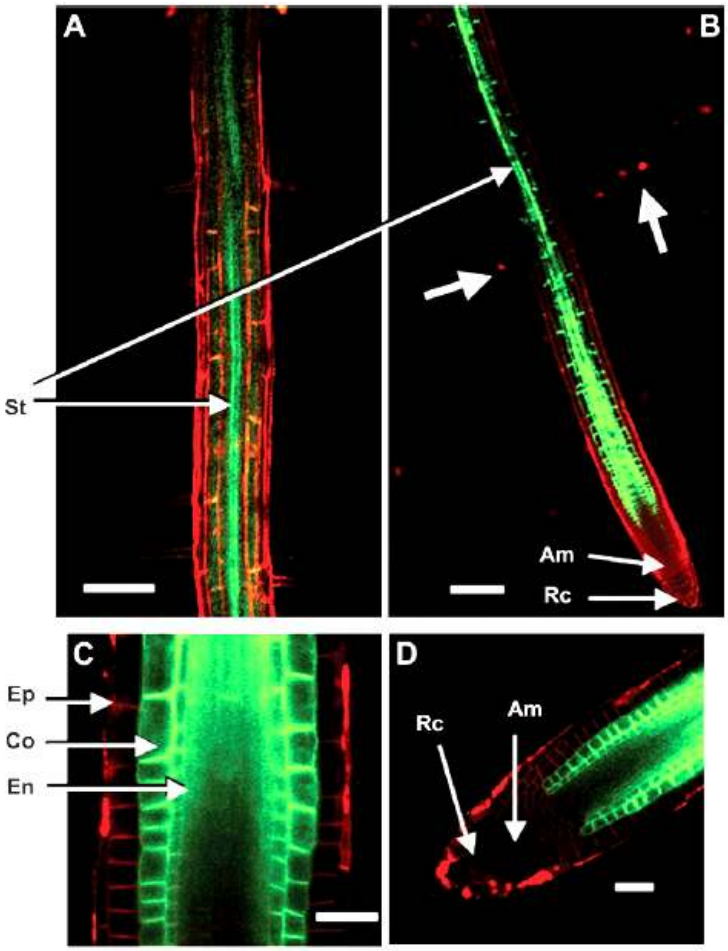

Figure 18. Distribution of PHOT1::GFP in roots of 4 days old etiolated seedlings.

A: Single low-magnification confocal section of mature root-hair zone. Note heavy expression of PHOT1::GFP along stele and polar distribution of signal in cortical cells, indicated by co-localization of PHOT1::GFP (green) and FM4-64 (red) resulting in a yellow color. Root hairs labeled only with FM4-64 are faintly visible (thick arrows). Am, apical meristem; Co, cortex; En, endodermis; Rc, root cap; St, stele (Bar = 100 µm).

B: Single low-magnification confocal section of root apex. Note heavy PHOT1::GFP expression in prevascular tissue and cortex, persisting in vascular region and showing distinct polar distribution in cortical cells. Epidermis shows signal only from FM4-64 and not from PHOT1::GFP (Bar=100 µm).

C: Single high-magnification confocal section of the root apex elongation zone. Note lack of the PHOT1::GFP signal in epidermal cells (FM4-64 red fluorescence only). Cortical cells heavily labeled at periclinal walls, only slightly labeled on the side toward the epidermis. Endodermal cells heavily labeled on the anticlinal walls, slightly labeled on the inner periclinal walls adjacent to stele. Whether heavy signal between endodermal and cortical cells arises from cortical or endodermal cells or both could not be resolved (Bar = 20 µm).

D: Single high-magnification confocal section of the extreme root tip. Labeling of cortex and endodermis precedes labeling of the prospective stelar tissue. Note the complete absence of any detectable PHOT1::GFP fluorescence from the root cap and apical meristem. The first detectable fluorescence appears in elongating cortical and endodermal cells (Bar = 20 µm).

at their anticlinal walls. There is only weak signal at their inner periclinal walls adjacent to the prestelar tissue. Hence, the opening of their ‘C’ faces is located inwards. At this time, it has not been possible to determine, whether the signal along the common walls between cortex and endodermis is of endodermal or cortical origin, or both.

3.2 BL-Induced Vesicular Re-localization of PHOT1::GFP Molecules

It has already been reported that BL illumination induces relocalization of PHOT1::GFP from the PM into the cytoplasm (Sakamoto and Briggs, 2002, Knieb et al., 2004). But the mechanisms and the pathways of this localization are still poorly understood. Here, the phenomenon is investigated at high resolution in a range of cell types in cotyledons, hypocotyls, and roots. I have also investigated the minimum requirement to induce re-localization and the onset of relocalization as a function of total blue-light fluence rate. Preliminary experiments showed that neither red nor green light induced any re-localization.

3.2.1 Hypocotyl Cells

The blue-light-induced changes in PHOT1::GFP localization appear as dramatic reorganization at the cell cortex and the fluorescence signal in the cytoplasm is clearly detected internal to the cell wall. Figures 19A – C show changes occurring at the cell membrane of several cortical cells in the hypocotyl elongation zone during their exposure to the BL from the scanning laser (25 $\mu mol \cdot m^{-2} \cdot s^{-1}$). At time zero, PHOT1::GFP is smoothly distributed over the entire cell surface. The line down the middle represents the wall of an unlabelled epidermal cell overlying the cortical cell (Fig. 19A). After 10 min of continuous BL treatment from the confocal microscope scanning laser, the uniformity once seen at the cell surface is drastically altered and the signal take on a mottled distribution with distinct dark areas outlined by more intense signal (Fig. 19B, arrows) and punctuate structures become evident. After 60 min, the mottling increases and more punctuate structures and dark circles are clearly visible (Fig.19C).

These dramatic changes are accompanied by detection of PHOT1::GFP in the cytoplasm. Figures 19D–F show a single section through the outermost cell layers (epidermis and cortex) from the elongating region of the hypocotyl. Again, the blue-light source was the confocal-microscope laser. Already, after 5 min of scanning with BL, what appear to be strands and blebs of PHOT1::GFP fluorescence are visible in the cytoplasm in both epidermal and outer and inner cortical cells (Fig. 19E, arrows). At 10 min, further changes in the intracellular distribution of signal in the two cell types are visible (Fig.19F).

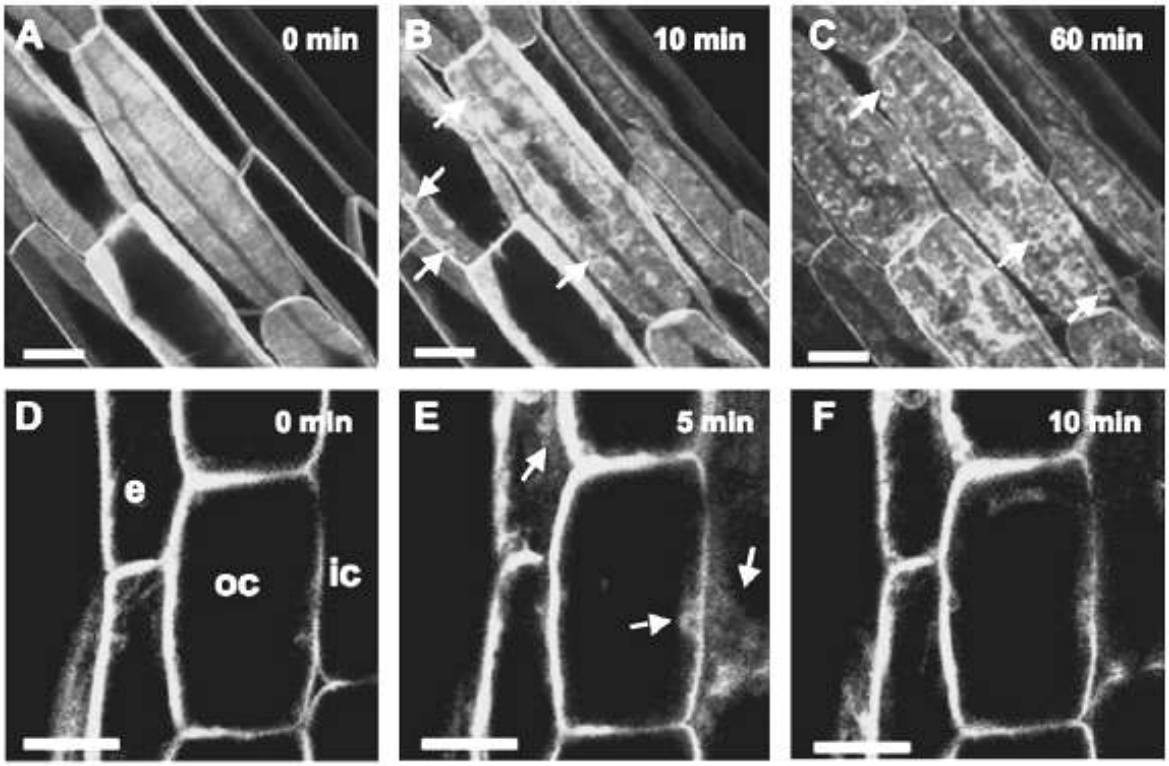

Figure 19. Blue-Light-induced changes in PHOT1::GFP distribution in cortical cells.

Changes in PHOT1::GFP distribution in cortical cells from the elongation region of the hypocotyl with time of blue-light treatment.

A–C: Image projection showing changes on the plasma membrane at the outer periclinal cell wall of a cortical cell during blue light treatment. The line down the center cell of A is likely the contact area to a neighboring cell out of the scanned field of depth. Arrows indicate circular areas devoid of signal.

D–F: Single images through cortical cells in the same region showing movement of PHOT1::GFP fluorescence into the cytoplasm. e, epidermis; oc, outer cortex; ic, inner cortex. Arrows indicate PHOT1::GFP in cytoplasm. Blue-light source: scanning laser (25 $\mu mol \cdot m^{-2} \cdot s^{-1}$). (Bar = 20µm)

Induction of these distributional changes of PHOT1::GFP is very sensitive to BL. The transgenic seedlings were exposed to three different intensities of BL for 10 min prior to observation in the confocal microscope immediately thereafter. A total fluence rate 3 of 300 $\mu mol \cdot m^{-2}$ was insufficient to induce any detectable change within that time period (Fig. 20A). However, 600 $\mu mol \cdot m^{-2}$ was sufficient to induce major changes in PHOT1::GFP distribution (Fig. 20B, arrows) and 3,000 $\mu mol \cdot m^{-2}$ likewise induced dramatic changes (Fig. 20C, arrows). Figure 14A provides a suitable dark control.

When seedlings were exposed to BL for 30 min (10 $\mu mol \cdot m^{-2} \cdot s^{-1}$) and then left in darkness for 1 h, there was still major reorganization of PHOT1::GFP in cortical cells in the hook region (Fig. 21A). Empty areas and small punctate structures are clearly

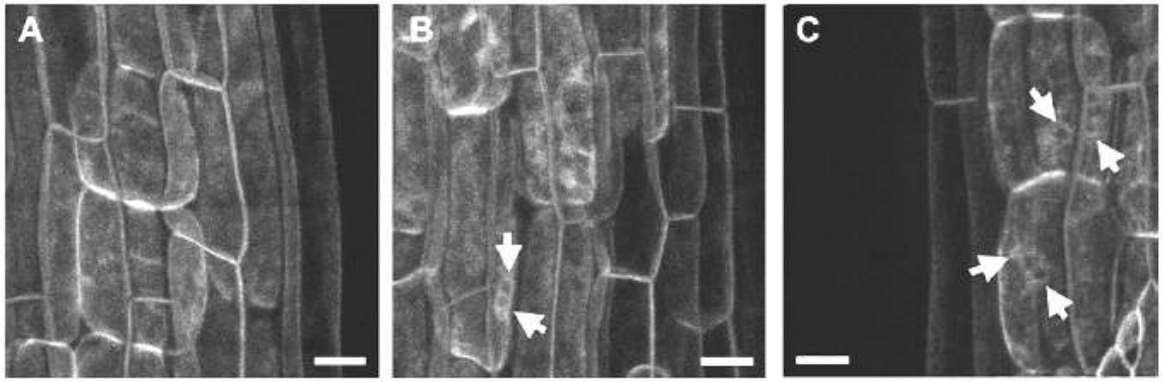

Figure 20. Sensitivity of PHOT1::GFP re-localization in hypocotyl cortical cells to blue light.

Top view of etiolated seedlings exposed to blue light for 10 min at 0.5 (A), 1 (B), or 5 (C) $\mu mol \cdot m^{-2} \cdot s^{-1}$ (total fluences 300, 600, and 3000 $\mu mol \cdot m^{-2}$, respectively). Projection images were reconstructed from z-series until 60 µm deep from surface by software. The line down the center cell of A is likely the contact area to a neighboring cell out of the scanned field of depth. Note circular areas devoid of signal in B and C (arrows). Blue-light source, halogen lamp plus blue filter (Bar = 20 µm).

evident in this image (arrows). However, after 2 hours of darkness (Fig. 21B), the signal assumed a more uniform distribution in several cells (thin arrows), although a few punctate structures and empty areas (thick arrows) persisted.

The time of onset of the re-localization process is a function of the total photon fluence of the initial blue-light stimulus (Fig. 22). Dark-grown seedlings were given total photon fluences ranging from 100 to 10,000 $\mu mol \cdot m^{-2}$, all given over a period of 100 s. A new seedling selected from each treatment was examined every 5 min in the confocal microscope to detect the first evidence for re-localization. When the total photon fluence was only 100 $\mu mol \cdot m^{-2}$, no significant response had occurred after 100 min (Fig. 22A). At 10 times the fluence, re-localization was first detectable after 45 min (Fig. 22B, arrow); at 20 times the fluence, after 20 min (Fig. 22C, arrow); and after 100 times the fluence, after 5 min (Fig. 22D, arrow). Hence, the greater the initial fluence was, the earlier the onset of the reorganization. The time of onset decreased approximately with the log of fluence, suggesting that the response was the consequence of a first-order photoreaction.

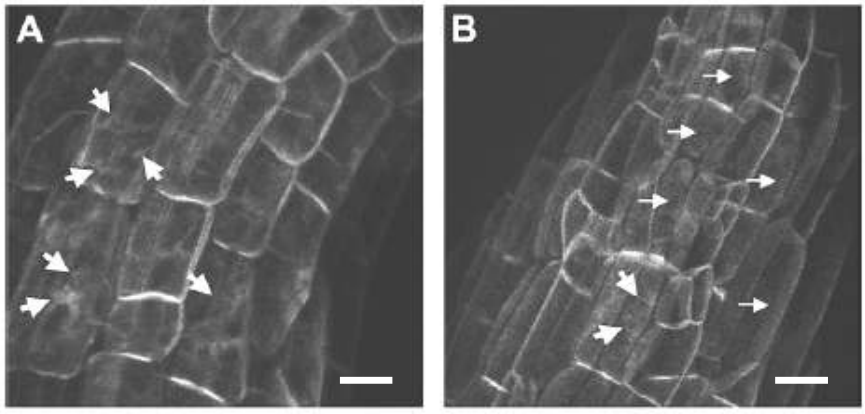

Figure 21. Disappearance of PHOT1::GFP from cytoplasm of hypocotyl cortical cells with time in the dark.

Brightest point projections. Etiolated seedlings were exposed to blue light (10 $\mu mol \cdot m^{-2} \cdot s^{-1}$) for 30 min before being returned to darkness.

A: Appearance after 1 h darkness. Some mottling and dark circular areas (arrows) still visible.

B: Appearance after 2 h. Signal at many cell surfaces mostly smooth (thin arrows), although a few empty circular areas persist (thick arrows). Blue-light source, halogen lamp plus blue filter (Bar=20 µm).

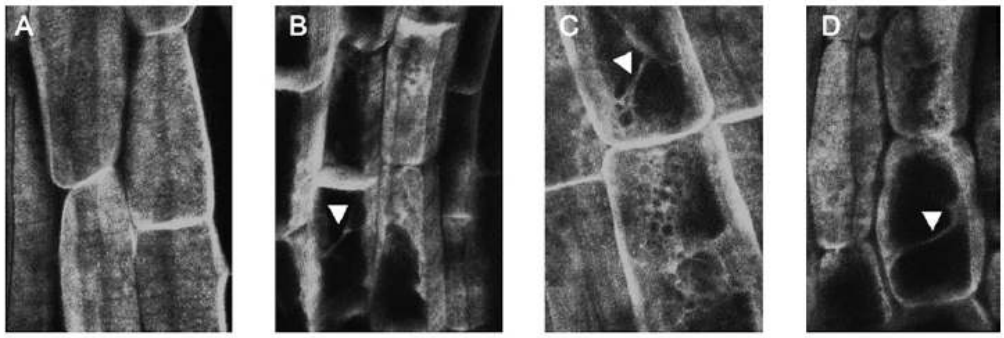

Total Fluence ($\mu mol\ m^{-2}$)	100	1000	2000	10000
Intensity ($\mu mol\ m^{-2}\ s^{-1}$)	1	10	20	100
Time in light (seconds)	100	100	100	100
Time in dark (minutes)	100	45	20	5

Figure 22. Blue-Light-Induced re-localization of PHOT1::GFP in hypocotyl cortical cells is sensitive to total photon fluence: (A) 100, (B) 1,000, (C) 2,000, (D) 10,000 $\mu mol\ m^{-2}$.

Time in dark refers to time in darkness between blue-light pulse and observation in the confocal microscope. Brightest point projections. Etiolated seedlings were exposed to blue light of various intensities for 100 s then returned to darkness. At 5-min intervals, hypocotyl cortical cells were examined in the confocal microscope for evidence of PHOT1::GFP re-localization (arrows).

3.2.2 Cotyledon Cells

Blue-light-activated PHOT1::GFP re-localization is also found in both the epidermal and mesophyll cells of the cotyledon. The Fig. 23 shows images of the surface near the cotyledon margin in single optical sections (A–C). As early as 6 min after the beginning of scanning (25 $\mu mol \cdot m^{-2} \cdot s^{-1}$), changes are visible in both cell types. The surfaces of the underlying mesophyll cells show the beginning of some mottling and there are small particulate structures within the epidermal cells (Fig.23B). After 12 min of scanning, there is further release of PHOT1::GFP signal into the cytoplasm of the epidermal cells (Fig. 23C) and the mottling on the upper surface of the mesophyll cells had increased.

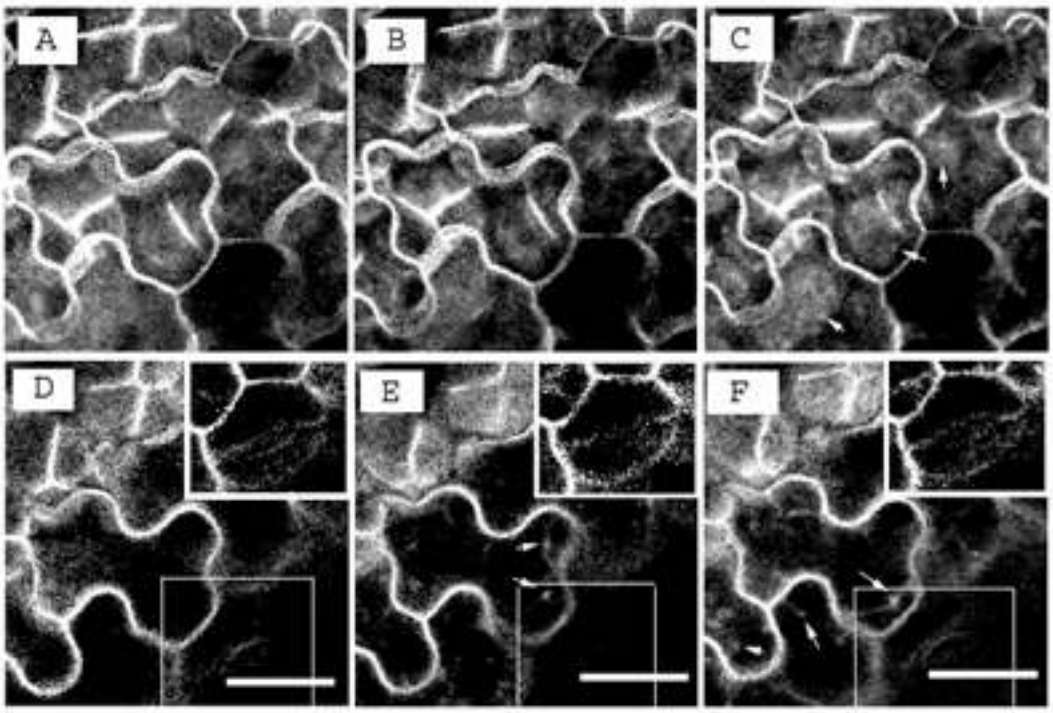

Figure 23. Blue-light-induced re-localization of PHOT1::GFP in cotyledon epidermal and mesophyll cells.

(A–C) Projective view of mesophyll cells and epidermal cells. Images were reconstructed from series of single optical sections scanning through 40μm depth under the epidermal surface. (D-F) Single optical sections through epidermal cells, chosen from same z-series. Three time points of illumination by the laser during scanning were chosen as: (A, D) zero time; (B, E) 6 min of scanning; (C, F) 12 min of scanning. These images show appearance of signal in the cytoplasm of epidermal cells with time (arrows in E, F), also the stimulation of GFP signals on the mesophyll PM as punctate structures (arrows in C). Blue light source was the laser light, which illuminated the specimens during confocal microscopic observation. In the inserts, two pairs of guard cells are shown to demonstrate that in guard cells PHOT1 did not relocate (Bar = 20 μm).

Examination of guard cells on the cotyledons of 4 days old etiolated seedlings shows that they are unique among the cell types examined in that they did not undergo a similar re-localization of PHOT1::GFP following blue-light treatment (Fig. 23 D-E). It might be that these guard cells were not fully functional at this stage of development. Alternatively, light-activated release of PHOT1::GFP into the cytoplasm simply may not occur in this cell type.

3.2.3 Root Cortical Cells

Because the PHOT1::GFP signal is weaker in the root tissues than in those of the hypocotyl and cotyledon and PHOT1::GFP is not localized on the outer surface of the root cortical cells either, it is not possible to see changes that might be occurring at the plasma membrane itself, comparable to those shown in Figs. 19-22. However, overall movement of the signal into the cytoplasm following blue-light treatment is easily observed. Figure 24A–C documents the changes in distribution of green fluorescence after 0, 6, and 12 min following excitation with the scanning laser. The signal moves through what appeared to be cytoplasmic strands that converge on a layer of cytoplasm surrounding the nuclear region (Fig24. arrows in B, C). Under higher magnification (Fig. 24D), some small punctate structures can be observed (arrows).

The sensitivity of root cells to BL appears similar to that found in hypocotyl cortical cells (Fig. 24E–G). Without blue-light treatment, no cytoplasmic PHOT1::GFP is detectable (Fig. 24E). Ten minutes of exposure to a total photon fluence of 600 $\mu mol \cdot m^{-2}$ is sufficient to induce small changes (Fig. 24F). However, 3000 $\mu mol\ m^{-2}$ induced clearly detectable migration of signal into the cytoplasm (Fig. 24G, arrows). As in the case with the hypocotyl cortical cells, cytoplasmic PHOT1::GFP in root cortical cells disappears in darkness following blue-light treatment. As shown in Fig. 24 D, the cytoplasm shows little signal after 1 h of darkness following a 30-min blue-light exposure (10 $\mu mol \cdot m^{-2} \cdot s^{-1}$). In root cortical cells, dark recovery appears somewhat more rapid than in hypocotyl cortical cells (Fig. 21).

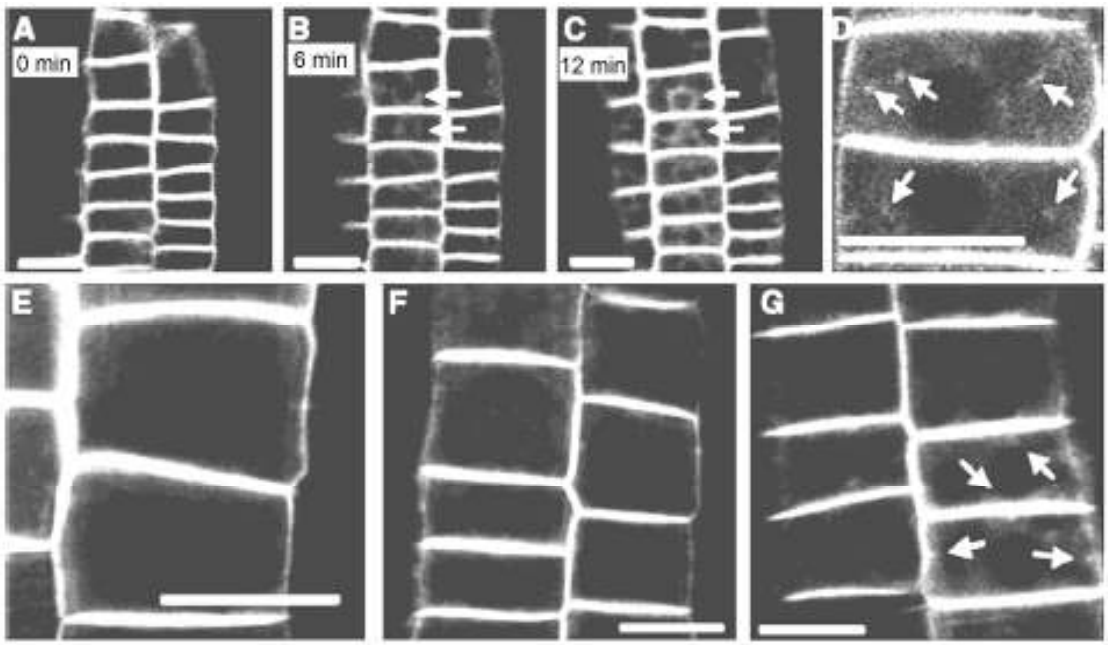

Figure 24. Blue-light-induced PHOT1::GFP re-localization in root cortical cells.

A–C: Zero, 6, and 12 min of blue-light exposure, respectively. Blue-light source is the scanning laser (25 µmol·m^{-2}·s^{-1}). (D) High-magnification image showing punctuate structures in cytoplasm. Note heavily labeled cross walls as compared to longitudinal walls (A, D) and signal surrounding the nuclear region (B, C). Blue-light source is the scanning laser (25 µmol·m^{-2}·s^{-1}).

E–G: Sensitivity of root cortical cells to blue light. Etiolated seedlings were exposed to blue light for 10 min at 0.5 (E), 1 (F), or 5 (G) µmol·m^{-2}·s^{-1} (total fluences 300, 600, and 3000 µmol·m^{-2}, respectively). Arrows in G indicate cytoplasmic PHOT1::GFP. Blue-light source is a halogen lamp fitted with a blue filter (Bar = 20 µm).

3.2.4 BL-Induced Movement and Dark Recovery in the Presence of a Protein Synthesis Inhibitor

Roots of 4 days old etiolated seedlings were treated with 50 µM cycloheximide (CHX) for 30 min in darkness prior to observation in the confocal microscope. This concentration, administered to 3 day old etiolated seedlings for 30 min, completely prevented the immediately subsequent incorporation of ^{35}S-methionine into protein (data not shown). Figure 25A shows that the inhibition of protein synthesis does not cause any changes of PHOT1 localization in root cortical cells. Migration of PHOT1::GFP into the cytoplasm in root cortical cells in the elongation region is clearly evident after 10 min of scanning (BL, 25 µmol·m^{-2}·s^{-1}) (Fig. 25B, arrows) and even more dramatic after 30 min (Fig. 25C, arrows). Hence, the re-localization itself

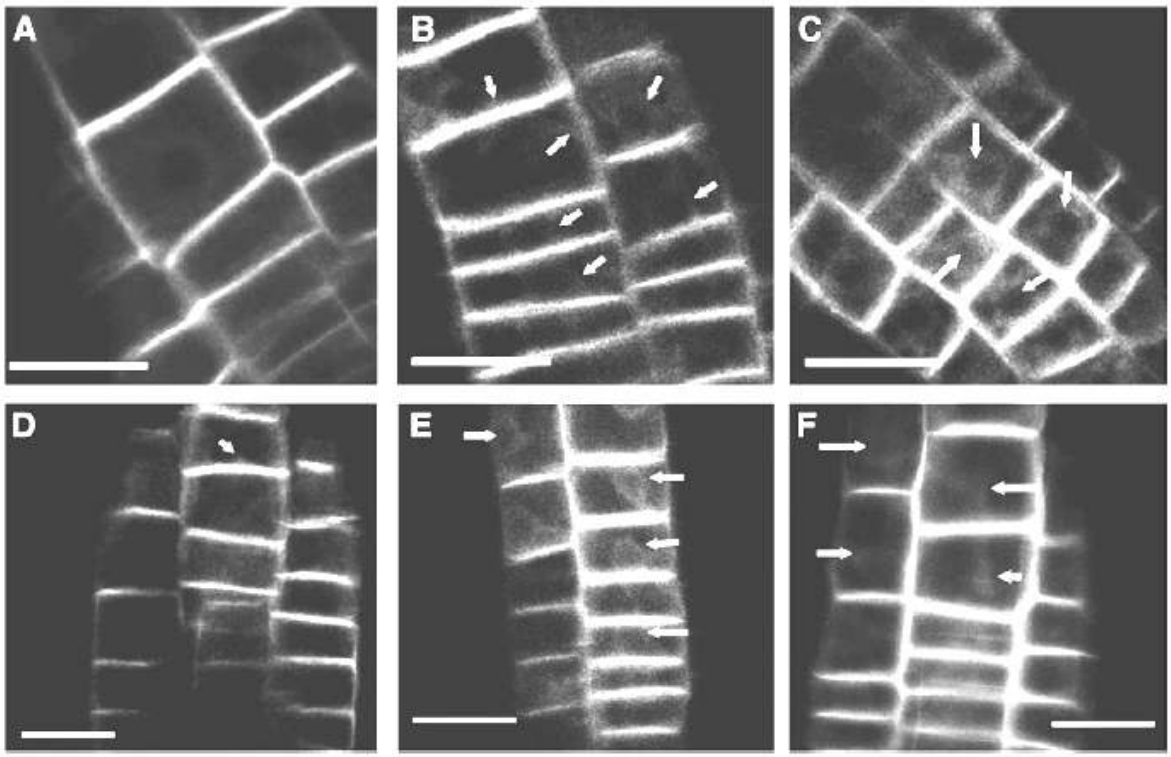

Figure 25. Effect of cycloheximide (CHX) on blue light-induced PHOT1::GFP re-localization and subsequent recovery in darkness.

A: Root cortical cells after 30 min CHX treatment in darkness. B: Root cortical cells after 30 min CHX treatment in darkness and 10 min blue-light treatment at 10 $\mu mol \cdot m^{-2} \cdot s^{-1}$. Cytoplasmic PHOT1::GFP is faintly visible. C: Root cortical cells after 30 min CHX treatment and 30 min blue-light treatment at 10 $\mu mol \cdot m^{-2} \cdot s^{-1}$. Cytoplasmic PHOT1::GFP clearly visible, especially surrounding the nuclear region (arrows, B, C). D–F: Root cortical cells following 30 min of blue light (10 $\mu mol \cdot m^{-2} \cdot s^{-1}$) and subsequent incubation in darkness in the absence of CHX (D: 60 min) or in the presence of CHX (E: 60 min, F: 120 min). Traces of signal after 2 h (F) in the presence of the inhibitor indicate that the disappearance of signal in root cortical cells is considerably slower in the presence of CHX than in its absence. Light source: halogen lamp plus blue filter (Bar = 20 µm).

brought on by BL does not require protein synthesis. When the roots were kept in darkness following 30 min of blue-light treatment (10 $\mu mol \cdot m^{-2} \cdot s^{-1}$) for 1h (Fig. 25D), in the absence of CHX, PHOT1::GFP gradually disappeared from the cytoplasm. In the presence of CHX, the signal also disappeared (Fig. 25E, 1 h darkness; Fig. 25F, 2h darkness). Hence, the disappearance from the cytoplasm might not require protein synthesis. Whether the disappearance results from return of the cytoplasmic PHOT1::GFP to the membrane or its degradation can not be resolved at this time, more experiments are designed to solve this question in next chapters. However, the disappearance from the cytoplasm (Figs. 25 E and F) is considerably slower than in the absence of the inhibitor (Fig. 25D).

3.2.5 BL-induced Internalization of Membrane-associated PHOT1 via Endocytosis

Endocytosis of PHOT1 was analyzed with the Zeiss 510-Meta laser scanning microscope in short time intervals (3.7 seconds per frame with 1.3 sec interval time). Figure 26 shows that PHOT1 is released from the plasma membrane via a vesicle-based process. The internalized portions of the PHOT1::GFP signals are colocalized with signals from the plasma membrane (PM) / endosome membrane marker, FM4-64 (Fig. 26). Because of limited passage of FM4-64 through the epidermal cells in to deeper cell layers, only epidermal cells in the hypocotyl region can be analyzed, but not cortical cells. In previous study, relocalizations of the PHOT1::GFP in epidermal and cortical cells showed similar behavior, when the membrane-associated portions of PHOT1::GFP were traced as mobile structures which were mobilized under illumination in the cortica cells too (See the Chapter 3.1).

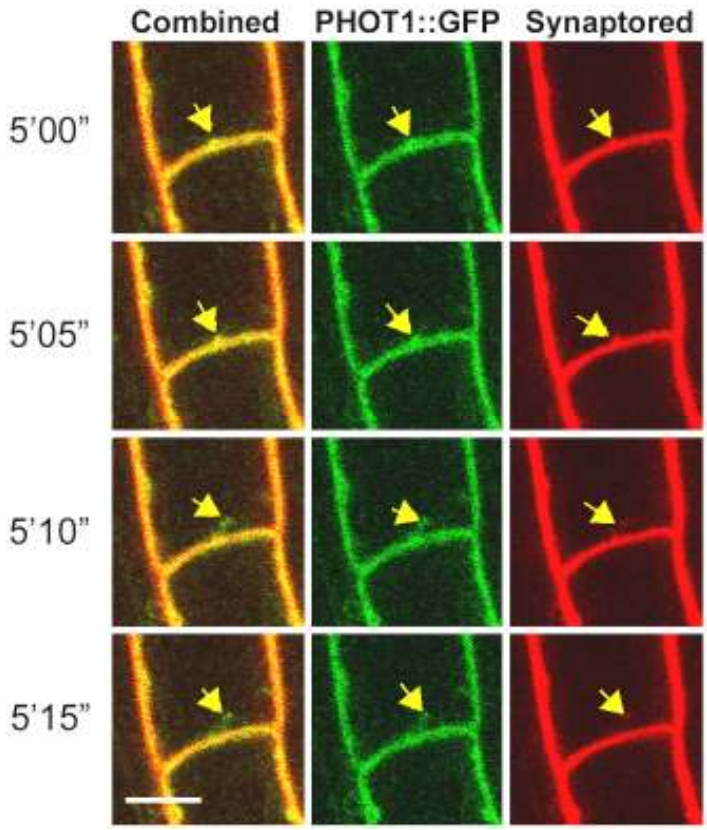

Figure 26. The Released PHOT1::GFP signals from PM of shoot epidermal cells is colocalized with endosome tracer FM4-64

4-day-old dark-grown seedlings were pre-treated with FM4-64 solution for 60 minutes in dark condition then put under the confocal laser scanning microscope. Duration of each scan is 3.7 seconds with 1.3 seconds interval time, total time for each scanning is 5 seconds. This sequence starts at the 5th minute of observation, the yellow arrows heads Figure out a vesicle releasing from cross-wall PM during the scanning. (Bar = 20 μm)

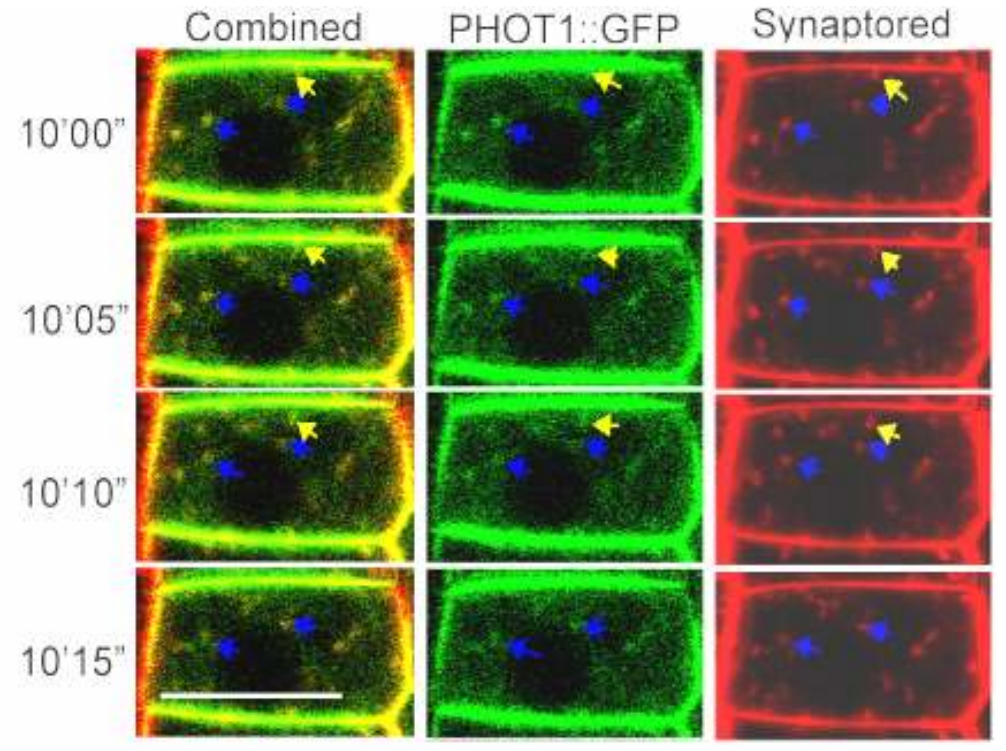

Figure 27. The Released PHOT1::GFP signals from the PM of root cortical cells co-localize with endosomes.

With pre-treatment of synaptored solution for 10 minutes in the dark, the roots of PHOT1::GFP transformed seedlings were scanned by blue laser for 15 minutes. The series starts at 10 minutes after beginning of observation, time for each scanning is 3.7 sec with 1.3 seconds interval time. total time for each frame 5 seconds. Yellow arrows point at an endosomal vesicle released from cross-wall membrane between two root cortical cells, while blue arrows show synaptored positive vesicles with less dynamic behavior. (Bar = 20 µm)

In addition, BL-induced punctate PHOT1::GFP-positive structures are scored also in the root cortex cells (Fig. 27). Again, BL-activated PHOT1::GFP colocalizes with FM4-64 -positive endosomes in the cytoplasm (arrows in the Fig. 27).

3.2.6 Endosomal PHOT1 Undergoes BL-Sensitive Vesicular Recycling

Brefeldin A (BFA) treatments trapped internalized PHOT1::GFP molecules within enlarged endosomal compartments in all three cell types analyzed in this study: shoot epidermis and cortex cells, as well as root cortex cells. Interestingly, these aggregates of enlarged endosomes, known as BFA-induced compartments, were formed in diverse cell types at different speed (Table 4). In darkness, the BFA exposure of 10 minutes was enough for a shift of the PHOT1::GFP-signal into the BFA-compartments while it

took about 50 minutes in shoot epidermis cells. In contrast, no compartments were detected for up to 135 minutes in the shoot cortex cells. BL illumination increased the speed of the formation of these BFA-compartments in all three cell types (Table 4). For example, shoot epidermal cells started to show PHOT1::GFP-containing compartments after 30 minutes of BFA treatment under BL illumination, and even the shoot cortex cells, which for more than 2 hours did not show any PHOT1::GFP positive compartments, formed them after 60 minutes (Table 4).

Table 4 . Speed of BFA induced compartment formation in different cell types (showing the fastest case from each kind of cells, n>3).

Cell Type	Blue-Light/BFA	Dark/BFA
Shoot epidermal	30 minutes	50 minutes
Shoot cortical	60 minutes	No detectable unit 135 minutes
Root cortical	8 minutes	10 minutes

Labelling with FM4-64 reveals endosomal colocalization with the PHOT1::GFP signals within the same BFA-induced compartments under darkness (Fig. 28). The regions positive for the PHOT1::GFP signal are larger than those positive for the FM4-64-signal (Figs. 28, 29), indicating that part of the cytoplasmic PHOT1::GFP signal is associated with structures or compartments in the immediate vicinity of endosomes. The time-lapse series (Fig. 29) document the process of BFA-induced trapping of endosomal membranes coinciding with the internalization of PHOT1::GFP molecules into the same endosomal compartments. The traces of PHOT1::GFP show more diffused pattern than the concentrated FM4-64-positive compartments, through this time series, PHOT1::GFP become more concentrated. Because of the photo-bleach effect from blue light laser, the whole process of trapping of PHOT1::GFP signals within concentrated BFA-induced compartments could not be shown (Fig. 29). With results from Fig. 30, the complete process to build up BFA-induced compartments are clear: Firstly, They are trapped within small sub-compartments, which are then aggregating into few large BFA compartments inside each cell. This phenomenon was repeated with different BL intensities: applying the same time of treatment, a stronger BL illumination caused a

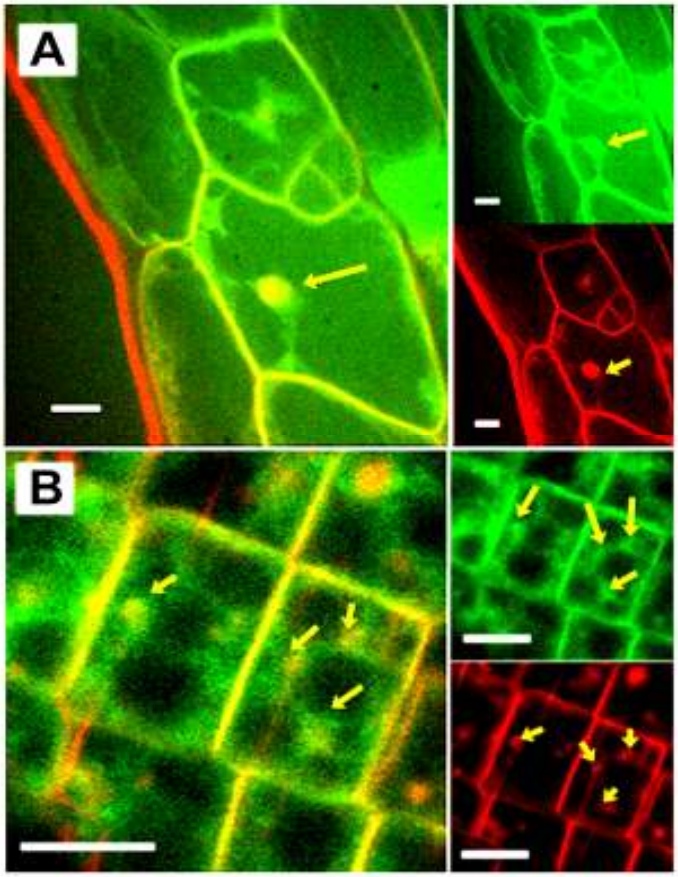

Figure 28. Colocalization of PHOT1::GFP and FM4-64 within BFA-induced endosomal compartments.

FM4-64 pre-incubated seedlings were treated with BFA for 60 minutes for hypocotyls (A) and 30 minutes for roots (B) in dark condition. Both shoot epidermal cells and root cortical cells were sensitive to BFA. Arrows indicate the colocalization sites of FM 4-64 and PHOT1::GFP signals. (Bar = 20 µm)

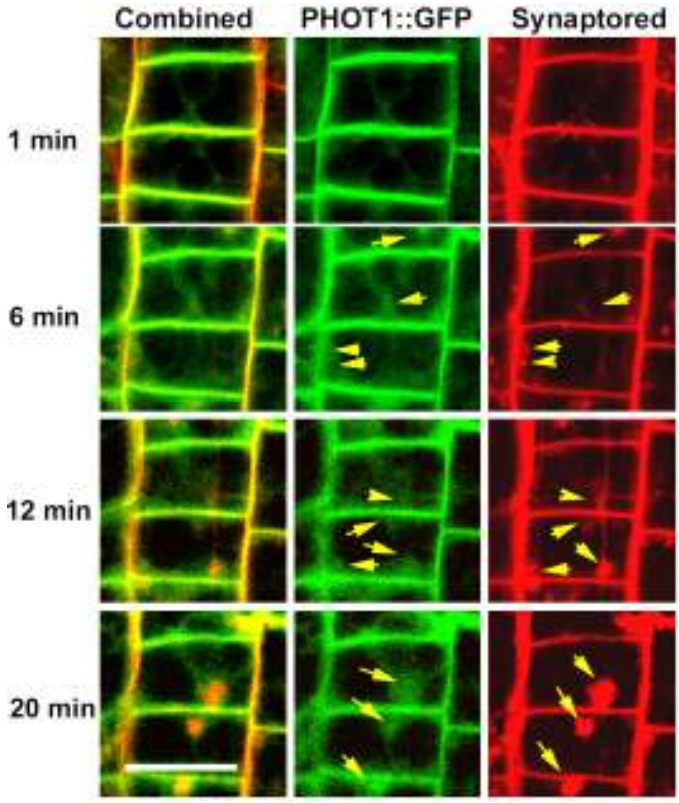

Figure 29. Still images from a time series of cells observed during BFA treatment.

PHOT1::GFP (middle column) and FM4-64 (right hand column) are becoming trapped within the same compartments during observation by confocal laser scanning microscopy. Time lapse series shows this process at time points of 1 minute, 6 minutes, 12 minutes and 20 minutes after scanning. Arrows figure out the colocalization sites of FM4-64 and PHOT1::GFP signals. (Bar=20µm)

bigger size of the PHOT1::GFP enriched compartments, while the number of these compartments per cell decreases (Figs. 30 A-C).

The inhibitor of endocytosis, wortmannin, also affected the localization of PHOT1::GFP under dark condition (Figs. 30E-F). Punctate structures appeares inside cytoplasm after short time treatment (Fig. 30E, 15 minutes) and signals inside cytoplasma were more diffuse than in the long time treated seedlings (Fig. 30F, 60 minutes). But long time treatment did not cause the formation of bigger compartments than in the short time treated roots. More dramatic impact had the inhibitor of actin polymerization, latrunculin B, which fully inhibited the assembly of BFA-induced compartments (Fig. 30G). In contrast, even full inhibition of protein synthesis by pre-treatment with cycloheximide (CHX) did not inhibit this process (Fig. 30D).

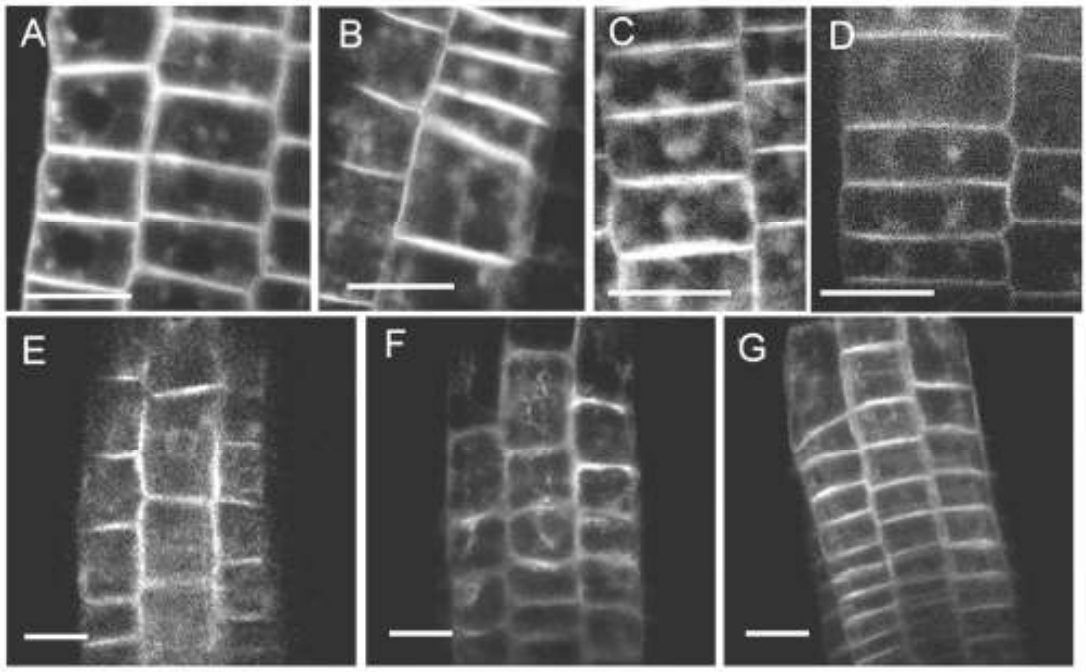

Figure 30. BFA-sensibility of root cortical cells in different conditions.

A-C show that illumination with higher BL intensity during BFA treatment caused larger phot1::GFP-positive endosomal compartments. The seedlings were treated with BFA (50 µmol l^{-}) under BL illumination with 0 (A), 12 (B), 20 (C) µmol $m^{-2}s^{-}$ intensities for 10 minutes.

In order to exclude effects from new-synthesized proteins, seedlings were pretreated for 1 hour by CHX (50) before incubation in BFA/CHX mixed solution in darknes for 30 minutes, the synthesis of proteins was stopped totally (see the Chapter 2.3.8). D shows that the formation of BFA-induced endosomal compartments is partly inhibited, because they are smaller and diffuser than by the BFA treatment without CHX. The pre-incubation with Latrunculin B can inhibit the formation of BFA-induced compartments totally, and results in numerous small vesicle-like structures during the same time of BFA treatments (G). The inhibitor of endocytosis, wortmannin, can also cause the relocalization of PHOT1::GFP molecules, the pattern of dark-wortmannin treatment for 15 minutes (E) and 60 minutes (F) is shown. (Bar = 20µm)

3.3 The Endosomal Recycling of PIN-formed Proteins is Sensitive to the BL Illumination

PIN proteins are putative facilitators of auxin efflux, and their recycling was suggested to be an adjustable pathway of polar auxin transport. In the following the question is addressed as to how the BL signal affects polar auxin transport (PAT) and how that in turn results in phototropic bending.

3.3.1 PIN2 is Essential for the BL-Induced Phototropic Responses in Roots

The growth direction of the null mutant line of *pin2*, named as *eir 1-4* (Luschnig *et al.,* 1998) was checked under lateral BL illumination. To this end, the seeds of *eir1*-4 mutant and WT (Col0) were put onto the same plate and grown under lateral BL illumination with the intensity of 2 μmol·m^{-2}·s^{-1}. Col0 seedlings had normal phototropic responses with an average angle for the shoot of 88.9˚ from the vertical position, while roots had an average angle of 17.5˚. In the *eir1* mutant, the lack of PIN2 protein apparently caused little effects on the shoot phototropic reaction as could be inferred from the angle of 76.0˚. However, roots of the *eir1* mutant lost their gravitropic responses completely with angles spreading between -38˚~+36˚ (Fig. 31A, n=12). Furthermore, roots of the *eir1* mutant seedlings had been

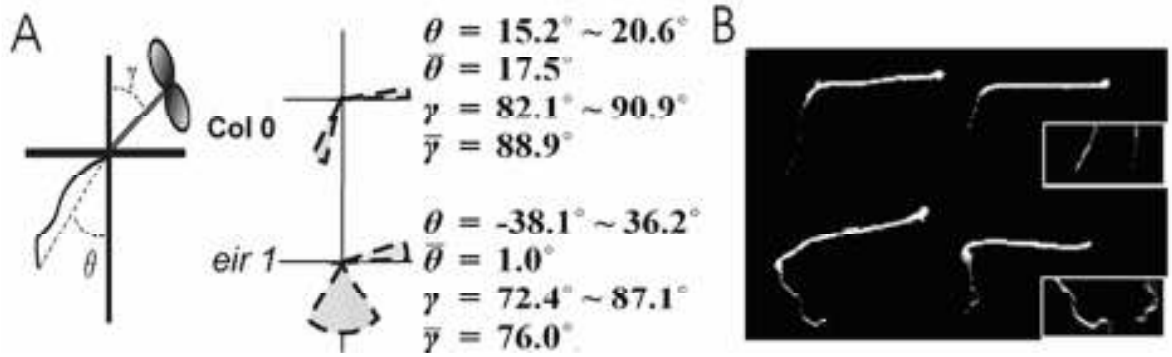

Figure 31. PIN2 is essential for root phototropic responses but has no effects in hypocotyl.

Blue light illumination with intensity of 2 μmol·m^{-2}·s^{-1} came from the right side during growth of 80 hrs. The angle of growth directions deviating from the vertical position were measured as γ (shoot) and θ (root). Because of the zigzag growth of *eir 1-4* roots, lines between the root tip and the initiation points were measured (A, left schema). 12 seedlings were measured in each *Arabidopsis* line, ranges of phototropic angels and mean value were recorded (A, right) and shown schematically (A, middle). B shows several images of both *Arabidopsis* line, the root parts are magnified (in white frames).

grown in zigzag patterns, irrespective of the light conditions during growth (Fig. 31B). Even the dark-grown seedlings showed this phenotype (data not shown).
Lack of PIN2 proteins caused nonphototropic responses of *Arabidopsis* roots. In order to define wether the polar auxin transport plays essential roles in this process, the following BFA experiments were designed.

3.3.2 Brefeldin A-inhibited BL-induced Responses in *Arabidopsis*

In order to study the endosomal cycling in root transition zone cells of *Arabidopsis,* and investigate the role of polar auxin transport in phototropic responses, the effect of Brefeldin A were checked during the light-induced responses in the *Arabidopsis* tissues (Fig. 32 and Table 5). The BL signal mediates various responses in plants, such as phototropism, spreading of leaves, synthesis of chloroplast, inhibition of hypocotyl elongation and increasing the elongation of root tissues. Figure 32 and Table 5 suggest that not all of these responses are inhibited by BFA, while the responses related to auxin are more sensitive than others. The shoot phototropism, root elonagtion and root phototropism have been inhibited or

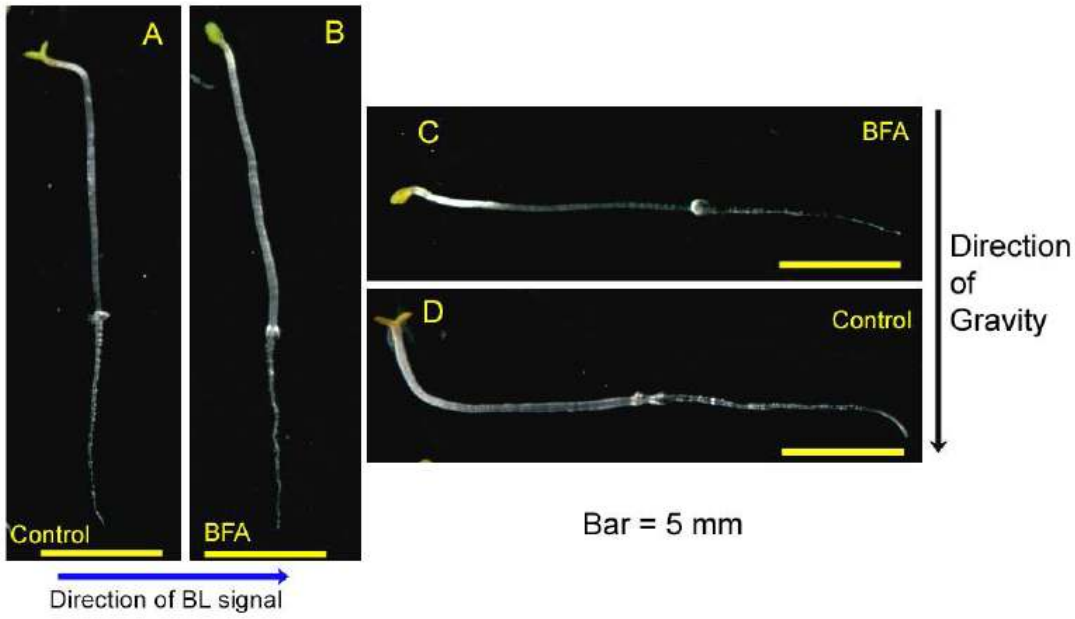

Figure 32. Brefeldin A inhibits responses to light and gravity.
3-days-old dark-grown *Arabidopsis* seedlings were chosen for phototropic- and gravitropic analysis, typical examples are showing as:
A, B: phototropic analysis with blue light from left side for 12 hrs.
C, D: gravitropic analysis in darkness with down side as shown for 12 hrs.
B, C: 500 µM brefeldin A were mixed in the 1/2 MS culture medium
A, D: 1/2 MS medium without BFA.

affected, while the Chloroplast development and the expanding of cotyledon remain in normal status (Table 5).

Table 5. Brefeldin A inhibits responses to light and gravity (Results are concluded from 15 *Arabidopsis* seedlings.)	
Chloroplast development	Not inhibited
Expanding of cotyledon	Decreased
Stomata opening	Inhibited
Shoot phototropism	Inhibited
Shoot gravitropism	Inhibited
Inhibition of shoot elongation	N/A, (because both BL and BFA can inhibit the elongation);
Root elongation	Inhibited from 1.3mm/12 hr to 0.3 mm/12 hr (n=16)
Root phototropism	Inhibited
Root gravitropism	Inhibited

3.3.3 BFA-Sensitive Recycling of PIN2 is Dependent on BL Illumination

Since the endosomal recycling of PIN2 is essential to the polar auxin transport, the above results suggested that both the lacks of PIN2 protein and inhibition of protein vesicular secretion could inhibit the phototropism of *Arabidopsis.* More experiments were preformed to understand the relationship between the light illumination and PIN2 recycling. These results are shown in Fig. 33.

Data presented in the Figs. 33A and B suggest that the dark-grown (B) and light-grown (A) *Arabidopsis* seedlings have different sensitivities to BFA. After 15 minutes treatment under white light illumination, BFA treatment caused more and larger PIN2::GFP positive compartments in cells of the light-grown seedlings (Fig. 33A, arrows) than those in cells of dark-grown seedlings (Fig. 33B, arrow heads). In dark-grown seedlings, BFA treatments under dark condition did not cause the disappearance of the PIN2-positive vacuole structures in cells (stars in Fig. 33C-2, comparing to Fig. 35 A), while the FM4-64-positive compartments (arrows in Fig. 33C-1) co-existed without colocalization with the PIN2::GFP compartments. In contrast, BFA treatments done under BL illumination resulted in different patterns when both the PIN2::GFP and

FM4-64-positive compartments colocalized within same compartments (arrow heads in Fig. 33D1 and D2).

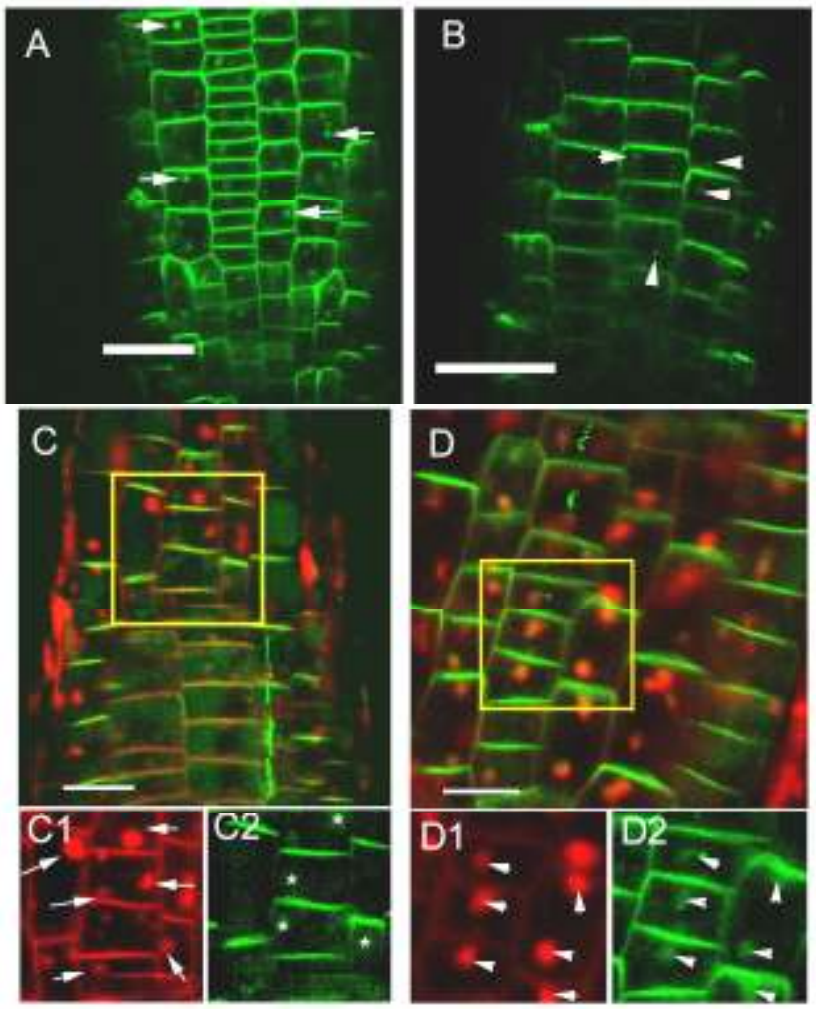

Figure 33. BFA-sensitive recycling of PIN2 is depended on blue light illumination.
A and B are showing the relocalization of PIN2::GFP in root cells of 4-days seedlings after treated by 50 µM BFA in light condition for 15 minutes. Seedling in image A was grown under white light illumination while seedling in image B was grown in dark condition. C and D are showing 4-days old dark-grown PIN2::GFP transformed seedlings treated by 50 µM BFA in dark condition (C) and under blue light illumination (D) for 60 minutes, red fluorescence signals are from synaptored. In dark-BFA treated seedlings, PIN2::GFP (green signals) remains in vacuole structures (defined by Laxmi et al., 2008) without co-localization with the synapto-red signals. While blue light illumination causes the dissappearence of PIN2::GFP positive vacuole structures, it involved co-localization of both fluorescence signals inside same BFA-compartments. Arrows are pointing out the BFA-induced compartments; stars are for the vacuole structures. Bar = 20 µm

3.3.4 BL Influences the Localization of PIN 1 and PIN2 Protein.

Since the inhibitor of protein secretion, BFA, stopped gravitropic responses in root tissues (Fig. 32) and BL affected the sensitivities of root cells to BFA (Fig. 33), it was reasonable to check, if BL affected localization of PINs via the endosomal vesicle recycling.

Figure 34 shows the localization of PIN1::GFP proteins in root tips in the dark (Fig. 34A) and the light (Fig. 34B) conditions. PIN1 is expressed mainly in central cylinder cells, in which they have polar localization in the light-grown plants. Figure 34B shows that the PIN1::GFP signals are stimulated at the cross-wall membrane, only weak signal is at side walls and the GFP signals absences in cytoplasm. However, in dark-grown plants, another pattern of PIN1::GFP localization is prevalent (Fig. 34A). The PIN1::GFP signal is weaker than in the light-grown plant and it does not show polar localization. In contract, the signal is found in vacuole-like structures (arrows). These differences of localizations could be reversed by changes of the growth conditions. When dark-grown seedlings were placed in white light for 12 hours, the polarity and the expression levels recovered (Fig. 34C), and no more signal was found in the vacuole-like structures. If the light grown PIN1::GFP-transformed plants were put into darkness for 12 hours, the GFP signals reappeared in the vacuole-like structures (Fig. 34D arrows).

Current hypothesis suggests that, whereas PIN1 acts as auxin transporter in the central cylinder cells in the direction towards the root apex, PIN2 protein is localized on the cross wall membrane of epidermal and cortical root cells, in which auxin is pumped upwards, i.e., away from the apex (see the Chapter 1.2). Therefore the localization of PIN2::GFP protein was checked in seedlings grown under dark and light conditions (Fig. 35). Figure 35A shows the localization of PIN2::GFP molecules in the dark-grown seeding. Both the cross wall membranes and the vacuole-like structures are labelled in dark-grown seedlings, whereas only the polar membranes were labelled in the light-grown seedlings (Fig. 35B). These localization patterns can be reversed too (Figs. 35C and D).

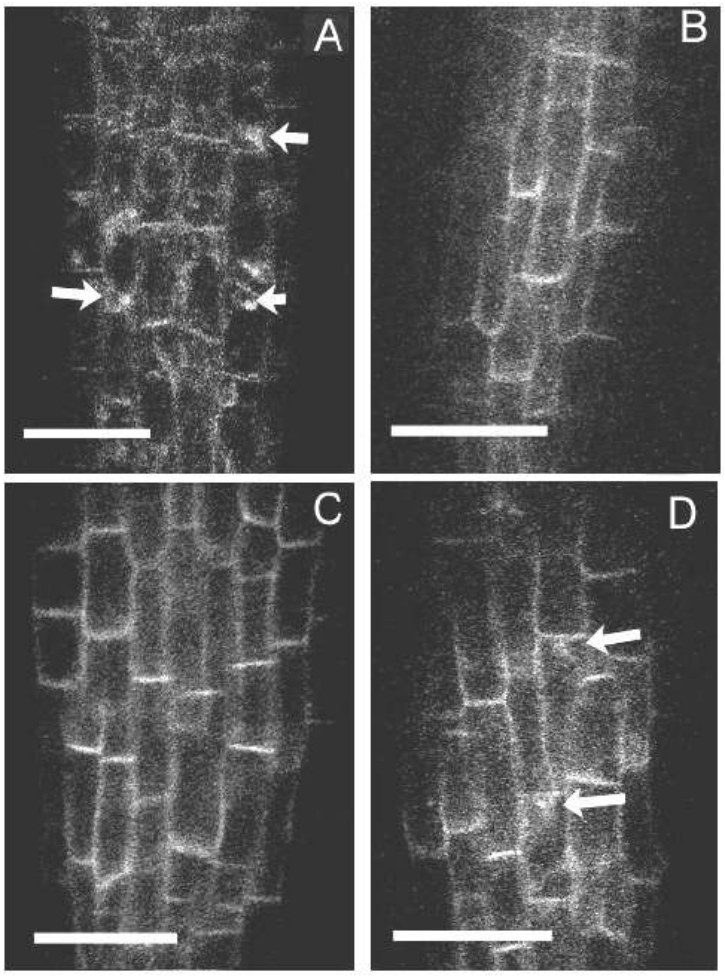

Figure 34. PIN1::GFP localization and relocalization in root cells under light and dark signals.

A: Root of 4 days-old dark-grown *Arabidopsis* seedling, arrows point at the vacuole-like structures. B: Root of 4 days-old light-grown *Arabidopsis* seedling. C: Root of 4 days-old dark-grown *Arabidopsis* seedling, which was transferred to light for the last 12 hours. D: localization of PIN1::GFP signals in root of 4 days-old light-grown *Arabidopsis* seedling, which was transferred to darknessthe for the last 12 hours. Arrows point at the vacuole-like structures (Bar = 20µm).

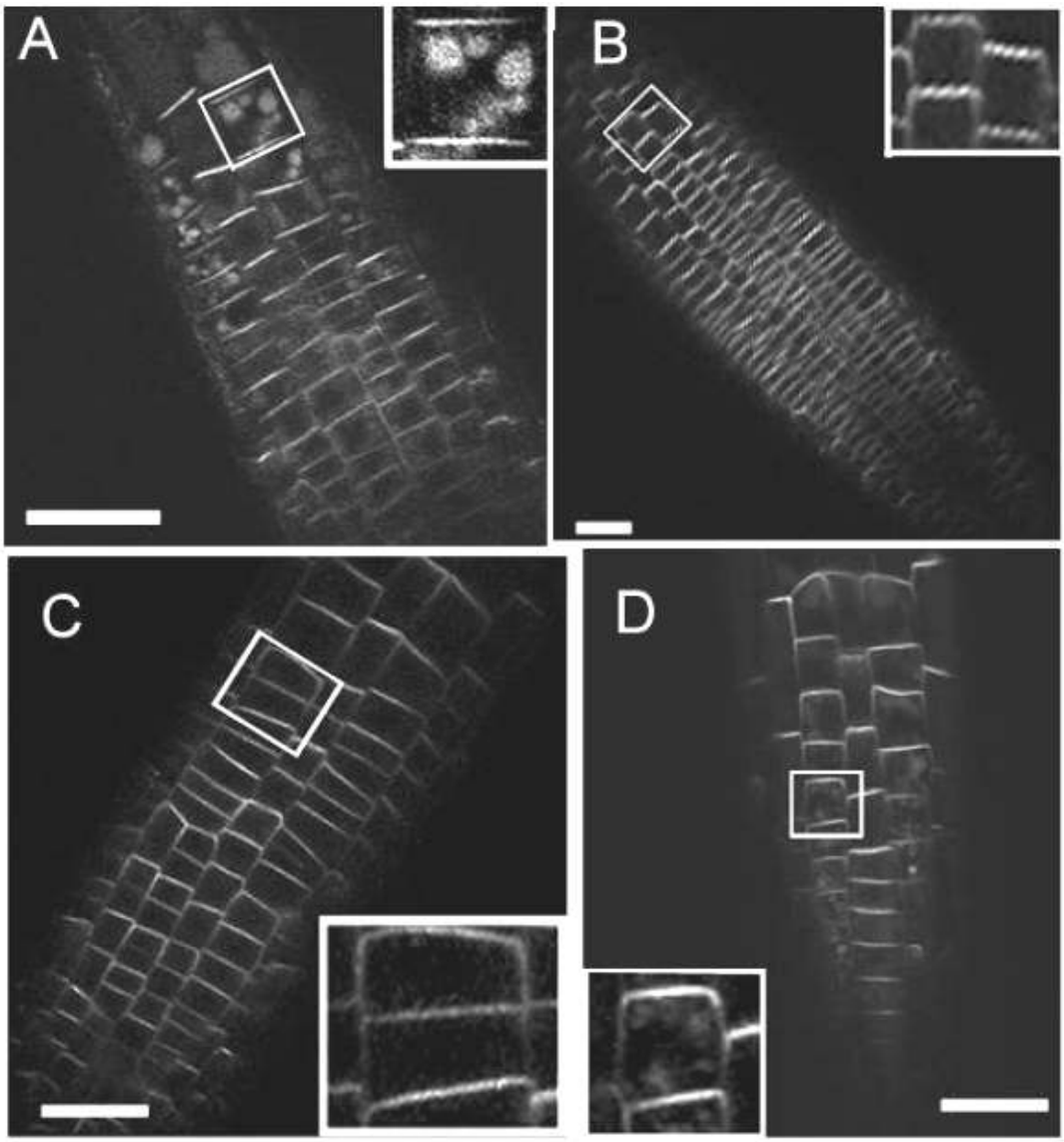

Figure 35. PIN2::GFP localization and relocalization in root cells under light and dark conditions.

A: Root of 4 days-old dark-grown *Arabidopsis* seedling, inset shows detail of vacuole-like structures. B: Root of 4 days-old light-grown *Arabidopsis* seedling, vacuole-like structures are absent. C: Relocalization of PIN2::GFP signals in root of 4 days-old dark-grown *Arabidopsis* seedling, which had been placed in light for the last 12 hours. D: Relocalization of PIN2::GFP signals in root of 4 days-old light-grown *Arabidopsis* seedling, which had been placed in darkness for the last 12 hours. (Bar = 20 µm)

3.3.5 Endocytosis and Fusion of Endosomal Vesicles are Accelerated by BL Illumination

In order to study the effects of BL on endocytosis and endosomal behavior, seedlings were stained stepwise with two different sterol dyes for PM and endosomes: FM1-43 and FM 4-64 (see Materials and Methods). This was combined with BFA treatments in order to visualize better the changes of endosomal recycling.

Firstly, the question was addressed as to whether FM1-43 and FM 4-64 stained different portion of the endosomal membrane fractions. When the seedlings were treated in solution with both dyes together, these two fluorescence signals showed very similar patterns of localization in root cells of seedlings grown either in dark or in light conditions (Figs. 36A and B). However, BFA-treatment revealed that the FM 4-64-labelled membranes had a more dynamic character than the FM1-43 positive membranes (Figs. 36 A-1 and A-2). Although BFA treatment caused trapping of both tracers within the same compartments, more green fluorescence (FM1-43) remained on the plasma membrane while stronger red fluorescence (FM4-64) was trapped within the BFA-induced compartments in darkness. Under BL illumination even more pronounced differences were evident between these two stains: red FM4-64 signal came mainly from the BFA-compartments, leaving only very weak staining on the plasma membrane (Fig. 36B-1), while the green FM1-43 signal shows more prominent plasma membrane labelling (Fig. 36 B-2).

In order to understand better these BL-mediated effects on the endocytosis and endosome recycling in general, FM1-43 was applied to pre-cooled seedlings incubated on ice for 5 minutes, then washed with liquid ½ MS medium for 10 minutes at room temperature. This should cause FM1-43 to be released from the plasma membrane by endocytosis into the endosomal compartment (early and late endosomes together). Next, FM4-64 was applied for 5min, which should only reveal the fraction of early endosomes. All staining steps were performed in darkness. After BFA treatments for relative long time (60 minutes) in both dark and light conditions, the FM1-43 and FM 4-64 positive endosomes were all fused together in BFA compartments (data not shown). However, when the time of BFA treatment was reduced to 15 minutes, only part of the early endosomes fused together. Using these incubation parameters under dark condition, fusion of endosomes was relatively low

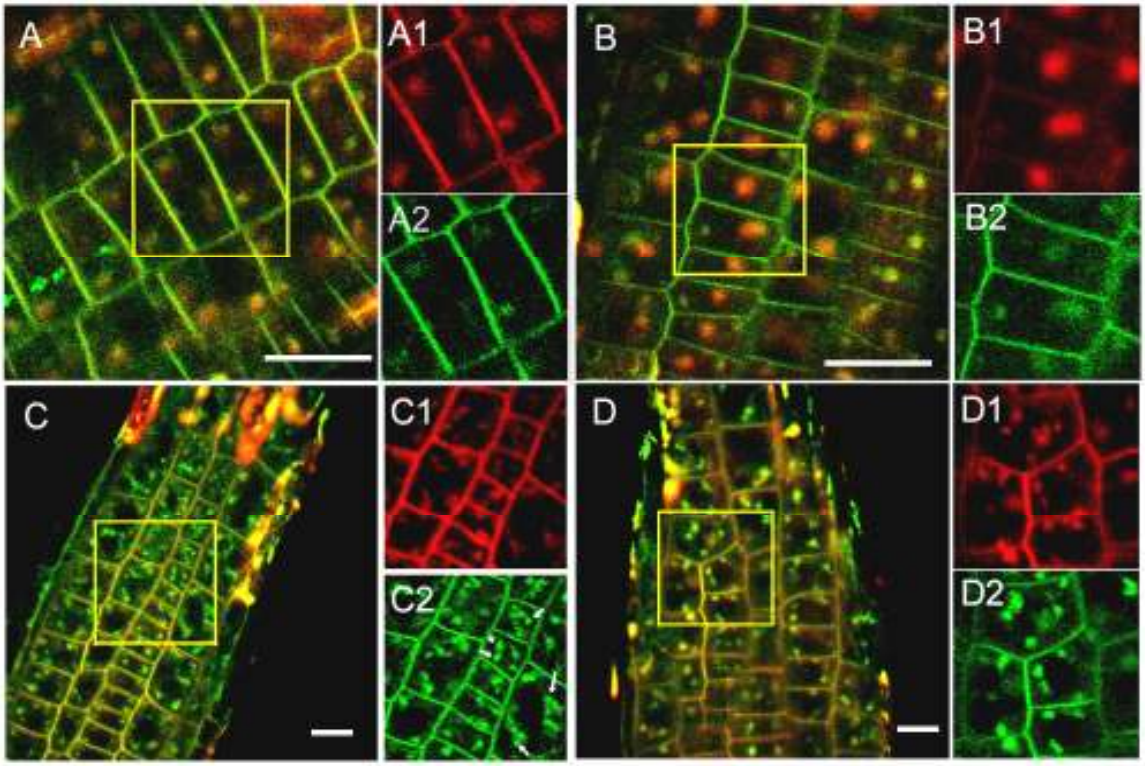

Figure 36. Sequential membrane labelling reveals an effect of light on the fusion of early and late endosome under BFA treatment.

4 days-old dark-grown seedlings were treated with synaptored (red signal) and FM1-43 (green signal) mixture (A, B) or treated with synaptored and FM 1-43 sequentially(C, D). Then the seedlings were treated by 50 µM BFA in darkness (A, C) or under blue light illumination (B, D).

A, B: These images show that both dyes were trapped within same BFA-compartments (30minutes), when the roots are treated in mixed solution. Synaptored tends to label endosomal vesicles, while FM1-43 is more strongly on the PMs (Compare A1 A2). Blue light illumination during the BFA treatment enlarged this difference (Compare B1 B2). Blue light illumination also increased the BFA-induced endosomal compartments (Compare A and B).

C, D: In order to ensure the different of time-separated endosomal pathways, the dyes were subjected sequentially and BFA treatments were shortened to 15 minutes. C: 15 minutes BFA treatment in darkness caused some of the stains to be trapped in the same compartment (yellow color shows co-localization of two stains), while FM 1-43 (green color) was present in additional compartments (white arrows); D: 15 minutes BFA treatment in the light resulted in a larger amount of coloclalization, i.e., only few exclusively green colored compartments could be found.

Bar = 20 µm

(Fig. 36C) whereas, under BL illumination, the same BFA treatment resulted in a much stronger fusion of endosomes (Fig. 36D).

Furthermore, the obtained pattern of FM 4-64 positive endosomal membrane fraction revealed also that the BL illumination accelerates general endocytosis. After 30 minutes of BFA treatment under BL illumination, only low level of the red fluorescence signal remained at the plasma membrane while most of the signal was trapped within the

enlarged BFA-induced compartments (Fig. 36 B-1). On the other hand, BFA treatment under dark condition resulted in well-labelled plasma membrane and small BFA-induced compartments (Fig. 36 A-1).

3.3.6 NPH3::GFP has Polar Localization at Root Tip Region

NPH3 is a scaffold protein related to photoreceptor PHOT1 and a homologous to regulator of PIN localization, PID (see Introduction, Chapter 1.4 and 1.5). In order to understand relationships between blue light induced relocalization of PHOT1 and PIN2, I created an *Arabidopsis* line that was transformed by *proS35::NPH3::GFP* constructor (see the Chapter 2.1.2). The preliminary studies are presented as Fig. 37.

In epidermal cells, NPH3::GFP signal was polarly arranged with the crosswalls showing the strong signals.

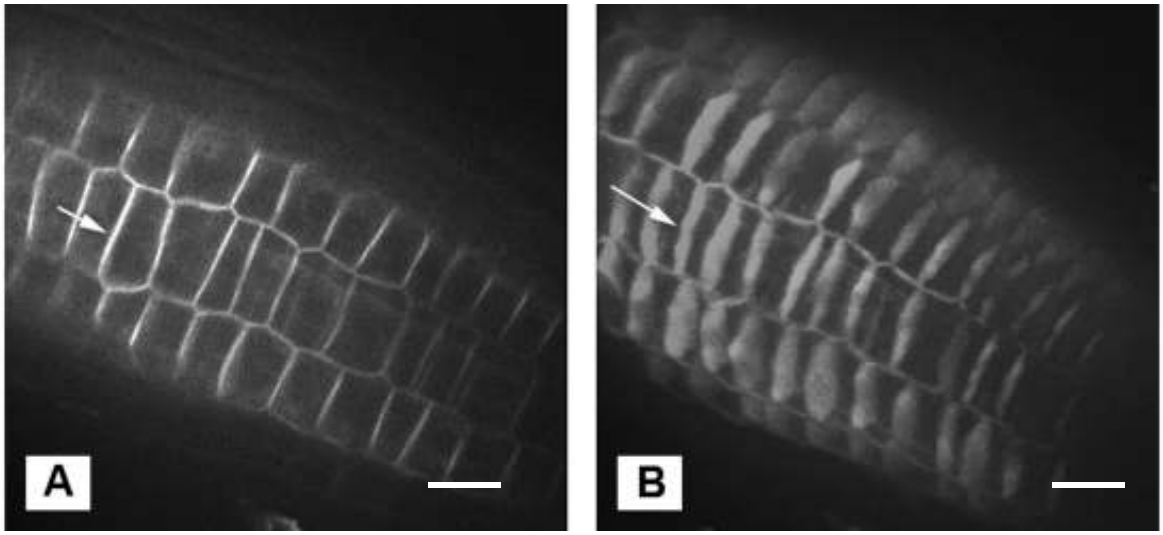

Figure 37. Cellular localization of NPH3::GFP in the root tip region.
Figures show the localization of NPH3::GFP in the root epidermal cells of 4 days old light-grown *Arabidopsis* seedlings. A: single scanning image from root epidermal cells; B: Projections reconstructed from series of images from surface of leaves to 30 µm deep inside. Arrows are pointing the location of NPH3::GFP on the cross wall of two cells. Bar = 20 µm

3.3.7 Illumination Changes the Size of Root Meristem and Transition Zone

The size of the apical root meristem was analyzed in *proCYCB1::GUS* transformed plant lines under dark and light conditions (see the Chapter 2.1.2). Under the control of the CYCB1 promotor, the expression of GUS gene pointed out the region of root meristem in different experiment conditions. When the *Arabidopsis* seedlings were grown under light condition, the length of the meristem and transition zones together was 134.6 µm (mean value from 6 seedlings, Fig. 38 A, B), but in the dark-grown seedlings it was only 78.2 µm (mean value from 6 seedlings, Fig. 38 C, D). The dark-grown seedlings only had a basic level of cyclin B promoter-drived *GUS* gene expression in this region, whereas seedlings grown under BL illumination had increased levels of *GUS* expression. The illuminated side of the roots always showed a stronger signal than the shaded side (more dark blue colored cells), and the length of cyclin B expression domain at the illuminated side gets longer than at the shaded side (Fig. 38E, red arrows). The changes in the light-grown seedlings are not so significant. But a line of dark blue colored cells was detected at the illuminated

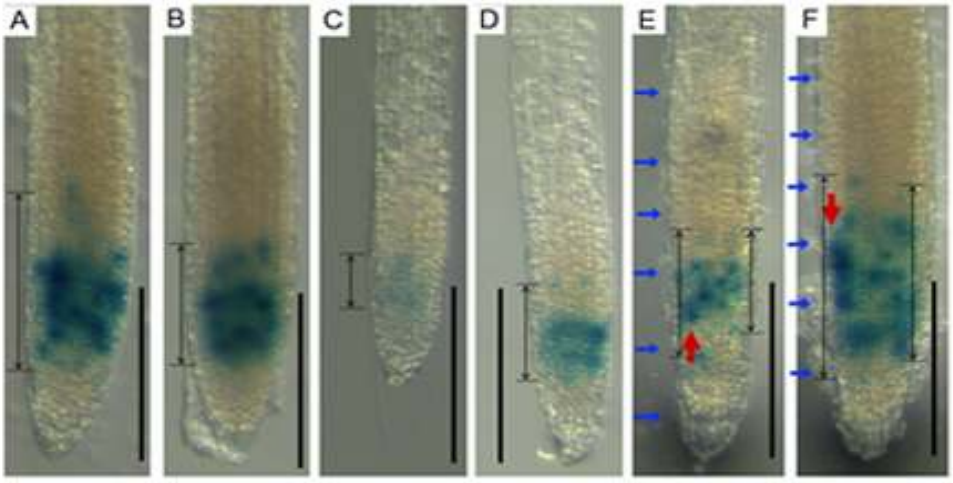

Figure 38. Expression pattern of *proCYC B1::GUS* in the root tip region.

A and B: Seedlings are grown under white light illumination for 4 days. The length of the expression region is 134.6 µm (mean value from 6 seedlings).

C and D: Seedlings are grown in dark condition for 4 days. The length of the expression region is 78.2 µm (mean value from 6 seedlings).

E: A dark-grown seedling with 1 hour blue light illumination from the left side (blue arrows).

F: A light-grown seedling with 1 hour blue light illumination from the left side (blue arrows).

Double dead arrows are indicating the length of root meristem, and red arrows are indicating the strongly expressing cells at the illuminated side of roots. (Bar = 200 µm)

side too (Fig. 38 F, red arrows). Figures 38 E and F are chosen from more than 10 seedlings for each experiment, most of them (about 70%) show the same changes.

3.3.8 Asymmetric Auxin Distribution is Affected by Lateral BL illumination

As shown above (see the Chapter 3.3.1-3.3.3) BL illumination determines the localization and trafficking of PIN2 proteins. In order to understand the importance of this phenomenon, auxin redistribution was analyzed by observing the GFP distribution in the *proDR5::GFP* transformed line of *Arabidopsis.*

The fluorescence of GFP is detected efficiently at the central column of the root cap (columella), and the distribution in the columella is symmetrical in the control root apices grown at diffuse illumination (Fig. 39A). Change of the gravity vector (Fig. 39B) or 2 hours or unilateral BL illumination with 2 µmol m^{-2} s^{-2} from the left side of seedlings stimulates a shift of the GFP signals towards the illuminated side (Fig. 39C).

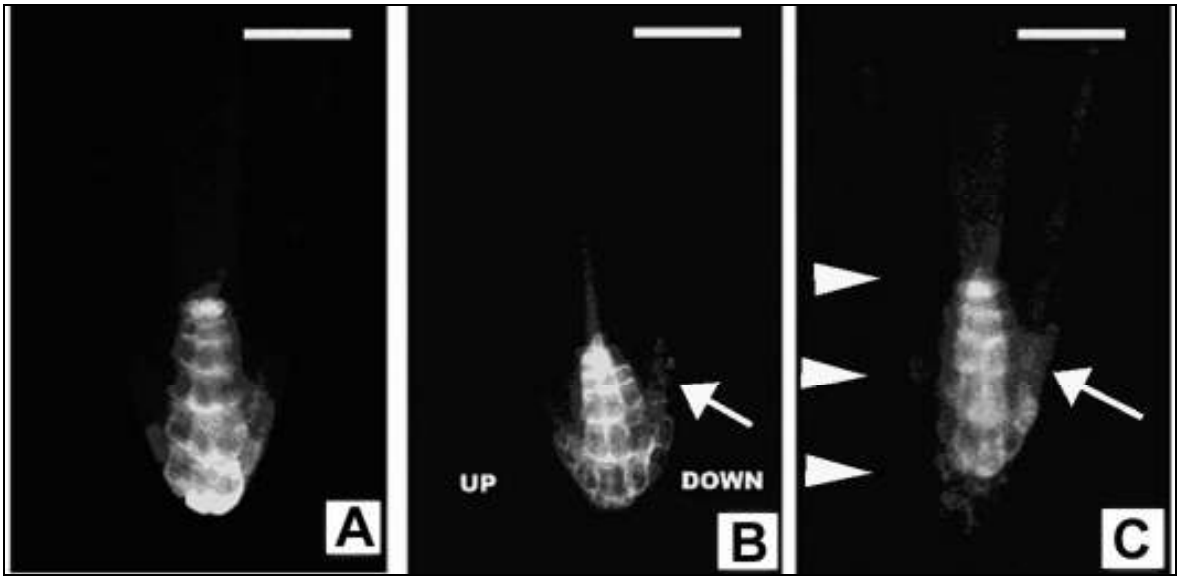

Figure 39. Expression pattern of *proDR5::GFP* at the root tip.
5 days old light-grown seedlings were observed under the confocal microscope. A: Control; B: The seedling was put into horizontal position for 2 hours. Up and down sides are labelled in this image; C: The seedling was illuminated with 2 µmol $m^{-2}s^{-1}$ blue light for 2 hours from the right side (Arrow heads). Red arrows point out the asymmetric distribution of GFP signals in root tip. Bar = 50 µm

3.3.9 PIN3 is an Essential Factor for Root Phototropism

The importance of PIN3 protein in the root phototropism was demonstrated by analyzing the phototropic growth of the mutant line *pin3-3* (null mutant for the PIN3) Seeds of *pin3-3* mutant and wild type (WS) were put onto the same plate and grown under lateral BL illumination with the intensity of 2 µmol·m^{-2}·s^{-1}. After 7 days of growth, images were taken (Fig. 40). It is evident from the zig-zag growth mode, that roots of the *pin3-3* mutant have lost their phototroipsm completely, with growth angles of the root between -25˚ and +22˚ (12 plants for each line, Fig. 40B). As compared to the roots of wild type (WS) seedlings, a normal phototropic response with an average growth angle of 63.0˚ was scored. However, for the shoots of the *pin3-3* mutant the lack of PIN3 caused little effects on the phototropic reactions as can be inferred from the average growth angle of 42.7˚ as compared to 56.4˚ in the wild type shoots.

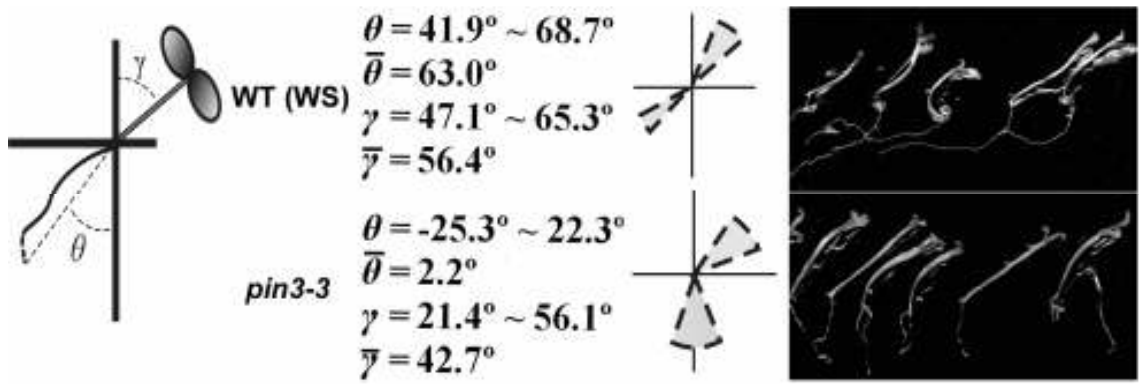

Figure 40. Analysis of phototropism in *pin3-3* mutants.

Wild type *Arabidopsis* seedlings have stronger hypocotyl phototropism (56.4°) than the *pin3-3* mutant (42.7°). The method of measurement is shown as scheme A, results are in part B. The mutant loses the root phototropism completely (only 2.2° as mean value), showing a zigzag formation of root growth (Arrow heads in image C). Schematic diagram C is showing the distribution of angles of hypocotyl and root growth.

4 Discussion

This study was intended to make progress in answering an “old” question: how can plants, which obviously lack ‘eyes’, sense light signals from the environment? Especially, how do blue light signals mediate phototropism? Since Charles Darwin began to study this phenomenon some 150 years ago (Darwin, 1880), researchers have suggested several hypotheses. Among them, the Went & Cholodny hypothesis is most widely accepted. Went and Cholodny suggested that the asymmetric distribution of auxin causes differential cell elongation rates at shaded and illuminated sides of plant organs (reviewed by Christie, 2007). This then causes the light-induced bending of the plant organs: hence phototropism. Here, the relocalization of auxin transporters of the PIN family was observed after blue light perception and this process is proposed to be one of the key events of phototropism.

Light signals which have their wavelengths in blue range have the most important roles in the phototropic responses. In 1995, family of blue light receptors were discovered by Winslow Briggs and his colleagues, and renamed them as PHOT1 and PHOT2 at 2002. PHOT1 and PHOT2 mediate most BL-intiated responses, such as phototropism, stomata opening, leaf expansion and chloroplast movement, but the mechanism of the signal transduction is still unclear (reviewed by Christie, 2007). Sakamoto and Briggs (2002) published a PHOT1::GFP transformed line of *Arabidopsis* plant and suggested new clues to understand the relationship between localization of PHOT1 and the PHOT1-mediated blue light signaling.

Based on these premier results and hypothesis, I observed in details subcellular localizations of PHOT1 in different cell types of various tissues with confocal microscopy. I have discovered that the blue light caused endosomal recycling of PHOT1 between PM and endosome. In the last part of my thesis, I am suggesting that the blue light affects the endosomal vesicular trafficking of PINs. This process could determine the direction of polar auxin transport and drive the phototropic bendings of plant organs.

4.1 The tissue distribution pattern of PHOT1 correlates with Physiological Responses

In the first part of this study (see the Chapter 3.1), the tissue expression and subcellular localization of PHOT1::GFP proteins in different kinds of plant cells has been described. These data support the conclusion that a link exists between

localization and function. In the following Chapter it will be discussed how the distribution of PHOT1 in different tissues is precisely consistent with its physiological role.

Before attempting to relate blue-light-induced changes in PHOT1::GFP to any physiological responses in wild-type plants, it was necessary to determine the relative physiological sensitivity of the transgenic seedlings to BL compared to wild-type seedlings. The results shown in the Table 2 suggest that the level of expression of the *proPHOT1::PHOT1::GFP* gene is either insufficient for full complementation of phototropism in the *phot1-5* mutant or the GFP-fusion protein is not fully functional. Expression of the GFP-tagged PHOT1 protein is nevertheless sufficient for at least partial PHOT1 function and to allow confocal examination of light-induced changes in PHOT1::GFP distribution and re-localization.

4.1.1 PHOT1::GFP Tissue Distribution Patterns with Respect to Physiological Responses

In the 4-days old dark-grown seedlings, PHOT1::GFP is localized in guard cells of the cotyledons and in the surrounding epidermal pavement cells. This result is consistent with the finding that PHOT1 mediates stomata opening (Kinoshita et al., 2001), and that pavement cells are likely the limiting factor in leaf expansion (Van Volkenburgh, 1999), respectively. The strong expression of phot1-GFP in the hypocotyls hook and elongation zone and in the root elongation zone are both to be expected, because these tissues have prominent roles in the phototropic response (Schwartz and Koller, 1980, Cho et al., 1996). Moreover, the distribution of phot1-GFP in mesophyll cells is consistent with its role in mediating the chloroplast avoidance response (Jarillo et al., 2001; Kagawa et al., 2001) and accumulation (Sakai et al., 2001) responses.

Early studies on the shoot phototropism of plants demonstrated the effects of apical hook position and cotyledon. When the side of hook is positioned away from the tropic curvature, the bending degree is maximized (Khurana et al., 1989). However, the authors did not see the possibility that these two organs had roles in light perception, they only addressed the question as to how their position affected the phototropic responses. By measuring the Ca^{2+} flux under blue light illumination Babourina et al. (2003) came to the conclusion that the light sensor site in the

hypocotyl is not limited to the hook region, although the top region of hypocotyl has the highest sensibility to blue light. This is consistent with the findings here, which show that the apical hook and elongation zone of hypocotyls have the strongest expression level of *proPHOT1::PHOT1::GFP*. PHOT1::GFP is localized on the outer periclinal PMs. These expression and localization data fit to the reaction site of shoot phototropism, i.e., the elongation zones (Sakamoto and Briggs, 2002). In summary, the PHOT1 distribution shown here corroborates all other data on apical hook opening and cotyledon unfolding stimulated by weak BL (Liscum and Hangarter, 1993).

Sakamoto and Briggs (2002) have noted a lack of detectable expression of PHOT1 in the root cap as well as the root apical meristem, although they reported a faint signal from the epidermis. In the present study, this observation was mostly confirmed except that PHOT1::GFP expression was also not detectable in the root epidermis. A difference in seedling age or growth conditions might account for this discrepancy. Historic publications on the identification of the site of root photosensitivity for phototropism reflect a complex situation. For instance, Naundorf suggested that the root cap of sun flower seedlings was the site of light signal perception at 1940, but Schneider (1964) reported that removing of the first 1mm tip of maize roots inhibited the negative phototropism of root. Mullen et al. (2002) disagreed with this result, and presented evidences that the root cap of maize seedlings is the site of photosensitivity for root phototropism. In their studies, white light applied via optic fibers to the root tip of mays induced curvature, whereas white light applied similarly to the elongation zone failed to produce a response. They suggested that the perception and response sites of root are separated. On the other hand, Liscum and Briggs (1995) demonstrated that it was PHOT1 that mediated phototropism in response to low-fluence BL in *Arabidopsis* roots. My analysis reveal that PHOT1::GFP is absent from the root cap and apical meristem in 4 days old etiolated seedlings. Either *Arabidopsis* and maize use different systems to regulate root phototropism or another photoreceptor is responsible for photoexcitation in the root cap. A gradient of light intensity between the illuminated and the shaded sides of a plant would be the physical basis for plant bodies to sense the direction of light. Optical fibers were used to measure the light gradient of the plant vessel tissues irradiated by unilateral BL. Light penetration, known to occur in etiolated tissues (Mandoli and Briggs, 1982) and light scattering (Vogelmann and Haupt, 1985), could

result in a light gradient in the elongation zone, even if only the root cap were directly illuminated but could not account for the greatest photosensitivity occurring in the cap region. This assumption is receiving quite some credibility, as is shown here, because roots illuminated with 2 $\mu mol \cdot m^{-2} \cdot s^{-1}$ of BL clearly curved away from the light in the absence of detectable PHOT1::GFP fluorescence in their apical meristems or root caps before or after phototropic stimulation (Fig. 18). As Mullen et al. (2002) suggest, perhaps the activation of phytochrome, known to be located almost exclusively in the root-cap columella cells in roots of maize and other etiolated grass seedlings (Pratt and Coleman, 1974), is required to potentiate a tropic response to BL in the phototropin-rich elongation region. BL can transform phytochrome *in vivo*, although the Pfr:Pr (far red : red) ratio is small and the quantum efficiency low compared to these parameters in RL (Pratt and Briggs, 1966). Because Mullen et al. (2002) used continuous BL, phytochrome activation certainly must have occurred.

It is not clear why PHOT1::GFP expression is high in the root–shoot transition region. Galen et al. (2007) have reported that PHOT1 serves a role in drought tolerance in field-grown *Arabidopsis*. Even if the zone is under the soil, penetrating light could provide sufficient phototropin activation to induce some sorts of response (Mandoli and Briggs, 1982). Under drought stress, blue-light-activated PHOT1 in the transition region might send signals to the roots that could modulate their growth rate or growth direction. Aspects of root phototropism, meristem size and positioning and PAT under BL illumination will be discussed in further detail in the Chapter 4.3.3.

4.1.2 Subcellular Distribution of PHOT1

With higher-resolution confocal microscopy a great deal better subcellular details of PHOT1::GFP localization can be observed than that found in the previous study by Sakamoto and Briggs (2002).

It has been well established for a number of plant species that PHOT1 is closely associated with the plasma membrane in dark-grown seedlings (Briggs et al., 2001). Results from the present study are consistent with that view. In dark-grown seedlings, PHOT1::GFP fluorescence is found closely associated with the outermost surface of the cytoplasm in all cell types in which we found it expressed. What is surprising is that different cell types and similar cell types at different stages of development may show unique patterns. In the cotyledons, distribution appears uniform at the plasma

membrane of mesophyll cells but is limited almost entirely to the anticlinal walls of the epidermal cells. Little, if any, signal was detected on the periclinal walls (Figs. 11, 14, 15). Expression in the marginal epidermal cells was especially weak compared to the cells on the abaxial surface of the cotyledons (Fig. 12). Like other epidermal cells, the guard cells also have PHOT1::GFP largely on their anticlinal walls (Fig. 12). However, it appears later in guard cells than in the other epidermal cells (Fig. 12B and 12E) and shows particularly strong expression on the contacting walls between the two guard cells of a single stoma (Fig. 12B). In the dividing tissue at the cotyledon margins, there is also exceptionally strong expression at what appears to be recently laid down cell walls of the mesophyll cells (Fig. 12A). Blue light mediates the expanding of cotyledons and leaves, Van Volkenburgh (1999) suggested that it is the layer of mesophyll cells increase cotyledon expanding but the epidermal cells limit the expanding. It is reasonable to suppose that the PHOT1 increase the dividing rare of mesophyll cells under illumination.More experiments are needed to support this hypothesis.

PHOT1 also mediates the chloroplast avoidance (Jarillo et al., 2001; Kagawa et al., 2001) and accumulation (Sakai et al., 2001) responses. The localization of PHOT1 gives clues to understand these processes. The chloroplasts develop in the mesophyll cells of 4 days old light-grown seedlings. In these cells, PHOT1::GFP signals are found on the surface of chloroplasts rather than the PM (Fig. 13). PHOT1 may interact with the J-domain protein, JAC1, in the process of initiating chloroplast movement (Suetsugu et al.,2005) and it has been shown that motor proteins of the myosin class VIII are involved in the PHOT1-dependent blue light-stimulated movement of chloroplast (Krzeszowiec et al., 2007). This suggests that the actin cytoskeleton plays an important role the PHOT1-mediated intercellular movements. Actually, disrupting actin filaments can stop the recycling of PHOT1::GFP too (Fig. 30 G).

In the hypocotyle hook and elongation zone, there is strong expression of PHOT1::GFP localized along the anticlinal and outer periclinal walls of cortical cells, moderate abundance along the end walls of elongating epidermal cells, and weak abundance at their outer walls (Figs.14 and 16). These PHOT1::GFP signals are forming a ‘C’-shaped pattern in longitudinal section, with the strongest signals from outer periclinal walls. This subcellular localization of PHOT1 reflexes the role of the hypocotyle hook and elongation zone in the phototropic responses (see the Chapter

4.1.1). The localization of PHOT1on the outer membrane provides an efficient pattern of photoreception. In elongating and mature tissues, as the cell surfaces become more completely labelled, outer periclinal walls do not have such priority. The polar localization of PHOT1 on the cross walls suggested that the PHOT1 may play intracellular roles here.

4.1.3 Cross-Wall Localization of PHOT1 in the Root Transition Zone Suggests Roles of PHOT1 in Polar Auxin Transport

Unlike the localization of PHOT1 in the shoot, most of the PHOT1::GFP signal is found along the cross walls in cortical cells of the root elongation region, especially the root transition zone, whereas the periclinal walls are only weakly labelled in these cells. These results are comparable to the subcellular localization of PIN2 protein, which is mainly localized on the cross-wall membranes of cortical and epidermal cells of the transition zone (Fig. 18 and Fig. 35).

At the root tip, members of PIN-formed proteins build up a transportation network to modify the distribution of auxin (Blilou et al., 2003). Under gravitropic and phototropic stimulation, they determine the asymmetry of distribution between both root sides, resulting in differential elongation of cells on both sides. PIN2 acts as the regulator for the auxin transport from the root tip upwards. PHOT and PINOID (PID) proteins have similar evolutionary ancestors and belong to the same protein family, namely the AGC kinases (Galván-Ampudia and Offringa, 2007). PID is well-known to affect the function of PIN proteins as *pid* mutants are losing the apical polar localization of PIN1 protein (Friml et al., 2004). PID and PIN1 and PIN2 proteins are partly co-localized at the cross-wall plasma membrane in *Arabidopsis* roots and hypocotyls. This observation suggests that PHOT1 and PIN2 proteins may not only be co-localized on the same plasmamembrane domain but may also functionally interact. Furthermore, PID is interacting with NPY1, which again shows a homology to NPH3 (Cheng et al., 2007). Cheng et al. hypothesized that the PID/NPY1 and PHOT1/NPH3 act via similar pathways to modify polar auxin transport. The result in Fig.37 supports this hypothesis well, because the localization of NPH3::GFP also shows perfect polarity, and NPH3::GFP localized all on the cross wall membrane of root cells. However, this hypothesis still needs more additional experiments to be verified.

The polar localization of PHOT1 in root cells is also one reason, why work in this thesis is focused on the root tip of *Arabidopsis* plants, which is not a popular object for phototropic analysis.

4.2 BL-Induced Relocalization of PHOT1::GFP is achieved by Receptor Mediated Endocytosis

Sakamoto and Briggs (2002) have reported blue-light-induced movement of PHOT1::GFP into the soluble fraction of the cytoplasm and Knieb et al. (2004) have obtained a similar result using native PHOT1 protein in solution. In both studies high-speed centrifugation was used to separate membrane and soluble proteins. Knieb et al. (2004) estimated that at least 20% of the total PHOT1 was released to the cytoplasm following blue-light treatment of etiolated mustard seedlings. Immunoblotting did not provided any evidences for breakdown products in either study. The question as to whether some of the cytoplasmic PHOT1::GFP is present within intracellular vesicles has remained unresolved so far, although results reported by Kong et al. (2006) indicate that PHOT2 appears to migrate into vesicles that co-localize with a Golgi marker upon blue light induction. In the following (Chapter 4.2.2), data will be presented, which support the localization of PHOT1 within endosomal vesicles.

4.2.1 Blue-Light Effects on PHOT1::GFP Subcellular Distribution

The reasons for blue-light-induced re-localization of PHOT1 and its movement into the cytoplasm are not clear. It could be a mechanism to desensitize plant tissues to BL by removing photoreceptor from the region of the plasma membrane, where it is required to interact with other PM-associated proteins. As mentioned in the introduction, BL induces some major ionic changes in plant tissues. It has been shown by Fuchs et al. (2003), that the potassium channel, ZMK1, is expressed as a gradient across unilaterally illuminated maize coleoptiles. However, the gradient developed relatively slowly, only after 60 min irradiation and therefore it is unlikely to be related directly to blue-light-induced changes in subcellular distribution. Cho and Spalding (1996) reported a rapid transient depolarization in *Arabidopsis* hypocotyls exposed to BL, attributable to the activation of anion channels. This transient response occurred well before we observed the first changes in PHOT1::GFP distribution (Figs. 19, 20). Whether these changes bear a causal relation to subsequent changes in PHOT1 distribution remains to be determined.

There are ionic changes with kinetics similar to those of the blue-light-mediated PHOT1::GFP re-localization and recovery described here. Baum et al. (1999) reported rapid but transient increases in calcium uptake in response to a blue-light pulse by light-grown *Arabidopsis* seedlings expressing the calcium sensing aequorin system. The overall changes lasted less than 100 s. However, a single blue-light pulse desensitized the system to subsequent pulses and recovery took place over 3–4 h, not unlike the dark recovery to a strict localization of PHOT1::GFP at the plasma membrane reported in the present study (Fig. 22). Two groups have reported blue-light-induced increases in calcium uptake by etiolated tissues of *Arabidopsis* (Stoelzle et al., 2003) and several other dicot species (Babourina et al., 2003), respectively. Stoelzle et al. (2003) found the response strongly reduced in a *phot1-5* mutant and completely absent in a *phot1-5/phot2-1* double mutant. In both studies, the kinetic was consistent with those for blue-light-induced PHOT1::GFP re-localization, with the changes detectable several minutes after the onset of BL and continuing for 15 or more minutes thereafter. It would be premature to do more than point out the correlation of these ionic changes with changes in the subcellular distribution of PHOT1::GFP. Further experimentation should be performed to determine, whether there is a causal relationship between these changes in calcium movement and the loss of PHOT1 from the plasma membrane in BL and its subsequent dark recovery to a plasma-membrane-only distribution.

4.2.2 Internalization of PHOT1 is Accomplished via Endocytosis

Data presented in section 3.2 showed that internalization of BL-activated PHOT1 sensor occurred in two separate steps. Firstly, PHOT1::GFP accumulates in punctate structures, which are then released from the plasma membrane and co-localize with endosomal membranes (Wan *et al.,* 2008). These PHOT1::GFP enriched endocytic vesicles can be traced by the quick scanning mode of the microscope (Fig. 26). The PHOT1::GFP signal is firstly assembled into aggregates associated with the plasma membrane. Subsequently, the PHOT1::GFP positive structures are released as discrete spots. The membrane endocytic marker FM4-64, which emits red fluorescence in the hydrophobic environment of the membrane, is a very useful tool for the studies of endocytosis. FM4-64 can not cross the double lipid layer of the plasma membrane, and the only way that this membrane tracer can get access to the cytoplasm is via

endocytosis. The data in the Figs. 26 and 27 prove that the PHOT1::GFP-positive vesicles are part of the membrane recycling endocytic system. FM4-64 labelled endosomes show PHOT1::GFP fluorescence, suggesting that at least part of PHOT1::GFP internalization is associated with endocytosis.

Prevacuolar compartments (PVC) and trans-Golgi networks (TGN) have a function in protein secretion and endosomal recycling (reviwed by Šamaj et al., 2005, Jürgens 2004.). In order to characterize the movement of endocytic PHOT1 in plant cells, the inhibitor of exocytosis and vesicle recycling, brefeldin A (BFA), and the endocytic inhibitor, wortmannin were applied. The results show, that consistent with other reports on BFA-action (Nebenfuhr et al., 2002), PHOT1::GFP molecules are trapped within the enlarged BFA-compartments. This finding provides strong evidence that internalization of PHOT1 occurrs along endosomal recycling pathways (Fig. 28). Protein synthesis is not required for this process, since cycloheximide pre-treatment does not stop the formation of PHOT1::GFP enriched BFA-induced compartments in dark treated cells (Fig. 30D).

Wortmannin, an inhibitor of PI3 kinase and PI3 kinase related enzymes, targets the early endosomal transportation in animal and plants cells (Simonsen *et al.,* 1998; Mills *et al.,* 1999). In plant cells, Wortmannin traps PVC-localized proteins within ring-like structures, while the TGN-localized proteins remain unaffected (Miao *et al.,* 2006). In addition, Tse *et al.* (2006) suggested that Wortmannin causes stacking of PVCs into enlarged endosomal structures, which are enriched also with endocytic PIN2 (Jaillais *et al.,* 2006). Secretion of proteins is not effected by Wortmannin. It is conceivable that wortmannin affects PHOT1 because of its membrane-bound nature (Figs. 30E and F). Taken together, the reactions to both inhibitors support the assumption that PHOT1 is recycled via PM-endosomal-TGN-PVC-PM recycling pathways. Additional experiments using the actin inhibitor latrunculin B (Fig. 30G) have proven that this pathway is dependent on the actin cytoskeleton.

4.2.3 ARF1-GTPase, the Key Regulator of Endocytosis, is Modified by PHOT1

ADP-ribosylation factors (ARFs) regulate vesicular trafficking and protein secretion/sorting in many kinds of organisms at the interfaces between Er and Golgi, endosomes and PM and possibly between other endomembrane compartments (Donaldson and Honda, 2005, Anders et al., 2008). GNOM is a plant specific

member of the ARF Guanosine Exchange Factor family (ARF-GEF) which activate ARFs in the processes of protein sorting und vesicle budding. GNOM has also been shown to modify the sorting and vesicular trafficking of PINs (Anders et al., 2008). As a key regulator of endocytosis, the functional role of ARF-GEFs is still far from clear. In *Arabidopsis,* GNOM regulates the vesicular trafficking between Endosomes and the Plasma membrane (Teh and Moore, 2007). Once activated by ARF-GEFs, ARFs recruit coat proteins such as COPI (Sun et al., 2007, Antonny et al., 2005) and regulate phospholipid metabolism; they also modulate the structure of actin filaments on the membrane surfaces (Myers and Casanova, 2008).

BFA specifically targets ARF-GEFs (Peyroche et al., 1999). The BFA-sensitivity of PHOT1 suggests, that the endosomal recycling of PHOT1 is related to the ARF-mediated pathways. Uhrig and coworkers (Botanisches Institut of University of Cologne, Joachim Uhrig, personal communication, unpublished data) analyzed the protein interaction between plant ARFs (ARF1, ARF6, and ARL1) and PHOT1, 2 proteins. By using the yeast two-hybrid assay, they found a direct linkage between the active form of ARF 1 (Q71L and д17) and both PHOT1 and PHOT2 proteins. The inactive form of ARF1 did not show such linkage to PHOT1 (Joachim Uhrig, unpublished).

Clearly, further studies are needed in order to determine the role of PHOTs in the interaction with ARFs. It is still unclear, whether the blue light-activated PHOT1 regulates the function of ARF molecules then modify the endosomal recycling, or the ARF-GEF complex is participating in the recycling of PHOT proteins. The first hypothesis may have more potential than the second one, because the level of PHOT1 recycling reflects the intensity of blue light illumination, this process seems to act as the trigger in the signaling pathways.

4.2.4 Endocytosis of PHOT1::GFP is Affected by BL Illumination

Under BL illumination, part of the PHOT1 molecules is released from the PM via endocytosis. In Chapters 3.1, it was suggested, that internalization is a two step process: at first, PHOT1::GFP signal are collected on the cell surface together, then it moves inside the cytoplasm. The speed and the level of this process reflect the amount of photons arrived on the surface of the plant. The fate of the internalized portion of PHOT1 is still unclear. Sakamoto & Briggs (2002) suggested that a part of the

internalized PHOT1 is degraded, because the total amount of PHOT1 decreased under continuous BL illumination. The data collected in this thesis support this hypothesis, because co-localization of PHOT1::GFP with FM4-64 was not identical and there were diffuse clouds of PHOT1 around the co-localized endosomal compartments. Immunoblotting studies also suggested that part of PHOT1 becomes soluble after illumination (Knieb et al., 2004), and Sakamoto suggested that after 24 hours of illumination, the total amount of PHOT1 proteins is decreased dramatically. All these studies suggest that the blue-light activated PHOT1::GFP is internalized via two different endocytic pathways: one targets on the activated PHOT1 for degradation and the other feeds into the endocytotic vesicular recycling pathway. Alternatively, there may be only one endocytic pathway and the internalized PHOT1 population would then be sorted subsequently either for degradation or for endocytic recycling.

Furthermore, the size of BFA-induced endosomal compartments corresponds to the rate of exocytosis of target proteins. After the inhibition of protein synthesis by CHX, PHOT1::GFP is still trapped within these BFA-induced compartments in both dark and light conditions. This fact suggests that the recycling of PHOT1 between the plasma membrane and endosomal membrane system is active even under dark conditions. However, the BL illumination increased the rate of PHOT1 recycling, as inferred from the increased size of the BFA-induced compartments. This is true for all cell types investigated in the present study (Table 4). Furthermore, increasing the BL intensity during BFA treatment also stimulates the size of PHOT1::GFP enriched BFA-induced endosomal compartments (Fig. 30 A-C). Comparing the time lapse images in Fig. 29, it can be concluded, that BL accelerates the recycling of PHOT1 between endosomes and the plasma membrane. It is very attractive to speculate, that this endosomal recycling of activated PHOT1 represent an integral part of BL-induced signal transduction.

4.2.5 Signaling Endosomes as Integrators of Environmental Signals?

From our knowledg of cell surface receptors in animal cells, such as receptors for epidermal growth factor and transferring (reviewed by Ibáñez, 2007), for example, we can infer that activated receptors will undergo endocytosis in plants too. Receptor mediated endocytosis (RME) has indeed been documented in plant cells. This was achieved by observing the uptake of recombinant human transferrin (hTfr) expressed

in *Arabidopsis* (Ortiz-Zapater *et al.,* 2006). Another recent example is the brassinosteroid receptor, BRI1, which is internalized by the RME process (Geldner *et al.*, 2007). Furthermore, the proteins that are essential for endosomal vesicle transport, such as SNAREs, Rabs and other proteins, are also found in plant cells. They are playing key roles in the transduction pathways (Chow et al., 2008, Anders et al., 2008, reviewed by Samaj et al., 2006). A dynamic motor protein, myosin VIII, has been found to be involved in the endosomal trafficking in *Arabidopsis* cells too. It proved an actin filament-dependent mechanism of RME in plant cells (Sattarzadeh et al., 2008). This thesis provides new evidences to understand relationships between the cell surface receptor of plant cells and the intercellular signal transduction. The rate of both, internalization as well as endosomal recycling of the BL activated PHOT1 is positively correlated with strength and duration of illumination. So it is reasonable to hypothesize, that BL-induced endocytic internalization of the activated PHOT1 is involved in BL signal perception and/or transduction. In this process, BL has a ligand-like role and activates the PHOT1 by conformation changes.

4.2.6 Model to Describe the PHOT1-Mediated Signaling by Endosomal Vesicular Relocalization.

Fig. 41 shows steps of PHOT1 relocalization schematically. Firstly, PHOT1 is localized on the PM uniformly and smoothly. The changes of molecular conformation or the status of phosphorylation cause internalisation of PHOT1 into endosomal vesicles. The mechanism of this process is still unclear. It may be speculated, that NPH3 acts as a scaffold (Pedmale and Liscum, 2007) and PHOT1 may be internalized as dimers (Salomon et al., 2004). As the first known component between endocytosis and BL receptor, ARF1 helps PHOT1 containing endosomal vesicles to fuse with the TGN or PVC compartments. This process even operates under dark condition, while blue light signals accelerate the internalisation of PHOT1. The experiments also suggested that the level of PHOT1 internalization reflexes the intensity and time of blue light illumination. Furthermore, the exchange of ARF-GEF-GDP (inactive form) for ARF-GEF-GTP (active form) is blocked by BFA. Thus, it can be expected that the recycling of PHOT1 is involved in the endomembrane pathways, and it accelerates recycling of endosomes (see Fig. 41). ARF-GEF is needed in this

process. Does this process have roles in signal transduction? How can it affect the auxin polar transport and involve in lateral differences in cell elongation?

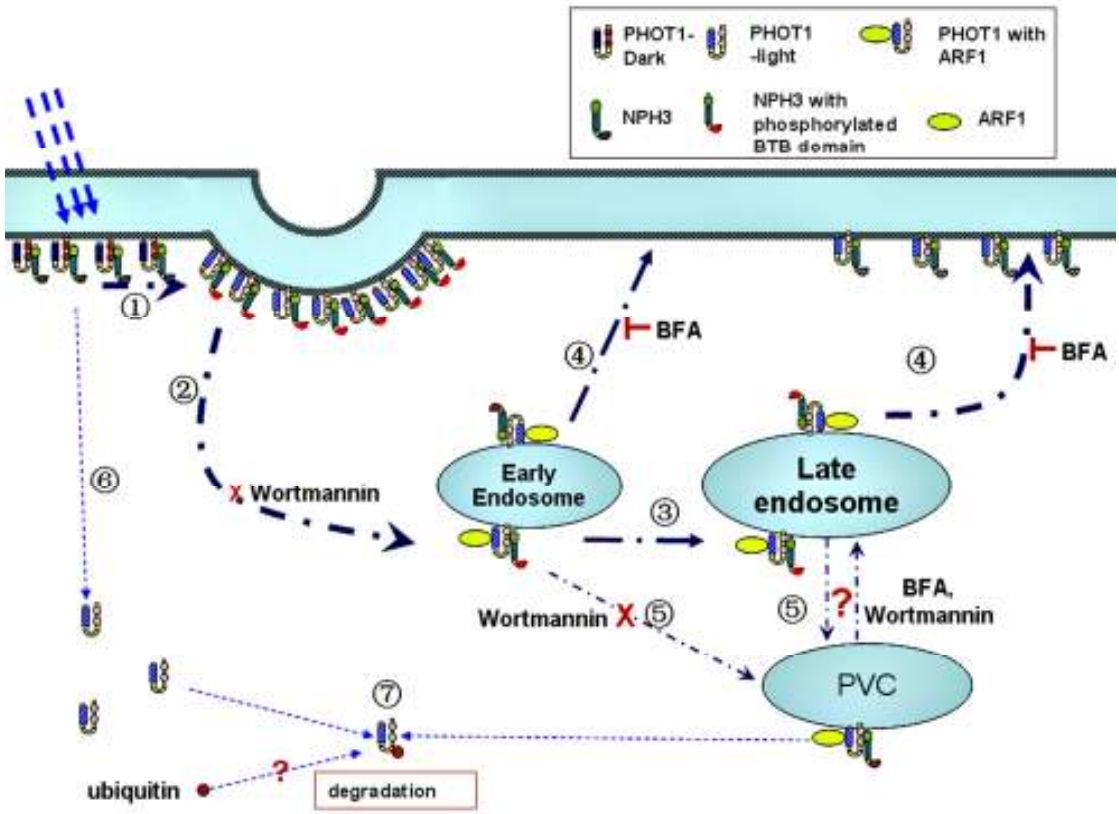

Figure 41: Model to explain PHOT1 movement under blue light illumination.

1. Activation of PHOT1 protein by blue light illumination, the activated PHOT1 molecules are collected at the PM domain of coated pit.
2. The forming of coated vesicles and internalization into endosomes is affected by wortmannin. This step is induced by blue light. The activated form of ARF factors supply docking sites for PHOT1.
3. Early and late endosomes are involved in the recycling pathway.
4. Recycling pathways of PHOT1 are sensitive to BFA, which blocks the exocytosis step by binding on the GNOM then stopping the activation of ARF,
5. Part of the PHOT1 molecules are recycling between endosomes and PVC compartments, this process is wortmannin-sensitive. These data suggest part of the internalized PHOT1 is shuttled between PVC and endosome.
6. Part (appr. 20%) of PHOT1 becomes soluble in the cytoplasm.
7. Soluble and vacuolar portion of PHOT1 is degraded. The degradation may be mediated by the ubiquitin proteasome pathway.

4.3 Intracellular Localization and Endosomal Recycling of PIN-formed Proteins are Determined by BL Illumiation

PIN – formed proteins (PINs) have been considered as auxin efflux carriers or facilitator ever since they have been discovered. As detailed in the Introduction, the recent *in vivo* analysis of auxin flow has drawn out a network of PIN-formed proteins in the root tip. This determines direction and rate of polar auxin transportation in response to gravi- and phototropic stimuli. In this network, PIN1 helps polar auxin transport from shoot to root tip through the cell files in the central cylinder, while the outer cell layers (cortex and epidermis) transport auxin backwards with the help of PIN2.

4.3.1 Light Signal Changes Subcellular Localization of PIN1 and PIN2 Proteins

The polar localization of PIN proteins on the cross-wall membrane is well-known, but only few studies have reported the relationship between polar localization and light signaling (Blakeslee et al., 2004, Laxmi et al., 2008). Laxmi also included that in dark condition, the PIN2 was localized in vacuolar compartments efficiently. In this thesis, data have been presented which allow to conclude that the polar localization of both PIN1 and PIN2 exist only in the seedlings grown under light condition. In dark condition, vacuolar compartments were labelled with PIN1::GFP or PIN2::GFP signals. Blue light illumination caused the disappearance of these vacuole-like accumulation of PINs (Figs. 34 and 35), Laxmi (2008) discovered that the disappearance of these compartments was inhibited by inhibitor of ubiquitin proteasome, this indicated that the vacuole-portion of PINs were destined for degradation under blue light illumination. In order to exclude the possibility that the vacuolar portion of PIN2 was removed via exocytosis, the seedlings were treated by BFA under blue light illumination. In this experiment, FM4-64 was also used to trace the endomembrane trafficking. When the roots were treated in BFA solution during the BL illumination, BFA can not inhibit the disappearance of these vacuolar compartments (Fig. 31). No more PIN2::GFP signals were found inside the vacuolar compartments. These results supported that the vacuole portion of PINs is going to the ubiquitim-depended degradation pathways, but not to the BFA-sensitive

exocytosis. The physiological function of this vacuolar portion of PIN2 is still unclear. Even more experiments were needed to discover its ultimate fates.

4.3.2 The BFA-Sensitive Endosomal Recycling of PIN2 is Depeneded on Blue Light Illumination.

Though the BFA did not inhibit the blue light -depended degradation of PIN2, the BFA-sensitive vesicular recycling of PIN2 was strongly effected by blue light illumination. The BFA-treatment under blue light illumination trapped PIN2::GFP signals within the enlarged endosomal compartments, in which the FM4-64 signals were colocalized. On other hand, the BFA treatment in dark condition did not cause the same pattern of PIN2 relocalization and FM4-64 colocalization. In the etiolated seedlings, formation of vacuolar compartments with PIN2::GFP was not changed by the dark-BFA treatment. This fact again indicted that the BFA-sensitive exocytosis of PIN2 was separated from the light-stimulated degradation of PIN2. In order to exclude all the exocytosis pathways from this PIN2 relocalization, a wide range of inhibitors need to be applied in the experiments.

BFA is an inhibitor specifically targets ARF-GEFs. BFA specifically targets ARF-GEFs. As a result of this action, the recycling of PIN1, PIN2 proteins and polar auxin transport are inhibited. The polar distribution of PIN proteins is also depended on the activation of ARF **(**Kleine-Vehn *et al.,* 2008). Sauer and colleagues (2006) suggested that the auxin signaling did not effects the transcription of PINs, but the polar localization of PINs was controlled by auxin molecules via feed back pathways.

As we discussed in Chapter 4.2.3, the ARF factor is also a key factor in blue light-mediated endocytic recycling of PHOT1. The results in my studies reveal logical linkages between BL signaling and rates of endocytic trafficking directly. Firstly, BL signals activate the PHOT1 by changing the protein conformation. Amount of PHOT1 internalized into cytoplasm depends on illumination time and on light intensities. Although the mechanisms are not clear, these dynamic parameters and the colocalization with FM4-64 suggest that the endocytosis of PHOT1 is accomplished *via* a receptor mediated endocytosis. Secondly, the GNOM localization in plant cells is specific on early/recycling endosomes which are targets of BFA. Therefore, PHOT1 is trapped within BFA-induced endosomal compartments together with FM4-64. At the same time, PIN1 and PIN2 proteins are also trapped in the FM4-64

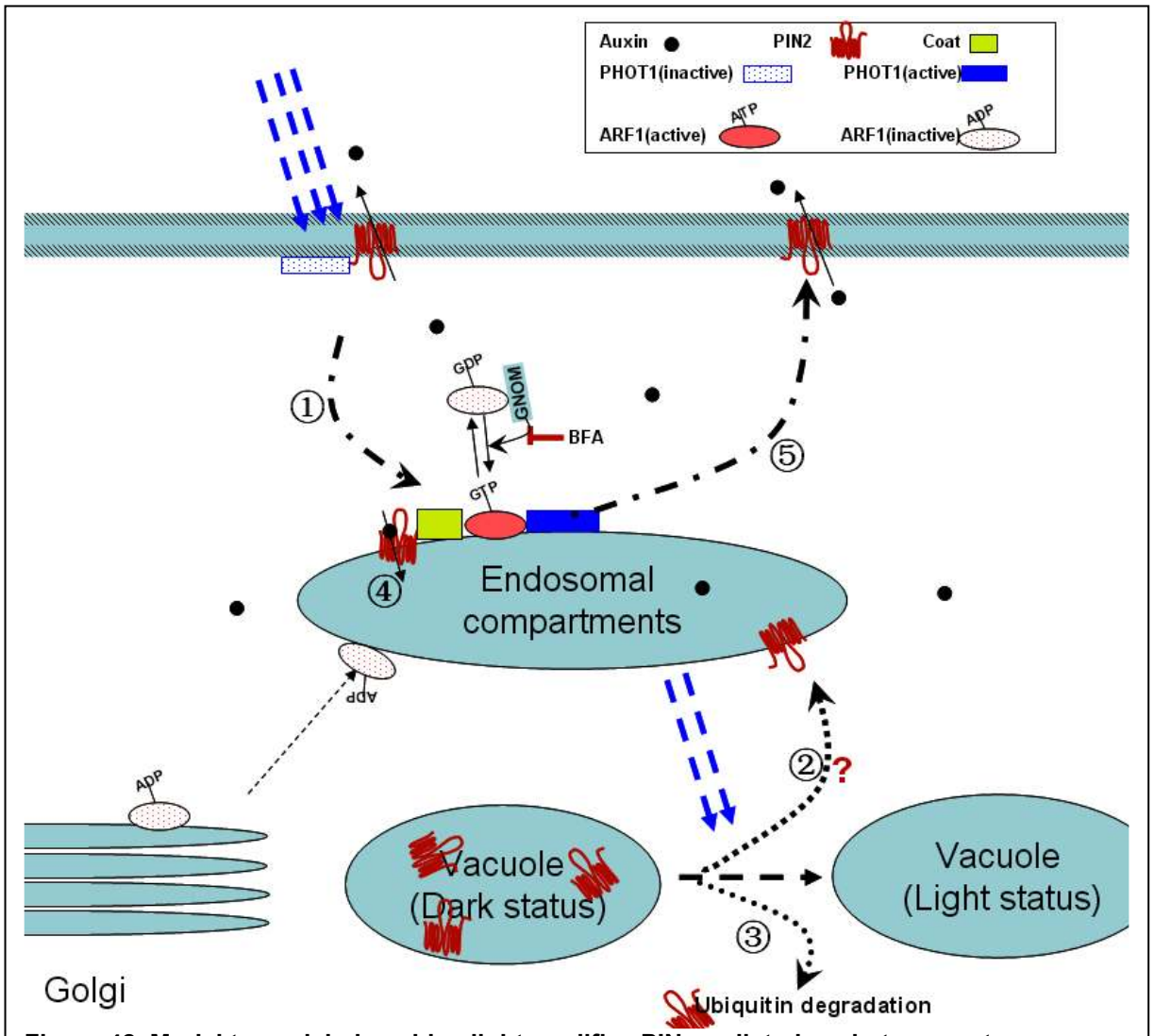

Figure 42. Model to explain how blue light modifies PIN-mediated auxin transport.

1. Blue light increases the endocytosis rate of PHOT1.
2. Under dark condition, small vacuoles (i.e., prevacuolar compartments) contain PIN2 which is released under blue light illumination via unknown pathways. PIN2 is then localized on the endosomal compartments and supports the efflux of auxin.
3. At least part of the vacuole localized PIN2 was degradated via ubiquitin pathways.
4. PIN2 supports transmembrane transport of auxin molecules. This process does not only exist across the PM, but also across the membrane of endosomes. Polar auxin transport depended on polar localization of this vesicular recycling pathway.
5. Vesicle-based export of auxin is BFA sensitive. BFA blocks exocytosis and stops the polar auxin transport.

enriched BFA-induced compartments. These data suggest that the blue light-activated PHOT1 can accelerate the recycling rate of PIN proteins and modify the auxin polar transport in a direct way. Thirdly, the active forms of ARF (ARF-GTP) have physical relationship with the PHOT1 on endosome compartments. The activated ARFs are likely to give PHOT1 docking sites at endosomal membranes. BL

stimulation increases the trafficking of PHOT1 in the cytoplasm via endocytosis, this process may affect the vesicle fusion in the trafficking pathways. Furthermore, the fusion of early and late endosome in BFA treatments are suporting this hypothsis (Fig. 35).

4.3.3 Root Phototropism

In this thesis, experiments were undertaken to elucidate the intracellular localization and fate of BL photoreceptors in response to illumination. As discussed in Chapter 4.3.2, that the endosomal trafficking of PHOT1 can modify the PIN2 recycling under BL illumination. Here I analyzed root phototropism of null mutant *pin2* (*eir1-4).* Mutant seedlings lost the abilities of phototropic response to BL signals completely, while the shoot organ was less influenced due to the lack of PIN2 (Chapter 3.3.1).

In *Arabidopsis* roots, PIN2 has similar distribution as PHOT1. Interestingly, both of them are not expressed in the root cap. This is surprising, at least in Zea mays, the root cap is supposed to be the organ of light perception (Mullen et al., 2002). The root cap has been suspected as the light perception organ of *Arabidopsis* too. However, there is still no direct analysis of this question. The analysis with *pin3-3* gives indirect evidences that the PIN3 has essential roles in the phototropic responses of root apices (Chapter 3.3.9). The relocalization of PIN3 proteins in the columella root cap cells are observed under reorientation of root in gravity vector, and has been supposed to be the mechanism to distribute auxin asymmetricly (Friml et al., 2002). Whether a similar mechanism plays a role under lateral illumination is still unclear. Moreover, asymmetric auxin distribution at root cap has been observed in the *proDR5::GFP* transformed *Arabidopsis* seedlings too (Chapter 3.3.8). Thus, root cap is clearly one of the sensory organs for photoreception. Because PHOT1 is not expressed in root caps, there must be other photoreceptors involved. PHYA and PHYB can be candidates with high potentials. PHYA and PHYB are essential to the RL induced root positive phototropism of *Arabidopsis* plants (Kiss et al., 2003) and BL can also activate these putative RL receptors and inhibit the gravitropic responses of *Arabidopsis* (Lariguet and Frankhauser, 2004). Studies with *phyA and phyB* mutants are important to discover the mechanism of root apex phototropisms. Another clue comes from the studies to analysis the region of meristem. Dark-grown

seedlings have smaller meristem than the light gown seedlings. Furthermore, the illuminated side shows extended and more active cell divisions than the shaded side.

Based on these results, it is clear that the PIN proteins are not only essential for the root gravitropic responses, but also for the root phototropisms. Asymmetric distribution of auxin occurs at illuminated root tips of *Arabidopsis* too. PIN3 is expressed at root caps and redistributes auxin to the shaded side under lateral light illumination. The signals of gravity and lateral light are sensed by root cap cells. Subsequently, the root tip bends to the light source at an angle of about 18 degree (Fig.40), until the competition of two kinds of signals reaches balance. More studies are needed to find out which photoreceptor(s) mediate(s) this process.

At the meristem and root apex transition zone, PHOT1 modifies the endosomal recycling of PIN2 in cortical cells. The recycling of PIN2 adjusts the rate of upward auxin transport and gives another clue to integrate both signals of gravity and light. This analysis results in a “delayed” response to light signals. Mullen (2000) found that the *Arabidopsis* roots response to light occur at the central elongation zone, while the roots respond to gravity at the root apex transition zone. Here I suppose that the root apex transition zone does not only act as reaction organ to gravitropism, but also as sensory region for integrating different environmental signals. Clearly, more detailed analysis is needed to improve our still limited understanding how sensory signals from gravi- sensing and light-sensing are integrated in order to allow all adaptive root growth behavior.

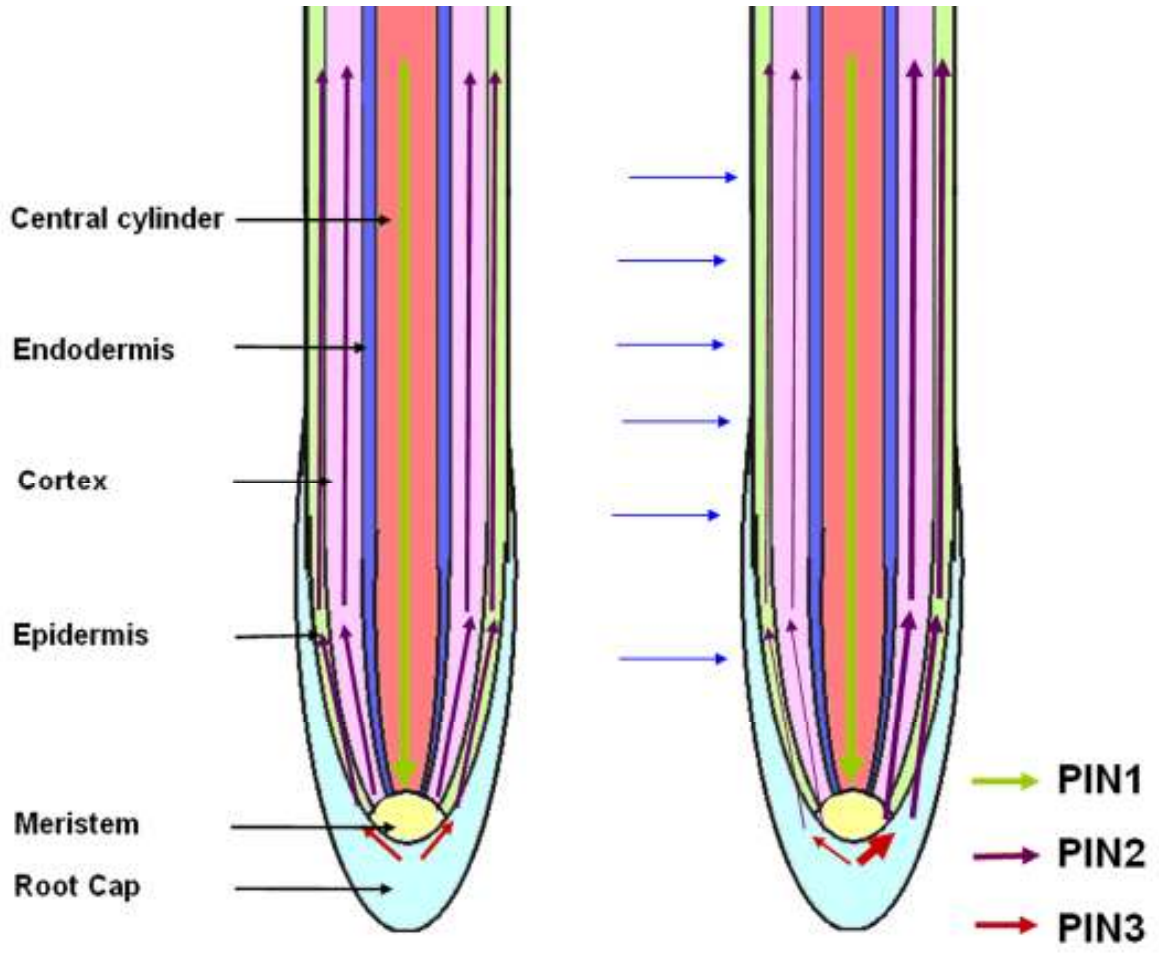

Figure 41 Schematic model to describe how the blue light modifies PAT pathways.
Arrows are showing the PAT pathways in the root tip of *Arabidopsis*. Left: root in vertical position without light signals; Right: root in vertical position with lateral blue light illumination (Blue arrows). Apical transportation of auxin via central cyclinder cells is modified by the auxin efflux facilitators PIN1 (green arrow). At the root cap, the PIN3 distributes auxin to the shaded side predominantly. The mechanism of this process is still unclear (Red arrow). PIN2 helps to shift the PAT towards the epidermis and cortex and PIN3 tansports auxin in basal direction through the epidermis and cortex (Purple arrow). This transportation pathway is enhanced by the blue light activated receptor PHOT1 via vesicular trafficking. For the sake of simplicity, I did not include PIN4 and PIN7 which are also expressed in cells of root tips.

5. Outlook

Based on results of this thesis, new problems are identified and new questions emerge. For example, it is unclear how PHOT1 and ARF molecules interact via their interaction domains. The recently published structure of PHOT1 does not give an answer to this question. Though it is widely accepted that polar localization and vesicular recycling of PINs is regulated by the ARF-GEFs, the particular molecular mechanisms are still unclear. Without understanding these mechanisms, it is not easy to explore further the exact signal transduction pathways linking PHOT1 endocytosis with the recycling of PINs.

To this end, it is important to conduct a domain analysis of ARF, ARF-GEF and PHOT1, and introduce point mutations to PHOT1. Of particular interest is the question wether the phosphorylation site of PHOT1 interacts with ARF. Furthermore, I have also crossed the PIN2::GFP construct into the *phot1-5, phot1-2/phot2-1* and *nph3-1* mutant backgrounds. This will allow identification of those members of the blue light signaling pathways which modify the PIN2 relocalization.

6. Summary

In this thesis, the subcellular localization and possible functions of the blue light receptor, PHOT1, is examined. Results are presented, which indicate that blue light-induced relocalization of auxin efflux carriers (PIN-proteins) is adjusted by PHOT1 via ARF-mediated and BFA-sensitive vesicle trafficking pathways.

PHOT1 was visualized by expressing the PHOT1::GFP reporter in *Arabidopsis* mutants which contain a dysfunctional copy of the endogenous PHOT1-gene. It is shown that the subcellular localization of PHOT1 in plant cells reflects the physiological functions and development stages of special kinds of cells. For example in guard cells, PHOT1 appears only in the mature developmental stage, when these cells begin to react to blue light signals. Especially, the specific roles of PHOT1 were addressed in root and shoot apical meristems. The obtained data suggest that PHOT1 has different roles in root and shoot phototropic responses. PHOT1 in root tissues acts to adjust the polar auxin transport, while PHOT1 in shoot tissues has more abundant roles. It is also suggested that the mechanism of phototropic responses in shoots and roots might be different from each other.

Interestingly, the PHOT1::GFP signals are quickly released from the plasma membrane and appear in intracellular vesicles, when cells are irradiated with blue laser light in the process of scanning in the confocal microscope. The level of PHOT1 relocalization reflects the amount of photons reaching the surface of the *Arabidopsis* cells. PHOT1-positive vesicles colocalize with the endosomal tracer, FM4-64, indicating that that light-induced movements of PHOT1-positive endosome are analogous to the ligand-induced receptor mediated endocytosis. PHOT1-mediated blue light sensing is sensitive to inhibitors of exocytosis and endocytosis and is also dependent on intact actin filaments.

Endosomal recycling of PIN proteins is considered as the mechanism to adjust the levels of polar auxin transport. Here it is demonstrated that blue light affects the recycling of PIN1 and PIN2 between the plasma membrane and the endosomal compartment. The *pin2* null mutant lacks phototropic responses in roots, while the shoot phototropism in this mutant is independent on PIN2. By taking into account the

polar transport of auxin under asymmetric illumination at the root tip, a testable model for the mechanism of root phototropism is proposed, which will helpful in guiding future phototropism research .

References

Abas L., Benjamins R., Malenica N., Paciorek T., Wiśniewska J., Moulinier-Anzola J.C., Sieberer T., Friml J., Luschnig C. (2006) Intracellular trafficking and proteolysis of the *Arabidopsis* auxin-efflux facilitator PIN2 are involved in root gravitropism. *Nat Cell Biol.* **8,** 249-256.

Ali G.S., Prasad K.V., Day I., Reddy A.S. (2007) Ligand-dependent reduction in the membrane mobility of FLAGELLIN SENSITIVE2, an *Arabidopsis* receptor-like kinase. *Plant Cell & Physiol.* **48,** 1601-1611.

Anders N., Nielsen M., Keicher J., Stierhof Y.D., Furutani M., Tasaka M., Skriver K., Jürgens G. (2008) Membrane association of the *Arabidopsis* ARF exchange factor GNOM involves interaction of conserved domains. *Plant Cell.* **20,** 142-151.

Azzam R., Chen S.L., Shou W., Mah A.S., Alexandru G., Nasmyth K., Annan R.S., Carr S.A., Deshaies R.J. (2004) Phosphorylation by cyclin B-Cdk underlies release of mitotic exit activator Cdc14 from the nucleolus. *Science.* **305,** 516-519.

Babourina O.K.,Newman I.A., Shabala S.N. (2003). Electrophysiological localization of blue light sensory sites in etiolated dicotyledon seedlings. *Plant Cell Environ.* **26,** 1505–1514.

Baluška F., Šamaj J., Menzel D. (2003) Polar transport of auxin: carrier-mediated flux across the plasma membrane or neurotransmitter-like secretion? *Trends in Cell Biology.* **13,** 282-285.

Baluška F., Volkmann D., Menzel D. (2005) Plant synapses: actin-based adhesion domains for cell-to-cell communication. *Trends in Plant Science.* **10,** 106-111.

Baluška F., Schlicht M., Volkmann D., Mancuso S. (2007) Vesicular secretion of auxin: Evidences and implications. *Plant Signaling & Behavior.* **3,** 254-256.

Baum G., Long J.C., Jenkins G.I., Trewavas A.J. (1999) Stimulation of the blue light phototropic receptor NPH1 causes a transient increase in cytosolic Ca^{2+}. *Proceedings of National Academy of Sciences USA.* **96,** 13554-13559.

Bennett C.L. (2005) Astrophysical observations: lensing and eclipsing Einstein's theories. *Science.* **307,** 879-884.

Blakeslee J.J., Bandyopadhyay A., Peer W.A., Makam S.N., Murphy A.S. (2004) Relocalizatin of the PIN1 auxin efflux facilitator plays a role in phototropic responses. *Plant Physiol.* **134,** 28-31.

Blilou I., Xu J., Wildwater M., Willemsen V., Popper I., Friml J., Heldstra R., Aida M., Palme K., Scheres B. (2005) The PIN auxin efflux facilitator network controls growth and patterning in *Arabidopsis* roots. *Nature.* **433,** 39-44.

Briggs W.R., Beck C.F., Cashmore A.R., Christie J.M., Hughes J., Jarillo J.A., Kagawa T., Kanegae H., Liscum E., Nagatani A., Okada K., Salomon M., Rüdiger W., Sakai T., Takano M., Wada M., Watson J.C. (2001) The phototropin family of photoreceptors. *Plant Cell.* **13,** 993-997.

Bonifacino J.S., Jackson C.L. (2003) Endosome-specific localization and function of the ARF activator GNOM. *Cell.* **112,** 141-2.

Bolte S., Talbot C., Boutte Y., Catrice O., Read N.D., Satiat-Jeunemaitre B. (2004) FM-dyes as experimental probes for dissecting vesicle traffickingin living plant cells. *Journal of Microscopy.* **214,** 159-173.

Briggs W.R., Christie J.M. (2002) Phototropins 1 and 2: versatile plant blue-light receptors. *Trends in Plant Science.* **7,** 204-210.

Chardin P., McCormick F. (1999)Brefeldin A: the advantage of being uncompetitive. *Cell.* **97,** 153-155.

Chen R., Masson P.H. (2006) Auxin transport and recycling of PIN proteins in plants. *Endocytosis in Plants. Plant Cell Monography.* **1,** 139-157.

Cheng Y., Qin G., Dai X., Zhao Y. (2007) NPY1, a BTB-NPH3-like protein, plays a critical role in auxin-regulated organogenesis in *Arabidopsis*. *Proceedings of National Academy of Sciences USA.* **104,** 18825-18829.

Cho M.H., Spalding E.P. (1996) An anion channel in *Arabidopsis* hypocotyls activated by blue light. *Proceedings of National Academy of Sciences USA.* **93,** 8134-8138.

Cho H.Y., Tseng T.S., Kaiserli E., Sullivan S., Christie J.M., Briggs W.R. (2007) Physiological roles of the light, oxygen, or voltage domains of phototropin 1 and 2 in *Arabidopsis*. *Plant Physiology.* **143,** 517-529.

Cholodny N. (1926) Beiträge zur Analyse der geotropischen Reaktion. *Jahrbuch für Wissenschaftliche Botanik* **65**: 447–459.

Chow C.M., Neto H., Foucart C., Moore I. (2008) Rab-A2 and Rab-A3 GTPases define a trans-golgi endosomal membrane domain in *Arabidopsis* that contributes substantially to the cell plate. *Plant Cell.* 20:101-123.

Christie J.M. (2007) Phototropin blue-light receptors. *Annual Reviews of Plant Biology.* **58,** 21-45.

Christensen S.K., Dagenais N., Chory J., Weigel D. (2000) Regulation of auxin response by the protein kinase PINOID. *Cell.* **100,** 469-478.

Correll M.J., Kiss J.Z. (2002) Interactions between gravitropism and phototropism in plants. *J Plant Growth Regul.* **21,** 89-101

DARWIN C. (1880) The Power of Movements in Plants (assisted by F. DARWIN). John Murray, London

De Marais D.J., (2000) Evolution. When did photosynthesis emerge on Earth? *Science.* **289,** 1703-1705

De Oliveira C.A., Mantovani B. (1988) Latrunculin A is a potent inhibitor of phagocytosis by macrophages. *Life Sci.* **43,** 1825-1830.

Dhonukshe P., Aniento F., Hwang I., Robinson D.G., Mravec J., Stierhof Y.D., Friml J. (2007) Clathrin-mediated constitutive endocytosis of PIN auxin efflux carriers in *Arabidopsis*. *Current Biology.* **17,** 520-527.

Dyall S.D., Brown M.T., Johnson P.J. (2004) Ancient invasions: from endosymbionts to organelles. *Science.* **304,** 253-257.

Eitoku T., Nakasone Y., Zikihara K., Matsuoka D., Tokutomi S., Terazima M. (2007) Photochemical intermediates of *Arabidopsis* phototropin 2 LOV domains associated with conformational changes. *Journal of Molecular Biology.* **371,** 1290-1303.

Esmon C.A., Pedmale U.V., Liscum E. (2005) Plant tropisms: providing the power of movement to a sessile organism. *International Journal of Developmental Biology.* **49,** 665-674.

Folta K.M., Maruhnich S.A. (2007) Green light: a signal to slow down or stop. *J Exp Bot.* **58,** 3099-3111.

Folta KM., Spalding EP. (2001) Unexpected roles for cryptochrome 2 and phototropin revealed by high-resolution analysis of blue light-mediated hypocotyl growth inhibition. *Plant J.* **26,** 471-478.

Folta K.M., Lieg E.J., Durham T., Spalding E.P. (2003) Primary inhibition of hypocotyl growth and phototropism depend differently on phototropin-mediated increases in the cytoplasmic calcium induced by blue light. *Plant Physiol.* **133,** 1464-1470.

Freddolino P.L., Dittrich M., Schulten K. (2006) Dynamic switching mechanisms in LOV1 and LOV2 domains of plant phototropins. *Biophysics Journal.* **91,** 3630-3639.

Friml J., Wisiewska J., Benkova E., Mendgen K., Palme K. (2002) Lateral relocation of auxin efflux regulator PIN3 mediates tropism in *Arabidopsis*. *Nature.* **415,** 806-809.

Friml J., Yang X., Michniewicz M., Weijers D., Quint A., Tietz O., Benjamins R., Ouwerkerk P.B., Ljung K., Sandberg G., Hooykaas P.J., Palme K., Offringa R. (2004) A PINOID-dependent binary switch in apical-basal PIN polar targeting directs auxin efflux. *Science.* **306,** 862-865.

Fuchs I., Phillipar K., Ljung K., Sandberg G., Hedrich R. (2003) Blue light regulates an auxin-induced K^+-channel gene in the maize coleoptile. *Proc Natl Acad Sci U S A.* **100,** 11795-11800.

Fujiwara T., Oda K., Yokota S., Takatsuki A., Ikehara Y. (1988) Brefeldin A causes disassembly of the Golgi complex and accumulation of secretory proteins in the endoplasmic reticulum. *J Biol Chem.* **263,** 18545-18552.

Ferreira P., Hemerly A., de Almeida Engler J., Bergounioux C., Burssens S., Van Montagu M., Engler G., Inzé D. (1994) Three discrete classes of *Arabidopsis* cyclins are expressed during different intervals of the cell cycle. *Proc Natl Acad Sci U S A.* **91,**11313-11317.

Galván-Ampudia C.S., Offringa R. (2007) Plant evolution: AGC kinases tell the auxin tale. *Trends in Plant Science.* **12,** 541-547.

Galen, C., Rabenold, J.J., Liscum, E. (2007). Functional ecology of a blue light photoreceptor: effects of phototropin-1 on root growth enhance drought tolerance in *Arabidopsis* thaliana. *New Phytol.* **173,** 91–99.

Geldner N., Friml J., Stierhof Y.D., Jurgens G., Palme K. (2001) Auxin transport inhibitors block PIN1 cycling and vesicle trafficking. *Nature.* **413,** 425-428

Geldner N., Anders N., Wolters H., Keicher J., Kornberger W., Müller P., Delbarre A., Ueda T., Nakano A., Jürgens G. (2003) The *Arabidopsis* GNOM ARF-GEF mediates endosomal recycling, auxin transport, and auxin-dependent plant growth. *Cell.* **112,** 219-230.

Geldner N., Hyman D.L., Wang X., Schumacher K., Chory J. (2007) Endosomal signaling of plant steroid receptor kinase BRI1. *Genes & Development* **21,**1598-1602.

Harada A., Sakai T., Okada K. (2003) PHOT and PHOT2 mediate blue light-induced transient increases in cytosolic Ca^{2+} differently in *Arabidopsis* leaves. *Proc Natl Acad Sci U S A.* **100,** 8583-8588.

Hause G., Šamaj J., Menzel D., Baluška F. (2006) Fine structural analysis of brefeldin A-induced compartment formation after high-pressure freeze fixation of maize root epidermis: Compound exocytosis resembling cell plate formation during cytokinesis. *Plant Signaling & Behavior* **1,** 134-139.

Hauser MT., Bauer E. (2000) Histochemical analysis of root meristem activity in *Arabidopsis* thaliana using a cyclin:GUS (β-glucuronidase) marker line. *Plant and Soil.* **226,** 1-10.

Hubert B., Funke G.L. (1937) The phototropism of terrestrial roots. *Biol Jaarboek.* **4,** 286–315.

Ibáñez C.F. (2007) Message in a bottle: long-range retrograde signaling in the nervous system. *Trends Cell Biol.* **17,** 519-528.

Iino M. (2006) Toward understanding the ecological functions of tropisms: interactions among and effects of light on tropisms. *Current Opinion in Plant Biology.* **9,** 89-93.

Inoue H., Randazzo PA. (2007) ARF GAPs and their interacting proteins. *Traffic.* **8,** 1465-1475.

Inada S., Ohgishi M., Mayama T., Okada K., Sakai T. (2004) RPT2 is a signal transducer involved in phototropin response and stomatal opening by association with phototropin 1 in *Arabidopsis thaliana*. *Plant Cell.* **16,** 887-896.

Jackson C.L., Casanova J.E. (2000) Turning on ARF: the Sec7 family of guanine-nucleotide-exchange factors. *Trends in Cell Biology.* **10,** 60-67.

Jacob T.C., Moss S.J., Jurd, R. (2008) $GABA_A$ receptor trafficking and its role in the dynamic modulation of neuronal inhibition. *Nature Reviews Neuroscience*. **9,** 331-343.

Jaillais Y., Fobis-Loisy I., Miège C., Rollin C., Gaude T. (2006) AtSNX1 defines an endosome for auxin-carrier trafficking in *Arabidopsis*. *Nature.* **443,** 106-109.

Jarillo J.A., Gabrys H., Capel J., Alonso J.M., Ecker J.R., Cashmore A.R. (2001) Phototropin-related NPL1 controls chloroplast relocation induced by blue light. *Nature.* **410,** 952-954.

Kagawa T., Sakai T., Suetsugu N., Oikawa K., Ishiguro S., Kato T., Tabata S., Okada K., Wada M. (2001) *Arabidopsis* NPL1: A photoropin homolog controlling the chloroplast highlight avoidance response. *Science.* **291,** 2138-2141.

Kaplinsky N.J., Barton M.K. (2004) Plant biology. Plant acupuncture: sticking PINs in the right places. *Science.* **306,** 822-823.

Khurana J.P., Best T.R., Poff K.L. (1989) Influence of hook position on phototropic and gravitropic curvature by etiolated hypocotyls of *Arabidopsis* thaliana. *Plant Physiol.* **90,** 376-379.

Kinoshita T., Doi M., Suetsugu N., Kagawa T., Wada M., Shimazaki K. (2001) PHOT1 and PHOT2 mediate blue light regulation of stomatal opening. *Nature* **414,** 656-660.

Kinoshita T., Emi T., Tominaga M., Sakamoto K., Shigenaga A., Doi M., Shimazaki K. (2003) Blue-light- and phosphorylation-dependent binding of a 14-3-3 protein to phototropins in stomatal guard cells of broad bean. *Plant Physiology.* **133,** 1453-1463.

Kiss J.Z., Ruppel N.J., Hangarter R.P. (2001) Phototropism in *Arabidopsis* roots is mediated by two sensory systems. *Adv Space Res.* **27,** 877-885.

Kiss J.Z., Mullen J.L., Correll M.J., Hangarter R.P. (2003) Phytochromes A and B mediate red-light-Induced positive phototropism in roots. *Plant Physiol.* **131,** 1411-1417.

Knieb E., Salomon M., Rüdiger W. (2004) Tissue-specific and subcellular localization of phototropin determined by immuno-blotting. *Planta.* **218,** 843-51.

Koller D. (2000). Plants in search of sunlight. *Advances Bot. Res.* **33,** 35–131.

Kong S.G., Suzuki T., Tamura K., Mochizuki N., Hara-Nishimura I., Nagatani A. (2006) Blue light-induced association of phototropin 2 with the Golgi apparatus. *Plant J.* **45,** 994-1005.

Krzeszowiec W., Rajwa B., Dobrucki J., Gabryś H.(2007) Actin cytoskeleton in *Arabidopsis thaliana* under blue and red light. *Biology of the Cell.* **99**, 251-260.

Lam S.K., Siu C.L., Hillmer S., Jang S., An G., Robinson D.G., Jiang L. (2007) Rice SCAMP1 defines clathrin-coated, trans-golgi-located tubular-vesicular structures as an early endosome in tobacco BY-2 cells. *Plant Cell* **19,** 296-319.

Lariguet P., Dunand C. (2005) Plant photoreceptors: phylogenetic overview. *J Mol Evol.* **61,** 559-569.

Lariguet P., Frankhauser C. (2004) Hypocotyl growth orientation in blue light is determined by phytochrome A inhibition of gravitropism and phototropin promotion of phototropism. *Plant J.* **40,** 826-834.

Lariguet P., Schepens I., Hodgson D., Pedmale U.V., Trevisan M., Kami C., de Carbonnel M., Alonso J.M., Ecker J.R., Liscum E., Fankhauser C. (2006)

PHYTOCHROME KINASE SUBSTRATE 1 is a phototropin 1 binding protein required for phototropism. *Proc Natl Acad Sci U S A*.**103,**10134-10139.

Laxmi A., Pan J., Morsy M., Chen R. (2008) Light plays an essential role in intracellular distribution of auxin efflux carrier PIN2 in *Arabidopsis thaliana*. *PLoS ONE* **3,** e1510

Li Q. H., Yang H. Q (2007) Cryptochrome signaling in plants. *Photochem Photobiol.* **83,** 94-101.

Liscum E., Briggs W. R. (1995) Mutations in the *NPH1* locus of *Arabidopsis* disrupt the perception of phototropic stimuli. *Plant Cell.* **7,** 473-485.

Liscum E., Briggs W. R. (1996) Mutations of *Arabidopsis* in potential transduction and response components of the phototropic signaling pathway. *Plant Physiol.***112,** 291-296.

Liscum E., Hangarter RP. (1993) Light-Stimulated Apical Hook Opening in Wild-Type *Arabidopsis* thaliana Seedlings. *Plant Physiol.***101,** 567-572.

Mandoli D.F., Briggs W.R. (1982) Optical properties of etiolated plant tissues. *Proc Natl Acad Sci USA.* ***7*9,** 2902-2906.

Mancuso S., Marras A.M., Mugnai S., Schlicht M., Zarsky V., Li G., Song L., Hue H.W., Baluška F. (2007) Phospholipase Dζ2 drives vesicular secretion of auxin for its polar cell-cell transport in the transition zone of the root apex. *Plant Signaling and Behavior* **2,** 240-244.

Matsuoka D., Tokutomi S. (2005) Blue light-regulated molecular switch of Ser/Thr kinase in phototropin. *Proc Natl Acad Sci USA.* **102,** 13337-13342.

Matsuoka D., Iwata T., Zikihara K., Kandori H., Tokutomi S. (2007) Primary processes during the light-signal transduction of phototropin. *Photochem Photobiol.* **83,** 122-30.

Michniewicz M., Zago M.K., Abas L., Weijers D., Schweighofer A., Meskiene I., Heisler MG., Ohno C., Zhang J., Huang F., Schwab R., Weigel D., Meyerowitz EM., Luschnig C., Offringa R., Friml J. (2007) Antagonistic regulation of PIN phosphorylation by PP2A and PINOID directs auxin flux. *Cell.* **130,** 1044-1056.

Mills I.G., Jones AT., Clague M.J. (1999) Regulation of endosome fusion *Mol Membr Biol* **16,** 73-79.

Molas M.L., Kiss J.Z. (2008) PKS1 plays a role in red-light-based positive phototropism in roots. *Plant Cell Environ.* **31,** 842-849.

Motchoulski A., Liscum E. (1999) *Arabidopsis* NPH3: A NPH1 photoreceptor-interacting protein essential for phototropism. *Science.* **286,** 961-964.

Mullen J.L., Wolverton C., Ishikawa, H., Evans M.L. (2000) Kinetics of constant gravitropic stimulus responses in *Arabidopsis* roots using a feedback system. *Plant Physiology.* **123,** 665–670.

Mullen J.L., Wolverton C., Ishikawa H., Hangarter R.P., Evans M.L. (2002) Spatial separation of light perception and growth response in maize root phototropism. *Plant Cell Environ*. **25,** 1191-1196.

Murashige T, Skoog F (1962) A revised medium for rapid growth and bio-assay with tobacco tissue cultures. *Physiol Plant*. **15,** 473-497.

Nebenführ A., Ritzenthaler C., Robinson D.G. (2002) Brefeldin A: deciphering an enigmatic inhibitor of secretion. *Plant Physiology* **130,** 1102-1108.

Obrig T.G., Culp W.J., McKeehan W.L., Hardesty B. (1971) The mechanism by which cycloheximide and related glutarimide antibiotics inhibit peptide synthesis on reticulocyte ribosomes. *J Biol Chem.* **246,** 174-181.

Orbovik V., Poff K. (1993) Growth distribution during phototropism of *Arabidopsis* thaliana seedlings. *Plant Physiology*. **103,** 157-163.

Ortiz-Zapater E., Soriano-Ortega E., Marcote M.J., Ortiz-Masiá D., Aniento F. (2006) Trafficking of the human transferrin receptor in plant cells: effects of tyrphostin A23 and brefeldin A. *Plant J*. **48,** 757-770.

Palmer J.M., Short T.W., Gallagher S., Briggs W.R. (1993) Blue light-Induced phosphorylation of a plasma membrane-associated protein in *Zea mays L*. *Plant Physiol.* **102,** 1211-1218.

Peyroche A., Antonny B., Robineau S., Acker J., Cherfils J., Jackson C.L. (1999) Brefeldin A acts to stabilize an abortive ARF-GDP-Sec7 domain protein complex: involvement of specific residues of the Sec7 domain. *Mol Cell.***3,** 275-285.

Poggioli, S. (1817) Della influenza che ha il raggio magnetico sulla vegeratione delle piante. *Bologna – Coi Tipi di Annesio Nobili Opusc Scientif Fasc I,* 9-23

Pratt, L.H., Briggs,W.R. (1966). Photochemical and non-photochemical reactions of phytochrome in vivo. *Plant Physiol* **41,** 467–474.

Pratt, L.H., Coleman, R.A. (1974). Phytochrome distribution in etiolated grass seedlings as assayed by an indirect antibody-labelling method. *Amer. J. Bot.* **61,** 195–202.

Ribchester R., Mao F., Betz W. (1994) Optical Measurements of Activity-Dependent

Membrane Recycling in Motor Nerve Terminals of Mammalian Skeletal Muscle. *Biological Sciences.* **255:** 61-66.

Russinova E., Borst J.W., Kwaaitaal M., Caño-Delgado A., Yin Y., Chory J., de Vries S.C. (2004) Heterodimerization and endocytosis of *Arabidopsis* brassinosteroid receptors BRI1 and AtSERK3 (BAK1). *Plant Cell.* **16**, 3216-3229.

Sakai T., Kagawa T., Kasahara M., Swartz T.E., Christie J.M., Briggs W.R., Wada M., Okada K. (2001) *Arabidopsis* nph1 and npl1: Blue light receptors that mediate both phototropism and chloroplast relocation. *Proc Natl Acad Sci USA.* **98,** 6969–6974.

Sakamoto K., Briggs W.R., (2002) Cellular and subcellular localization of phototropin 1. *Plant Cell.* **14,** 1723-1735.

Salomon M., Lempert U., Rüdiger W. (2004) Dimerization of the plant photoreceptor phototropin is probably mediated by the LOV1 domain. *FEBS Lett.* **572,** 8-10.

Šamaj J., Read N.D., Volkmann D., Menzel D., Baluška F (2005) The endocytic network in plants. *Trends Cell Biol*. **15**, 425-433.

Sattarzadeh A., Franzen R., Schmelzer E. (2008) The *Arabidopsis* class VIII myosin ATM2 is involved in endocytosis. *Cell Motil Cytoskeleton.* **65,** 457-468.

Sauer M., Balla J., Luschnig C., Wisniewska J., Reinöhl V., Friml J., Benková E. (2006) Canalization of auxin flow by Aux/IAA-ARF-dependent feedback regulation of PIN polarity. *Gene Dev.* **20,** 2902-2911.

Sharrock, R. A., Quail, P. H. (1989). Novel phytochrome sequences in *Arabidopsis thaliana*: structure, evolution, and differential expression of a plant regulatory photoreceptor family. Genes Dev. 3, 1745–1757.

Schepens I., Duek P., Fankhauser C. (2004) Phytochrome-mediated light signaling in *Arabidopsis*. *Curr Opin Plant Biol.***7,** 564-569.

Schepens I., Boccalandro H.E., Kami C., Casal J.J., Fankhauser C. (2008) HYTOCHROME KINASE SUBSTRATE4 Modulates Phytochrome-Mediated Control of Hypocotyl Growth Orientation. *Plant Physiol.* **147,** 661-71.

Schlicht M., Strand M., Scanlon M.J, Mancuso S., Hochholdinger F., Palme K., Volkmann D., Menzel D. , Baluška F. (2006) Auxin immunolocalization implicates vesicular neurotransmitter-like mode of polar auxin transport in root apices. *Plant Signaling & Behavior.* **1,** 122-133.

Schwartz A., Koller D. (1980) Role of the Cotyledons in the Phototropic Response of Lavatera cretica Seedlings. *Plant Physiol.* **66,** 82-87.

Shankaran H., Resat H., Wiley H.S. (2007) Cell surface receptors for signal transduction and ligand transport: a design principles study. *PLoS Computional Biology* **3,** 986-999.

Short T.W., Porst M., Palmer J., Fernbach E., Briggs W.R. (1994) Blue Light Induces Phosphorylation at Seryl Residues on a Pea (Pisum sativum L.) Plasma Membrane Protein. *Plant Physiol.* **104,** 1317-1324.

Simonsen A., Lippé R., Christoforidis S., Gaullier J.M., Brech A., Callaghan J., Toh B.H., Murphy C., Zerial M., Stenmark H. (1998) EEA1 links PI(3)K function to Rab5 regulation of endosome fusion. *Nature* **394**, 494–498.

Solomon S.G., Lennie P., (2007) The machinery of colour vision. *Nat Rev Neurosci.* **8,** 276-286.

Stoelzle S., Kagawa T., Wada M., Hedrich R., Dietrich P. (2003) Blue light activates calcium-permeable channels in *Arabidopsis* mesophyll cells via the phototropin signaling pathway. *Proceedings of National Academy of Sciences USA.* **100,** 1456-1461.

Suetsugu N., Kagawa T., Wada M. (2005) An auxilin-like J-domain protein, JAC1, regulates phototropin-mediated chloroplast movement in *Arabidopsis*. *Plant Physiology.* **139,** 151-162.

Takemiya A., Inoue S.I., Doi I., Kinoshita T., Shimazaki K.I. (2005) Phototropins promote plant growth in response to blue light in low light environments. *Plant Cell.* **17,** 1120-1127.

Teh O.K., Moore I. (2007) An ARF-GEF acting at the Golgi and in selective endocytosis in polarized plant cells. *Nature.* **448:**493-496.

Tse Y.C., Mo B., Hillmer S., Zhao M., Lo S.W., Robinson D.G., Jiang L. (2004) Identification of multivesicular bodies as prevacuolar compartments in Nicotiana tabacum BY-2 cells. *Plant Cell.* **16,** 672-693.

Tse Y.C., Lo S.W., Hillmer S., Dupree P., Jiang L. (2006) Dynamic response of prevacuolar compartments to brefeldin a in plant cells. *Plant Physiology* **142,** 1442-1459.

Tokutomi S., Matsuoka D., Zikihara K. (2008) Molecular structure and regulation of phototropin kinase by blue light. *Biochimica Biophysica Acta* **1784,** 133-142.

Ulmasov T., Murfett J., Hagen G., Guilfoyle T.J. (1997) Aux/IAA proteins repress expression of reporter genes containing natural and highly active synthetic auxin response elements. *Plant Cell.* **9,** 1963-1971.

Van Volkenburgh E. (1999). Leaf expansion – an integrating plant behavior. *Plant Cell Environ*. **22**, 1463–1473.

Vitha S., Zhao L., Sack F.D. (2000) Interaction of root gravitropism and phototropism in *Arabidopsis* wild-type and starchless mutant. *Plant Physiol*.**122,** 453-461

Vogelmann T.C., Haupt W. (1985) The blue light gradient in unilaterally irradiated maize coleoptiles:Measurement with a fiber optic probe. *Photochem Photobiol.* **41,** 569-576

Wan Y.L., Eisinger W., Ehrhardt D., Kubitscheck U., Baluška F., Briggs W. (2008) The subcellular localization and blue-light-induced movement of phototropin 1-GFP in etiolated seedlings of *Arabidopsis thaliana***.** *Molecular Plant.* **1,** 103-117.

Went F.W. (1928) Wuchsstoff und Wachstum. *Rec trav Bot Neel,25,* 1-116.

Whippo C.W., Hangarter R.P. (2006) Phototropism: bending towards enlightenment. *Plant Cell* **18,** 1110-1119.

Wymann, M.P. (1996), Wortmannin inactivates phosphoinositide 3-kinase by covalent modification of Lys-802, a residue involved in the phosphate transfer reaction. *Mol Cell Biol.* **16**, 1722-1733.

Xiong J., Fischer W.M., Inoue K., Nakahara M., Bauer C.E. (2000) Molecular evidence for the early evolution of photosynthesis. *Science.* **289,**1724-1730

Publications

Wan Y-L., Eisinger W, Ehrhardt D., Kubitscheck U., Baluška F., Briggs W. (2008) The subcellular Localization and Blue-Light-Induced Movement of Phototropin 1-GFP in Etiolated Seedlings of Arabidopsis thaliana. *Molecular plants,* **1:**103-171.

Baluška F., Schlicht M., **Wan Y-L.**, Burbach C., Volkmann D. (2008) Intracellular domains and polarity in root apices: from synaptic domains to plant neurobiology. *Nova Acta Leopoldina*, In Press

Shen H., Hou N-Y., Schlicht M., **Wan Y-L**., Mancuso S., Baluška F. (2008)Aluminium toxicity targets PIN2 in Arabidopsis root apices: inhibitory effects on PIN2 endocytosis, vesicular recycling, and polar auxin transport. *Chinese Science Bulletin,* 2008,**53.** 2480-2487

Wan Y-L., Kubitscheck U., Briggs W., Baluška F. (2008) Darkness and Blue Light Illuminations Control Endocytosis and Vesicle Recycling at the Plasma Membrane of Plant Cells. In preparation.

Award

Awarded by Signal Transduction Society **(STS)** at STS meeting 2007, for the works at *Root apex transition zone: integration of gravitropic and phototropic responses via endocytic vesicle recycling?*

Conferences

Wan Y-L., Gabrys H., Baluška F., Menzel D. (2005) Blue Light-Regulated Vesicular Recycling of Phototropin 1 in the Root Transition zone. The First Symposium on Plant Neurobiology, Florence, Italy. poster.

Wan Y-L., Gabrys H., Baluška F., Menzel D. (2005) Blue Light-Regulated Vesicular Recycling of Blue Light Receptor PHOT1 at Cellular End-Poles in the Root

Transition Zone, DGZ, Heidelberg, *European Journal of Cell Biology,* **84(55)**. poster

Wan Y-L., Eisinger W., Krzeszowiec W., Gabrys H., Baluška František., Ehrhardt D., Briggs W. (2006) The Subcellular Localization and Blue Light-induced Dynamic Relocalization of Phototropin 1 in Root and Shoot cells of Arabidopsis thaliana. Second Symposium on Plant Neurobiology. Beijing, China, poster.

Wan Y-L., Eisinger W., Baluška František., Ehrhardt D., Briggs W. (2006) The subcellular localization and blue light-induced movement of phototropin 1 in etiolated seedlings of Arabidopsis. European Plant Endomembrane Meeting. Marienburg at Zell/Mosel, Germany,lecture,

Wan Y-L., Kubitschek U., Chen R-J., Volkmann D., Baluška F. (2007) Darkness and blue light illuminations control endocytosis and vesicle recycling at the plasma membrane of plant cells. The Third Symposium on Plant Neurobiology. Strbske Pleso, Slovakia, poster.

Wan Y-L., Eisinger W, Ehrhardt D., Kubitscheck U., Baluška F., Briggs W. (2007) The subcellar localization and blue-light-induced movement of Phototropin 1-GFP in etiolated seedlings of Arabidopsis thaliana. The Third Symposium on Plant Neurobiology. . Strbske Pleso, Slovakia, poster.

Wan Y-L, Kubitscheck U., Volkmann D. and Baluška F. (2007) Endocytosis and Vesicle Trafficking in Gravitropism and Phototropism**.** Botanical Congress by the Deutsche Botanische Gesellschaft. Hamburg, Germany, poster.

Wan Y-L., Baluška F., Volkmann D., Menzel D. (2007) Root apex transition zone: integration of gravitropic and phototropic responses via endocytic vesicle recycling? Signal Transduction: Receptors, Mediators and Genes. Weimar, Germany, poster.

Acknowledgments

I thank Prof. Dr. František Baluška, who supervised this study, for teaching me the theories and methods in field of plant cell biology and supporing me excellent ideas in this study.

I thank Prof. Dr. Diedrik Menzel and Prof. Dr. Dieter Volkmann for supporting and leading our wonderful working teams and teaching me many knowledge in plant biology.

I thank Prof. Dr. Winslow Briggs, in Carnegie institute of Washingtong, department of plant science, Stanford, US. He hosted me for 6 month research works in his group, taught me a lot about light physiology and plant sensory biology, gave me helps in writing and publication of scientific papers.

I thank Prof. Dr. Ulrich Kubitscheck for allowing me use the confocal microscopy in his group, teaching me the methods of laser scanning confocal microscopy.

I also thanks all members in our research group. Especially, I thank Dr. Josef Šamaj, Dr. Jan Jasik, Dr. Boris Voigt and Markus Schlicht for discussing and helping me for new techniques and exchanging new ideas with me in the plant cells biology. Dr. Olga Samajova, Claudia Heym and Ulla Mettbach supported a nice working atmosphere and working conditions.

Erklärung

Ich versichere hiermit, dass ich die vorliegende Arbeit in allen Teilen selbst und ohne jede unerlaubte Hilfe angefertigt habe. Diese oder eine ähnliche Arbeit ist noch keiner anderen Stelle als Dissertation eingereicht worden. Die Arbeit ist an nachstehend aufgeführten Stellen auszugsweise veröffentlicht worden:

Wan Y-L., Eisinger W, Ehrhardt D., Kubitscheck U., Baluška F., Briggs W. (2008) The subcellular Localization and Blue-Light-Induced Movement of Phototropin 1-GFP in Etiolated Seedlings of Arabidopsis thaliana. *Molecular plants,* **1:**103-171.

Ich habe früher noch keinen Promotionsversuch unternommen.

Bonn, den 23,10,2008